



**NAVAL  
POSTGRADUATE  
SCHOOL**

**MONTEREY, CALIFORNIA**

**THESIS**

**REDUCING HUMAN RADIATION RISKS ON DEEP  
SPACE MISSIONS**

by

Kathryn A. Worden

September 2017

Thesis Advisor:  
Co-Advisor:  
Second Reader:

Stephen Tackett  
Jennifer Rhatigan  
Mark Rhoades

**Approved for public release. Distribution is unlimited.**

THIS PAGE INTENTIONALLY LEFT BLANK

REPORT DOCUMENTATION PAGE			Form Approved OMB No. 0704-0188	
Public reporting burden for this collection of information is estimated to average 1 hour per response, including the time for reviewing instruction, searching existing data sources, gathering and maintaining the data needed, and completing and reviewing the collection of information. Send comments regarding this burden estimate or any other aspect of this collection of information, including suggestions for reducing this burden, to Washington headquarters Services, Directorate for Information Operations and Reports, 1215 Jefferson Davis Highway, Suite 1204, Arlington, VA 22202-4302, and to the Office of Management and Budget, Paperwork Reduction Project (0704-0188) Washington, DC 20503.				
<b>1. AGENCY USE ONLY</b> (Leave blank)	<b>2. REPORT DATE</b> September 2017	<b>3. REPORT TYPE AND DATES COVERED</b> Master's thesis		
<b>4. TITLE AND SUBTITLE</b> REDUCING HUMAN RADIATION RISKS ON DEEP SPACE MISSIONS			<b>5. FUNDING NUMBERS</b>	
<b>6. AUTHOR(S)</b> Kathryn A. Worden				
<b>7. PERFORMING ORGANIZATION NAME(S) AND ADDRESS(ES)</b> Naval Postgraduate School Monterey, CA 93943-5000			<b>8. PERFORMING ORGANIZATION REPORT NUMBER</b>	
<b>9. SPONSORING /MONITORING AGENCY NAME(S) AND ADDRESS(ES)</b> N/A			<b>10. SPONSORING / MONITORING AGENCY REPORT NUMBER</b>	
<b>11. SUPPLEMENTARY NOTES</b> The views expressed in this thesis are those of the author and do not reflect the official policy or position of the Department of Defense or the U.S. Government. IRB Protocol number ____N/A____.				
<b>12a. DISTRIBUTION / AVAILABILITY STATEMENT</b> Approved for public release. Distribution is unlimited.			<b>12b. DISTRIBUTION CODE</b>	
<b>13. ABSTRACT (maximum 200 words)</b>  <p>This paper uses a systems engineering approach to address radiation exposure risks for humans on the first missions to Mars. Alternatives are reviewed in the areas of Mars mission architectures, various shielding technologies, and medical treatment options to help mitigate the risks of radiation doses received. The over-arching goal of this study is to determine if any alternatives will reduce astronaut radiation exposure on a mission to Mars to below the NASA space worker limits, while concurrently minimizing launch weight, costs, and risks.</p> <p>All alternatives are compared via a combination of existing trade studies and swing matrices. Using these tools, it is determined that boronated nitride nanotubes are the highest potential composite for vehicle shielding, and it is recommended that Martian regolith should be used in parallel for any long-stay by the crew on the Martian surface. Two medical countermeasures (Amifostine and Neupogen) are found to have the highest potential due for use, given that they are already FDA approved. It is also determined that no single shielding alternative will reduce crew exposure below existing limits, but further research may determine that a combination of composite shielding and regolith barriers may improve this outlook.</p>				
<b>14. SUBJECT TERMS</b> space radiation protection, human Mars mission, human deep space mission, space radiation shielding, medical countermeasures, Mars mission architecture			<b>15. NUMBER OF PAGES</b> 187	
			<b>16. PRICE CODE</b>	
<b>17. SECURITY CLASSIFICATION OF REPORT</b> Unclassified	<b>18. SECURITY CLASSIFICATION OF THIS PAGE</b> Unclassified	<b>19. SECURITY CLASSIFICATION OF ABSTRACT</b> Unclassified	<b>20. LIMITATION OF ABSTRACT</b> UU	

THIS PAGE INTENTIONALLY LEFT BLANK

**Approved for public release. Distribution is unlimited.**

**REDUCING HUMAN RADIATION RISKS ON DEEP SPACE MISSIONS**

Kathryn A. Worden  
Lieutenant Commander, United States Navy Reserves  
B.S., Rensselaer Polytechnic Institute, 2004

Submitted in partial fulfillment of the  
requirements for the degree of

**MASTER OF SCIENCE IN SYSTEMS ENGINEERING MANAGEMENT**

from the

**NAVAL POSTGRADUATE SCHOOL**  
**September 2017**

Approved by: Stephen Tackett  
Thesis Advisor

Jennifer Rhatigan, Ph.D., P.E.  
Co-Advisor

Second Reader  
Mark Rhoades

Ronald Giachetti, Ph.D.  
Chair, Department of Systems Engineering

THIS PAGE INTENTIONALLY LEFT BLANK

## **ABSTRACT**

This paper uses a systems engineering approach to address radiation exposure risks for humans on the first missions to Mars. Alternatives are reviewed in the areas of Mars mission architectures, various shielding technologies, and medical treatment options to help mitigate the risks of radiation doses received. The over-arching goal of this study is to determine if any alternatives will reduce astronaut radiation exposure on a mission to Mars to below the NASA space worker limits, while concurrently minimizing launch weight, costs, and risks.

All alternatives are compared via a combination of existing trade studies and swing matrices. Using these tools, it is determined that boronated nitride nanotubes are the highest potential composite for vehicle shielding, and it is recommended that Martian regolith should be used in parallel for any long-stay by the crew on the Martian surface. Two medical countermeasures (Amifostine and Neupogen) are found to have the highest potential due for use, given that they are already FDA approved. It is also determined that no single shielding alternative will reduce crew exposure below existing limits, but further research may determine that a combination of composite shielding and regolith barriers may improve this outlook.

THIS PAGE INTENTIONALLY LEFT BLANK



# TABLE OF CONTENTS

<b>I.</b>	<b>BACKGROUND .....</b>	<b>1</b>
<b>II.</b>	<b>RADIATION IN OUTER SPACE .....</b>	<b>3</b>
<b>A.</b>	<b>GALACTIC COSMIC RADIATION .....</b>	<b>3</b>
<b>B.</b>	<b>SOLAR PARTICLE EVENTS .....</b>	<b>6</b>
<b>C.</b>	<b>IMPROVEMENTS TO MEASUREMENTS OF SPACE RADIATION .....</b>	<b>10</b>
<b>1.</b>	<b>Mars Science Lab Space Measurements.....</b>	<b>11</b>
<b>2.</b>	<b>Curiosity Rover Surface Measurements.....</b>	<b>15</b>
<b>D.</b>	<b>TRAPPED RADIATION .....</b>	<b>22</b>
<b>III.</b>	<b>BIOLOGICAL EFFECTS OF DEEP SPACE RADIATION.....</b>	<b>25</b>
<b>A.</b>	<b>TYPES OF RADIATION.....</b>	<b>25</b>
<b>1.</b>	<b>Electromagnetic Radiation.....</b>	<b>25</b>
<b>2.</b>	<b>Particulate Radiation.....</b>	<b>26</b>
<b>3.</b>	<b>Expansion on Solar Particle Events .....</b>	<b>26</b>
<b>B.</b>	<b>MEASUREMENT OF RADIATION.....</b>	<b>27</b>
<b>C.</b>	<b>BIOLOGICAL IMPACT MECHANISMS .....</b>	<b>28</b>
<b>1.</b>	<b>Mechanisms of Cancer from Radiation Exposure.....</b>	<b>28</b>
<b>2.</b>	<b>Non-cancerous Impacts from Radiation Exposure.....</b>	<b>30</b>
<b>D.</b>	<b>REVIEW AND BASIS OF EXISTING EXPOSURE LIMITS .....</b>	<b>31</b>
<b>E.</b>	<b>DOSIMETRY REVIEW AND RESEARCH IMPROVEMENTS.....</b>	<b>34</b>
<b>1.</b>	<b>Dosimetry Review and Improvements .....</b>	<b>35</b>
<b>2.</b>	<b>Research on Dose Estimate Improvements .....</b>	<b>36</b>
<b>F.</b>	<b>CURRENT EXPOSURE FORECASTS .....</b>	<b>39</b>
<b>1.</b>	<b>General Predictive Models.....</b>	<b>40</b>
<b>2.</b>	<b>Mission-Specific Models .....</b>	<b>51</b>
<b>IV.</b>	<b>REDUCING EXPOSURE THROUGH MISSION ARCHITECTURE .....</b>	<b>55</b>
<b>A.</b>	<b>OPPOSITION CLASS MISSION ARCHITECTURE .....</b>	<b>55</b>
<b>B.</b>	<b>CONJUNCTION CLASS MISSION ARCHITECTURE.....</b>	<b>58</b>
<b>C.</b>	<b>COMPARISONS OF MISSION ARCHITECTURES.....</b>	<b>60</b>
<b>1.</b>	<b>Propulsion Requirements.....</b>	<b>60</b>
<b>2.</b>	<b>Scientific Exploration .....</b>	<b>63</b>
<b>3.</b>	<b>Human Health Hazards.....</b>	<b>64</b>
<b>V.</b>	<b>REDUCING RISK OF EXPOSURE THROUGH MISSION SHIELDING TECHNOLOGY .....</b>	<b>69</b>

A.	<b>INITIAL MISSION DESIGN AND SHIELDING ASSUMPTIONS.....</b>	<b>69</b>
1.	<b>Pre-Deploy Configuration Summary .....</b>	<b>70</b>
2.	<b>All-Up Configuration Summary .....</b>	<b>71</b>
3.	<b>Mass Reference for Transit Vehicles.....</b>	<b>71</b>
B.	<b>SHIELDING CONSIDERATIONS FOR MARS SURFACE HABITAT .....</b>	<b>74</b>
C.	<b>HYDROGEN-FOCUSED SHIELDING RESEARCH.....</b>	<b>78</b>
D.	<b>ADVANCED LIGHTWEIGHT SHIELDING RESEARCH .....</b>	<b>87</b>
E.	<b>FIELD-BASED SHIELDING RESEARCH.....</b>	<b>90</b>
VI.	<b>REDUCING IMPACTS OF EXPOSURE THROUGH MEDICAL COUNTERMEASURES .....</b>	<b>91</b>
A.	<b>ETHICAL GUIDELINES FOR SPACE EXPLORATION.....</b>	<b>91</b>
B.	<b>MEDICAL COUNTER-MEASURES.....</b>	<b>93</b>
VII.	<b>DETERMINATION OF OPTIMAL SOLUTIONS .....</b>	<b>99</b>
A.	<b>OVERVIEW OF RISK-INFORMED DECISION MAKING METHOD .....</b>	<b>99</b>
B.	<b>OBJECTIVES HIERARCHY .....</b>	<b>105</b>
1.	<b>Existing Risk Analysis Data and Gap Assessments .....</b>	<b>107</b>
2.	<b>Definition of Project-Specific Swing Weight Objectives and Matrix .....</b>	<b>112</b>
3.	<b>Definition of Objective Rating Scales and Assumptions .....</b>	<b>118</b>
C.	<b>EVALUATION OF MISSION ARCHITECTURE ALTERNATIVES .....</b>	<b>121</b>
D.	<b>EVALUATION OF SHIELDING ALTERNATIVES.....</b>	<b>124</b>
1.	<b>Simplification of Decision Regarding Launch Configuration .....</b>	<b>124</b>
2.	<b>Analysis of Shielding Alternatives.....</b>	<b>125</b>
E.	<b>EVALUATION OF MEDICAL COUNTERMEASURES .....</b>	<b>136</b>
F.	<b>REVIEW OF SOLUTIONS AND SENSITIVITY ANALYSIS .....</b>	<b>143</b>
1.	<b>Explanation of Sensitivity Analysis for Swing Matrices .....</b>	<b>144</b>
2.	<b>Sensitivity Analysis Results.....</b>	<b>145</b>
VIII.	<b>CONCLUSIONS .....</b>	<b>151</b>
	<b>LIST OF REFERENCES.....</b>	<b>155</b>
	<b>INITIAL DISTRIBUTION LIST .....</b>	<b>159</b>

## LIST OF FIGURES

Figure 1.	GCR Fluence for Selected Elemental Species Relative to Solar Cycle. Source: Rojdev and Atwell (2015, 61). .....	4
Figure 2.	Shielding Effectiveness of GCR at Solar Minimum. Source: NASA Space Radiation Analysis Group (2016).....	6
Figure 3.	Measured Fluence for Three Significant SPEs. Source: NASA Space Radiation Analysis Group (2016). .....	7
Figure 4.	Shielding Effectiveness for Three Significant SPEs. Source: NASA Space Radiation Analysis Group (2016).....	8
Figure 5.	Measured Fluence for Significant SPEs. Source: Adams et al. (2005).....	9
Figure 6.	Dose Rate as Measured by the RAD in Deep Space. Source: Köhler et al. (2013). .....	12
Figure 7.	Dose Rate for Solar Particle Events as Compared by the RAD (Black Lines) versus the GOES-11 Satellite (Grey Lines). Source: Köhler et al. (2013). .....	14
Figure 8.	RAD Dose Rate Measurements on Martian Surface. Source: Hassler et al. (2013, 8). .....	16
Figure 9.	RAD Dose Rate versus Atmospheric Pressure on Martian Surface. Source: Hassler et al. (2013, 8). .....	16
Figure 10.	April 2014 SPE as Compared by Various Instruments. Source: Hassler et al. (2013, 10). .....	18
Figure 11.	Comparison of Radiation Dose Equivalents. Source: Hassler et al. (2013, 9). .....	19
Figure 12.	Radiation Environment Measured by MSL/Rover for GCR Only. Source: Hassler et al. (2013, 11). .....	20
Figure 13.	Radiation Environment Measured by MSL/Rover for GCR Only. Source: Hassler et al. (2013, 11). .....	21
Figure 14.	Radiation Environment Measured by MSL/Rover for GCR Only. Source: Hassler et al. (2013, 11). .....	21

Figure 15.	Anticipated Dose Rates for Astronauts in 28.5-Degree Incline Earth Orbit Flights. Source: NASA Space Radiation Analysis Group (2016).....	23
Figure 16.	Areas of Investigation within the Radiation Health Program. Source: NASA Space Radiation Analysis Group (2016).....	35
Figure 17.	Comparison of Quality Factors Using Both Traditional and “Acute” RBE Models. Source: Cucinotta (2015, 4). ....	38
Figure 18.	Predictions of REID over a One-Year Space Mission at Deep Solar Minimum. Source: Cucinotta (2015, 11). ....	39
Figure 19.	Organ Doses for Males with 5g/cm <sup>2</sup> Aluminum Shielding. Source: Cucinotta et al. (2011, 30).....	41
Figure 20.	Organ Doses for Males with 20g/cm <sup>2</sup> Aluminum Shielding. Source: Cucinotta et al. (2011, 31).....	42
Figure 21.	Organ Dose Quantities/Equivalents. Source: Cucinotta et al. (2011, 33). ....	43
Figure 22.	REIC Comparison for Mixed Cancer Types versus Exposure Age per Sv of Dose Received. Source: Cucinotta et al. (2011, 40).....	45
Figure 23.	REIC Comparison for Organ-Specific Cancer Types versus Exposure Age per Sv of Dose Received. Source: Cucinotta et al. (2011, 41).....	46
Figure 24.	Effective Dose Rates versus Shielding Depth in Deep Space. Source: Cucinotta et al. (2011, 88).....	47
Figure 25.	Effective Dose Rates versus Shielding Depth for Multiple Cancer/Organ Effects. Source: Cucinotta et al. (2013, 3).....	48
Figure 26.	REID Distributions versus Density of Ionization for Particle Tracks. Source: Cucinotta et al. (2013, 4). ....	49
Figure 27.	Estimates of GCR Organ Doses over Recent Solar Cycles at 0g/cm <sup>2</sup> and 20g/cm <sup>2</sup> Shielding. Source: Cucinotta et al. (2013, 4).....	50
Figure 28.	Organ Specific REICs for a Typical Mars Mission. Source: Cucinotta et al. (2013, 6).....	52
Figure 29.	Combined REIDs for Various Mission Types. Source: Cucinotta et al. (2013, 7). ....	53

Figure 30.	Typical Opposition Class Mission Trajectories. Source: Drake (2009, 50).....	56
Figure 31.	Opposition Class Mission Departure Years with Swing by versus Long-Stay Architecture. Source: Drake (2009, 56).....	57
Figure 32.	Typical Conjunction Class Mission Trajectories. Source: Drake (2009, 51).....	58
Figure 33.	Comparison of Mission Class Transit Times, Stay Times, and Total Durations. Source: Drake (2009, 52).....	59
Figure 34.	Delta V Comparisons. Source: Drake (2009, 57). .....	62
Figure 35.	Nominal Six-Person, 1000-Day Duration Mass Allocation Break-Out for Mars Transit Vehicle. Source: Drake and Watts (2014, 369). .....	73
Figure 36.	Dose Equivalent and Effective Doses versus Shielding Depth on the Martian Surface Compared to $\frac{1}{2}$ Free Space Approximations. Source: Slaba et al. (2013, 6).....	75
Figure 37.	MOF Material Formulas and Densities Used for Radiation Transport Calculations. Source: Rojdev and Atwell (2015, 64). .....	80
Figure 38.	CNT Material Formulas and Densities Used for Radiation Transport Calculations. Source: Rojdev and Atwell (2015, 65). .....	81
Figure 39.	MH Material Formulas and Densities Used for Radiation Transport Calculations. Source: Rojdev and Atwell (2015, 66). .....	82
Figure 40.	Selected MOF Shielding Effectiveness Results Compared to Conventional Materials for GCR. Source: Rojdev and Atwell (2015, 68). .....	83
Figure 41.	Selected CNT Shielding Effectiveness Results Compared to Conventional Materials for GCR. Source: Rojdev and Atwell (2015, 69). .....	84
Figure 42.	Selected MH Shielding Effectiveness Results Compared to Conventional Materials for GCR. Source: Rojdev and Atwell (2015, 70). .....	85
Figure 43.	Selected Base, Hydrogen, and Methane-Loaded MOF Shielding Effectiveness Results for SPEs. Source: Rojdev and Atwell (2015, 72). .....	86

Figure 44.	Selected Base, Hydrogen, and Methane-Loaded CNT Shielding Effectiveness Results for SPEs. Source: Rojdev and Atwell (2015, 73).	86
Figure 45.	Effectiveness of 5% BNNT against GCR Exposure Compared to Conventional Shielding Materials. Source: Thibeault et al. (2012, 5).	88
Figure 46.	Effectiveness of Selected BNNTs against GCR Exposure Compared to Conventional Shielding Materials. Source: Thibeault et al. (2012, 6).	89
Figure 47.	Effectiveness of Selected BNNTs against SPE Exposure Compared to Conventional Shielding Materials. Source: Thibeault et al. (2012, 7).	89
Figure 48.	Human Health and Performance Challenges. Source: Drake (2009, 293).	101
Figure 49.	Human Health, Life Support, and Habitation System Goals. Source: NASA Office of the Chief Technologist (2016).	102
Figure 50.	Human Exploration Destination System Goals. Source: NASA Office of the Chief Technologist (2016).	103
Figure 51.	The RIDM Process. Source: Dezfuli et al. (2010, 14).	104
Figure 52.	Risk Assessment for Radiation Carcinogenesis. Source: NASA Human Research Roadmap (2016).	108
Figure 53.	Risk Assessment for Acute Radiation Syndrome Due to SPEs. Source: NASA Human Research Roadmap (2016).	109
Figure 54.	Risk Assessment for Cardiovascular Disease and Other Degenerative Tissue Effects. Source: NASA Human Research Roadmap (2016).	111
Figure 55.	Risk Assessment for Acute Nervous System Effects from Radiation Exposure. Source: NASA Human Research Roadmap (2016).	111
Figure 56.	Objective Hierarchy Summary	116
Figure 57.	Advantages and Disadvantages for Behavioral Health and Performance Discipline. Source: Drake (2009, 77).	121
Figure 58.	Long and Short-Stay Architecture Mass Comparisons. Source: Drake (2009, 79).	122

Figure 59.	Summary of Long versus Short-Stay Trade Space. Source: Drake (2009, 81).....	123
Figure 60.	Summary of Pre-Deploy versus All-Up Trade Space. Source: Drake (2009, 89).....	124
Figure 61.	Normalized Weights and MOEs for Selected Shield Alternatives .....	145
Figure 62.	Optimized Weights and MOEs for Selected Objectives.....	146
Figure 63.	MOE Response to H&S 1 Objective Weight Adjustment .....	147
Figure 64.	MOE Response to C&W 1 Objective Weight Adjustment.....	147
Figure 65.	MOE Response to Sked 2 Objective Weight Adjustment .....	148

THIS PAGE INTENTIONALLY LEFT BLANK



## LIST OF TABLES

Table 1.	Radiation Quality Factors. Adapted from United States Nuclear Regulatory Commission (2016).....	27
Table 2.	Career Effective Dose Limits. Source: Williams (2015).....	32
Table 3.	Organ-Specific Exposure Limits for Space Workers. Source: Williams (2015).....	32
Table 4.	Relative Biological Effectiveness Assumptions for Non-cancer Effects. Source: Williams (2015).....	33
Table 5.	Mission Assumptions for Human Health and Performance Assessments .....	65
Table 6.	Sample Swing Weight Table .....	106
Table 7.	Assigned Swing Weight Matrix and Normalized Values .....	117
Table 8.	Normalized Weights by Objective and Objective Category Weighting.....	118
Table 9.	Definition of Objective Rating Scales and Assumptions.....	119
Table 10.	Review of NASA Career Effective Dose Limits .....	126
Table 11.	Shielding Sample Calculations .....	127
Table 12.	Objective Ratings for Martian Regolith Shielding .....	130
Table 13.	Objective Ratings for BNNT Shielding .....	131
Table 14.	Objective Ratings for MOF Shielding .....	132
Table 15.	Objective Ratings for CNT Shielding.....	133
Table 16.	Objective Ratings for MH Shielding .....	134
Table 17.	Objective Ratings for Field-Based Shielding .....	135
Table 18.	Summary of MOE Calculations.....	136
Table 19.	Objective Ratings for Amifostine .....	138
Table 20.	Objective Ratings for Neupogen.....	139

Table 21.	Objective Ratings for Entolimod .....	140
Table 22.	Objective Ratings for Recilisib.....	141
Table 23.	Objective Ratings for Romylocel-L.....	142
Table 24.	Summary of MOEs for Medical Countermeasures.....	143

## LIST OF ACRONYMS AND ABBREVIATIONS

ACE	Advanced Composition Explorer
AERO	aerospace
AG	artificial gravity
AIAA	American Institute of Aeronautics and Astronautics
ALARA	as low as reasonably achievable
ASCO	American Society of Clinical Oncology
AU	astronomical unit
BEIR	biological effects of ionizing radiations
BFO	blood forming organs
BNNT	hydrogenated boron nitride nanotubes
BRYNTRN	baryon transport
CAMERA	computerized anatomical man model
CFR	Code of Federal Regulations
CME	coronal mass ejection
CNS	central nervous system
CNT	nanoporous carbon composites
CT	computed tomography
CPDS	Charged Particle Directional Spectrometer
C&W	cost and weight
DAV	descent/ascent vehicle
DC	District of Columbia
DDREF	dose and dose rate effectiveness factor
DLOC	dose locations
DNA	deoxyribonucleic acid
DRA 5.0	Design Reference Architecture 5.0
EuCPAD	European Crew Personal Active Dosimeter
EVA	extravehicular activity
FDA	Food and Drug Administration
FOM	figure of merit
GCR	Galactic Cosmic Radiation

GINA	Genetic Information Non-Discrimination Act
GLE	ground level event
GOES	Global Online Enrollment System
HDPE	high density polyethylene
H&S	health and safety
HZE	high atomic number and energy
ISRU	in situ resource usage
ISS	International Space Station
JSC	Johnson Space Center
LAR	lifetime attributable risk
LEO	low Earth orbit
LET	linear energy transfer
L1	Lagrangian Point
LOC	loss of crew
LTV	Lunar Transfer Vehicle
MER	Mars Expedition Rover
MH	metal hydride
MOE	measure of effectiveness
MOF	metal organic framework
MSFC	Marshall Space Flight Center
MSL	Mars Science Laboratory
MSR	Mars sample return
MTV	Mars transit vehicle
NASA	National Aeronautics and Space Administration
NCRP	National Council on Radiation Protection and Measurements
NIAC	NASA Innovative Advanced Concepts
NLSI	NASA Lunar Science Institute
NRC	Nuclear Regulatory Commission
NSCR	NASA space radiation cancer risk
NTR	nuclear thermal
OSHA	Occupational Safety and Health Administration
PC	probability of causation

QF	Quality Factor
RAD	Radiation Assessment Detector
RBE	relative biological effectiveness
REIC	risk of exposure induced cancer
REID	risk of exposure induced death
RIDM	risk informed decision making
SAA	South Atlantic Anomaly
SEP	solar energetic particle
SHAB	surface habitat
Sked	schedule
SOHO	Solar Heliospheric Observatory
SP	standard procedure
SPE	Solar Particle Event
STD	standard
SV	science value
TEPC	Tissue Equivalent Proportional Counter
TA	technology area
TM	technical manual
TP	technical procedure
TRL	technology readiness level
U.S.	United States
UV	ultraviolet

THIS PAGE INTENTIONALLY LEFT BLANK

## EXECUTIVE SUMMARY

Sending humans to deep space is arguably one of the greatest technical challenges of our time. There are scientific benefits that may be gained by sending humans to Mars in conjunction with the Mars Expedition Rover (MER) missions that are already underway. However, the risks required to send humans so far from Earth are also high. In the face of more obvious risks such as mission equipment failure or human error, a less overt but equally significant risk is that of the consequences of radiation exposure that astronauts will receive on such missions. This study aims to address the following question: **How can systems engineering techniques be applied to suggest optimal combinations of mission architectures, shielding designs, and medical counter-measures; with the goal of helping to ensure that human radiation health criteria are met on missions to Mars?**

In the first chapter, the types of radiation encountered in deep space are reviewed. Galactic Cosmic Radiation (GCR) is a constant flux of high velocity particles from outside our solar system, which varies slightly with solar cycle due to the radiation shielding provided by solar wind. It is also a challenge to protect against given that the effectiveness of common shielding materials levels is asymptotic as “shielding thickness” (i.e., density per unit area) is increased. Solar Particle Events (SPEs) occur at higher frequencies during the maxima of our solar cycles, and originate from the waves of particles released during solar storms, flares, and coronal mass ejections. Solar Particle Events do not have the same velocity as GCR flux, but due to the fact that their particles may possess much higher energy during severe events, and that such severity increases with proximity to the sun—they have the potential to deliver significant exposure and to cause acute and even potentially lethal effects for astronauts if proper shielding is not provided.

The second chapter summarizes the anticipated doses that would be received by astronauts in various Mars mission models. Radiation types are reviewed, including non-ionizing (electromagnetic) and ionizing (particulate) fluxes. The concept of Quality Factor (QF) is introduced, which equates to the level of biological damage that each

radiation particle type is capable of doing for a given energy level. Biological impact mechanisms for different types of radiation are reviewed, including a summary of the complex phases that determine whether cell impacts will metastasize into cancer or not. Current research on both improved space-based dosimetry technology and improved models for Quality Factor to account for the variation in linear energy transfer (LET) in GCR flux is also discussed. While this research helps to reduce uncertainty in radiation dosage estimates—summaries for anticipated astronaut doses on Mars mission models conclude that astronauts will vastly exceed the current limit for a career-based 3% increase in risk of exposure induced death (REID) over the course of a typical mission, that these impacts are worse for women versus men given the higher risks to reproductive organs and lungs (Cucinotta and Durant 2010, 126), and that a large degree of uncertainty for anticipated exposures still exists.

Next, mission architecture options are reviewed and compared from a stand-point of human health risks. Short-stay or Opposition Class missions are those which comprise overall shorter mission durations, with a very short (roughly 30-day) stay on the Martian surface, and overall longer transit times between Earth and Mars. Long-stay or Conjunction Class missions involve shorter transit times, but with a very long Martian surface stay (~540 days) to permit time for optimal orbital alignment on the return trip. The longer transit times, combined with trajectories that will require passage within the orbit of Venus (or closer) to the Sun, equate to overall higher radiation concerns for Short-stay missions due to the risk of Solar Particle Events. The Short-stay mission class also has less potential scientific benefit when compared to the Long-stay. Conversely, Short-stay missions do also yield slightly less mission duration risk due to their overall shorter length, and significantly lower risks for the uncertainty of the conditions that will be encountered during their relatively short periods on the Martian surface.

Shielding alternatives are discussed in Chapter V. Existing shielding designs are reviewed, including the use of aluminum structure and water walls for the design reference Mars transit vehicle designs. Shielding considerations on the Mars surface are discussed in a series of studies that overall suggest the need to consider novel shielding materials and the use of Martian regolith in order to gain substantial shielding benefits



verses the effects of secondary radiation interactions with aluminum shielding materials on the surface. Finally, multiple novel shielding studies are discussed, highlighting the potential of hydrogen or methane rich materials, and in particular, Hydrogenated boron nitride nanotube technologies to provide shielding improvements or at least equivalent shielding when compared to pure hydrogen or polyethylene materials (which are too impractical and too heavy to use on their own, respectively). The nanotube technologies are particularly promising in part because of their potential cross-application for structural materials as well.

In Chapter VI, the ethical principles that serve as the basis for NASA exposure limits and policy are reviewed. These principles create a complex decision process where the balance must be maintained between providing autonomy to crew members who knowingly assume the very high risks associated with space exploration, and the obligation of NASA to protect them against long term harm from cancers and the like. Medical countermeasures for radiation exposure are also reviewed, with a highlight on several drugs currently in the early stages of use or development. These drugs work either by preventing radiation damage, or by mitigating radiation sickness symptoms after acute exposure. While the potential benefits and cost savings provided by these drugs are high in the sense that medicine takes up relatively little cargo space/launch mass, the use of such countermeasures must be weighed against several concerns. These include the schedule risk incurred by the very lengthy testing and approval process mandated by the FDA, the risks of side effects if the drugs are used, and the limitations of shelf lives for drugs on lengthy deep space missions. Exciting potential technology does exist, however, which may mitigate some of these concerns by permitting remote synthesis of new or existing drugs through the use of computer systems and basic substrate chemicals while a mission is underway.

Chapter VII conducts the analysis of all alternatives reviewed in Chapters IV through VI. Simplifying assumptions are made based on existing trade studies in the Drake's publications, which conclude that Long-stay missions are preferable to Short-stay missions and that Pre-Deploy mission configurations are superior to All-Up configurations. The concept of swing weight matrices is reviewed as a powerful tool to

calculate measures of effectiveness (MOEs) for various alternatives. Crew mission objectives are defined in the context of priorities for NASA missions in general, and using NASA risk roadmaps that are pertinent to human radiation concerns on deep space/planetary missions. Using objective rating scales, a detailed shielding analysis reveals that BNNTs are the most promising shielding composite under study. In parallel, it is recommended that Martian regolith should be used for any Long-stay surface portion of a Mars mission, and that field-based shielding should continue to be researched as a high potential shielding option in the longer term. Finally, a swing weight analysis is also conducted for medical countermeasures alternatives, where it is determined that Amifostine and Neupogen have the highest potential for use right away, with three other options that may also be viable for concurrent use once they are FDA approved.

## **Reference**

Cucinotta, Francis A., and Marco Durant. 2010. "Risk of Radiation Carcinogenesis." In *Human Health and Performance Risks of Space Exploration Missions*, edited by Jancy C. McPhee and John B. Charles, 119–169. Washington, DC: NASA.

## **ACKNOWLEDGMENTS**

I offer many thanks to my doctors for helping me to get through some challenging months, so I could finally complete this program. Even greater thanks to my professors and advisors for their continued patience, and to my friends and family for their constant support.

THIS PAGE INTENTIONALLY LEFT BLANK

## I. BACKGROUND

Sending astronauts to space has many inherent risks. One significant risk is radiation exposure; this risk drove the Occupational Safety and Health Administration (OSHA) to classify all astronauts as radiation workers in 1982 (Sieffert 2014, 21). Because OSHA's Earth-based limits were deemed too restrictive for effective space exploration, NASA was soon granted a waiver to establish its own set of radiation limits for ionizing exposure to astronauts in low Earth orbit (LEO). While these overall limits allow higher career doses than currently permitted for Earth-based radiation workers, they are still governed by the overarching principal of maintaining space worker exposure "as low as reasonably achievable," or ALARA.

However, radiation exposure in *deep space* is significantly higher than in LEO, where the planet's magnetosphere provides shielding from both Galactic Cosmic Rays (GCR) and Solar Particle Events (SPE). Studies have predicted that a human on a typical mission to Mars may receive levels of exposure that nearly double or triple the existing OSHA limits for astronauts working on the International Space Station (Cucinotta et al. 2013). These same studies reveal that for astronauts returning home, this may result in significant loss of lifespan and quality of life due to increased risk of cancer, cardiovascular abnormalities, and other organ abnormalities.

This thesis attempts to answer the overarching question: How can systems engineering techniques suggest optimal mission architectures, shielding designs, and medical counter-measures in order to ensure human radiation health criteria are met on missions to Mars? To answer this question, first background is provided on the types of radiation encountered in space, and the anticipated dose rates and biological effects of such radiation on astronauts in various proposed Mars mission architectures.

Next, this paper consolidates information from existing research and development efforts in regards to various Mars mission architectures. These cover aspects of mission schedule, potential transit vehicle/habitat shielding technologies, and medical treatments

that may be used to reduce the overall exposure level or biological impacts of radiation doses received by personnel on such a mission.

Finally, we employ a combination of weighted metric decision matrices and optimization curve techniques to evaluate potential combinations of methods as discussed above. For the sake of controlling the scope of these systems assessments, the following key points must be reviewed:

- That radiation exposure has not only significant human risks for missions to Mars, but also carries equipment risks as well. It is well-documented that radiation hardening and other shielding are needed to protect sensitive electronics and other vessel systems from failure in the harsh deep-space and Martian environments—and that such failures could contribute to mission compromise or even loss of crew (LOC). However, these points are not addressed by this study in an effort to maintain focus on the overarching solutions that will provide the greatest extent of *human* radiation exposure reduction/mitigation.
- That the sampling of solution sets carried forward through full systems engineering assessment should be distilled down to the three or four “most promising” options for final comparison, so resources are not wasted in assessing other permutations of alternatives that are not as favorable.

The application of these techniques aim to determine the optimal solution set(s) that yield the highest promise as far as lowering dose levels from existing mission models to Mars below the OSHA space worker limits while concurrently minimizing added weight, and therefore, costs.

## II. RADIATION IN OUTER SPACE

Astronauts and spacecraft will encounter various sources and types of radiation depending on spacecraft location relative to planetary orbit, and solar cycles. The three key types of radiation that will be encountered on any interplanetary/deep space mission are discussed in the following subsections.

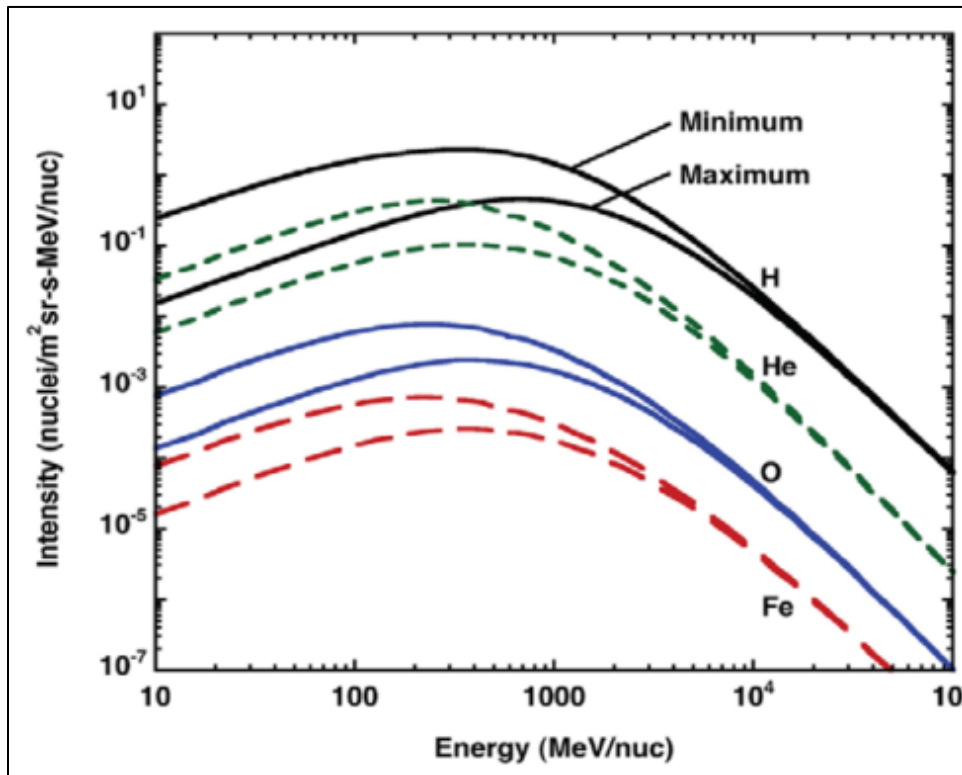
### A. GALACTIC COSMIC RADIATION

Galactic Cosmic Radiation (GCR) is a primary concern for any mission that will take astronauts beyond the range of the Earth's protective magnetic field. There, spacecraft are exposed to a small, isotropically distributed, high-energy flux that originates from outside the solar system, in the form of ionized charged atomic nuclei. This ion flux is comprised of largely hydrogen nuclei (i.e., protons, approximately 85%), and helium nuclei (i.e., alpha particles, approximately 14%), with some traces of other heavy nuclei (Adams et al. 2005, 2). These High (H) charge (Z), high energy (E) nuclei consist of any elements heavier than helium and are also given the shorthand name of HZE (Cucinotta et al. 2013, 1).

What makes GCR so damaging to biological tissue is the extremely high velocity at which the particles are moving (in some cases nearly the speed of light), and thus the kinetic energy they impart. Depending on the type of particle and its mass (described in more detail in this section), these particles are capable of either directly damaging human cells or DNA structures if they are not attenuated by shielding prior to entering the body; or alternately they may cause further damage through a process called secondary interaction, in which heavier GCR particles that are attenuated by shielding in turn release other particles (often neutrons and other ions) which are still energetic enough to cause biological damage. The topic of biological damage from radiation exposure is reviewed in greater detail in Chapter III.

A sample diagram of GCR Flux versus energy levels is shown in Figure 1. The diagram also demonstrates a key point in how GCR flux varies with each 11-year solar cycle, as discussed by the NASA Space Radiation Analysis Group (2016). At solar

maximum, the sun’s magnetic field (solar wind) actually provides some measure of protection by attenuating a large portion of the lower energy particles in the GCR flux. Measurements have shown that particles with energies  $<2000$  MeV/u (where “u” is atomic mass unit) are most significantly reduced (Cucinotta et al. 2010, 6). Higher energy particles are not affected as much, but the net difference still demonstrates that GCR dose rate is notably higher at solar minimum versus maximum (NASA Space Radiation Analysis Group 2016). For further context, where this figure refers to particle energy levels in terms of mega-electron-volt per nucleus (MeV/nuc)—it is helpful to reference 1 MeV as about twice the rest energy ( $E=mc^2$ ) of an electron, and 200 MeV as the amount of energy released in a single fission of a Uranium-235 atom.



Atomic symbol legend: H=Hydrogen, He=Helium, O=Oxygen, Fe=Iron.

Figure 1. GCR Fluence for Selected Elemental Species Relative to Solar Cycle.  
Source: Rojdev and Atwell (2015, 61).



According to the NASA Space Radiation Analysis Group (2016), the typical unshielded dose to internal organs that would be encountered by astronauts on a deep space mission occurs at an annual rate of 60 Rem/year, where Rem are units of equivalent radiation dose. Equivalent radiation dose is a measure of the biological damage that a radiation dose is capable of delivering, which is explained in further detail in Section B of Chapter III. Shielding can help to reduce this amount, but only to a limited extent as shown in Figure 2 which shows dose equivalent to blood forming organs (BFO) as compared to different shielding thicknesses. Shield thickness is a unit that is discussed repeatedly throughout this paper—it indicates the mass of shielding that is placed between an object to be protected and the source of radiation, per unit area. Thus, where aluminum has a density of  $2.7\text{g/cm}^3$  as shown in the figure, an aluminum shield thickness of  $5\text{g/cm}^2$  would correlate to an actual shield that is just under 2cm thick, and so forth. BFO are also referenced throughout this paper, and consist of the lymph nodes, bone marrow, spleen, and liver.

Secondary interactions account for the plateaus in shielding effectiveness seen in Figure 2. Secondary interactions occur when the primary source of radiation (in this case, GCR particles) interacts with another material (such as people, clothing, spacecraft shielding), which in turn causes scattering where other particles (such as neutrons) are freed and in turn become a part of the radiation flux themselves. The figure shows how thicker shields eventually cause an increase in the resulting secondary particle flux, which then causes the level of dose that can be prevented to level off (NASA Space Radiation Analysis Group 2016).

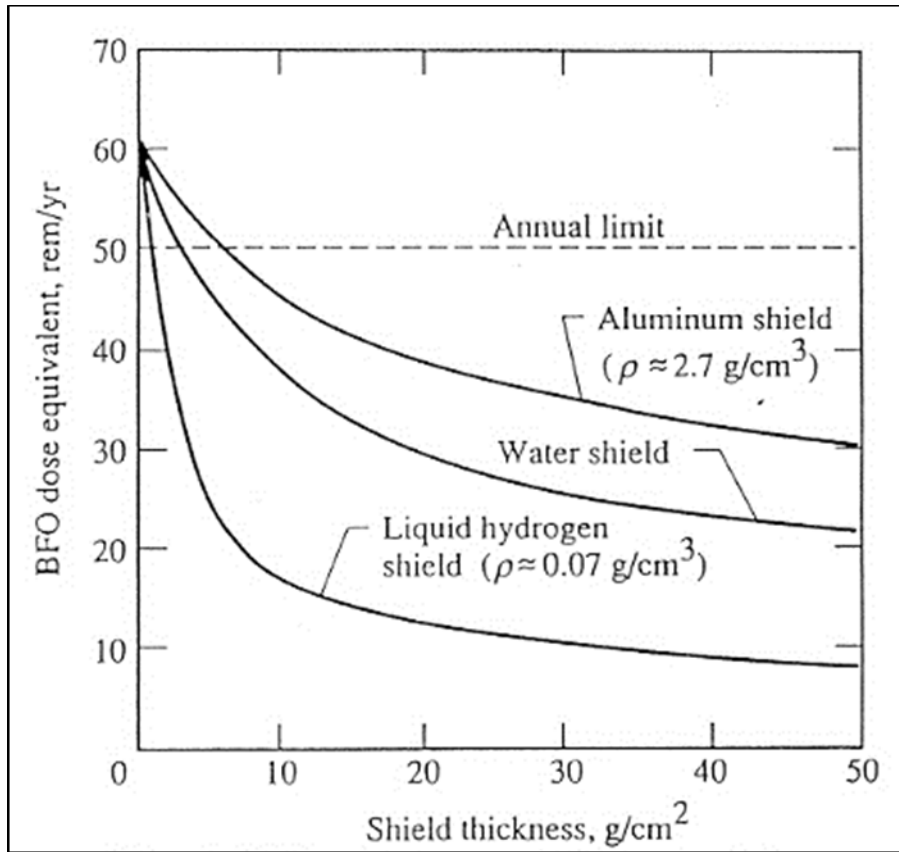


Figure 2. Shielding Effectiveness of GCR at Solar Minimum. Source: NASA Space Radiation Analysis Group (2016).

Biological mechanisms of the radiation interaction with living tissue are detailed further in the next chapter. Overall, GCR is considered to be one of the most limiting factors in near term human missions to deep space.

## B. SOLAR PARTICLE EVENTS

According to the NASA Space Radiation Analysis Group website, Solar Particle Events (SPE) are short-term expulsions of protons, alpha particles, and other heavier nuclei from our own sun which are seen during flares, solar storms, and coronal mass ejections (CME) that may occur at any time, but also more frequently during periods of elevated solar activity (2016) Logically, these events occur at higher frequencies during solar maximums—but due to their short-term nature (minute to day durations) and often isolated trajectories, there is a high degree of uncertainty associated with their prediction

for mission risk assessment. Sample figures for three historically severe SPEs are shown in Figures 3 and 4. Figure 3 depicts the overall spectra for each event, which is represented as fluence (particles passing through a unit of area integrated over the time of the event) versus the energy level of the particles observed. It shows that the quantity of higher energy particles seen during these events is relatively small, but also that the fluence observed for lower energy particles is relatively high. Figure 4 provides sample curves for what the effective dose to blood forming organs (BFO) would be when compared with varying levels of aluminum shielding. When one considers the “nominal” shielding values for spacecraft which range from 5–20g/cm<sup>2</sup> as are reviewed for various studies later in this paper, one can see the risk of receiving a significant dose (20 to over 100 Rem) in the course of a worst-case event would be almost certain. The effects of such a dose are reviewed further in Chapter III.

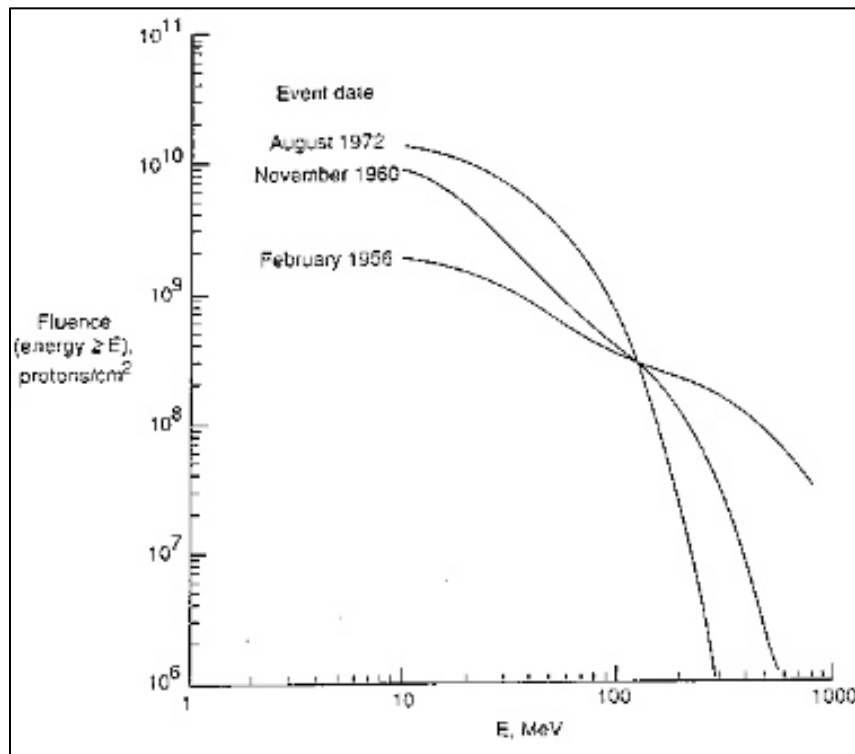


Figure 3. Measured Fluence for Three Significant SPEs. Source: NASA Space Radiation Analysis Group (2016).

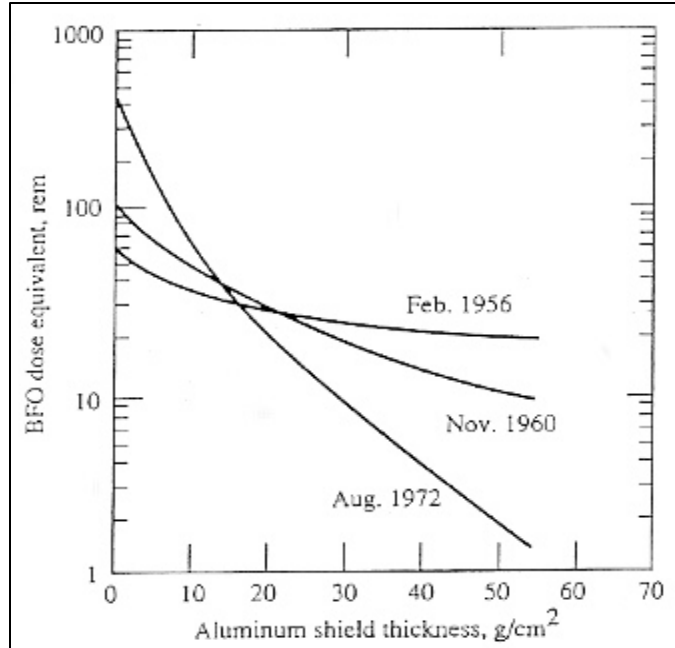


Figure 4. Shielding Effectiveness for Three Significant SPEs. Source: NASA Space Radiation Analysis Group (2016).

SPEs also differ from GCR in that while the particles generated during solar events overall have lower energy levels, their fluence is much higher within the directional trajectory of the given event (Adams et al. 2005, 2). Higher fluence is more damaging in many cases because more particles moving through a unit area integrated over time increases the likelihood of those particles causing more interactions (and therefore potential cell or tissue damage) in that time. Figure 5 shows this fluence not just for the earlier significant SPEs that have been recorded in the last century, but also for a cycle that generated three extremely powerful flares in the span of three months of higher activity in 1989. For context, this figure refers to fluence in units of protons/cm<sup>2</sup> whereas earlier discussion of GCR fluence in Figure 1 applied units of nuclei/m<sup>2</sup>. There are 10<sup>4</sup> cm<sup>2</sup> per m<sup>2</sup>, so one may scale the Y axis in Figure 5 up by that factor to get a better comparison. Overall, the comparison shows that the fluence of a SPE is quite high (up to an order of 10<sup>15</sup> protons/m<sup>2</sup> versus the fluence on the order of 10<sup>-1</sup> protons/m<sup>2</sup> seen in Figure 1), while the energies of the particles themselves may be somewhat lower (up to 10<sup>3</sup> MeV compared to GCR particles at 10<sup>5</sup> MeV).

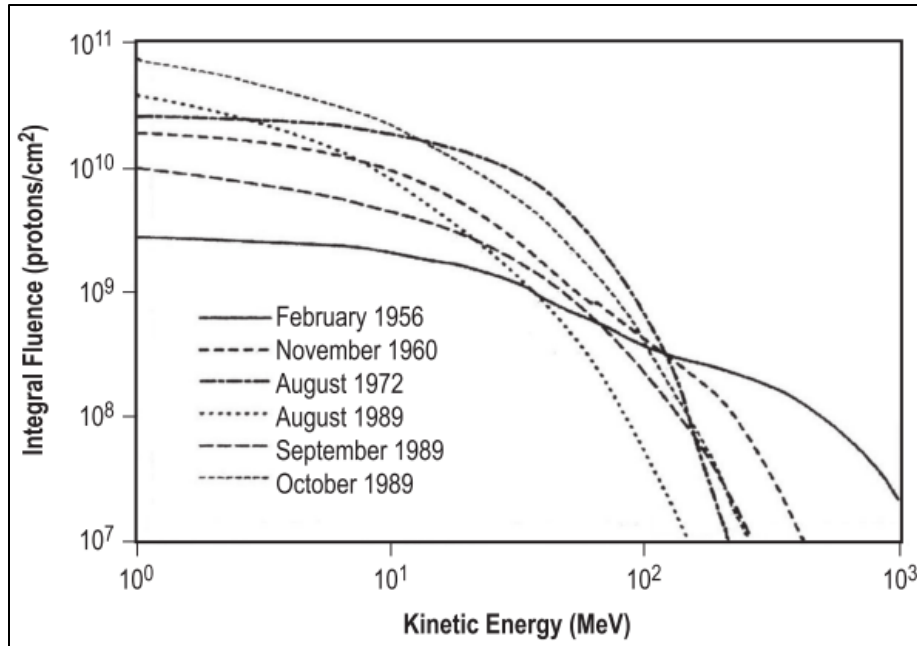


Figure 5. Measured Fluence for Significant SPEs. Source: Adams et al. (2005).

Due to the uncertain nature of SPEs, historical observations of frequency of occurrence versus all solar maxima are relevant for probability analysis. Such research has been well documented both through direct observations within the last century, and through polar ice measurements which enabled scientists to document SPEs going back as far as the 15<sup>th</sup> century (Cucinotta et al. 2010, 15). Cucinotta's study reviews data that show that in the last five solar cycles, 13 events have occurred in which the measured omnidirectional proton fluence exceeded 30 MeV at a density greater than  $10^9$  protons/cm<sup>2</sup>. Going back through polar ice history, 71 SPEs with the same energy levels at a fluence of greater than  $2 \cdot 10^9$  protons/cm<sup>2</sup> were measured from the years 1561 to 1950. SPEs with a fluence of less than 30 MeV and less than  $10^8$  protons/cm<sup>2</sup> are typically ignored for shielding studies because such levels will not yield a significant dose to spacecraft crew with nominal (5g/cm<sup>2</sup>) shielding present.

Solar Particle Events are also notoriously difficult to predict because while some have occurred during peak activity or sunspots during solar maximum, many others have occurred at different times during the cycle and in particular at random intervals during the ascent/descent from the maximum cycle (Cucinotta et al. 2010, 15). According to the

same research paper by Cucinotta et al., while resources have been dedicated to conduct probability analyses in an effort to determine whether consistent event size distributions can be mapped for the last five solar cycles, no definitive pattern has been identified. However, in spite of this random behavior, the short duration of one to two days for SPEs does make them easier to design into mission structure. In cases such as these, deep space crews could easily shelter in a small-volume space with heavier shielding to ride out the worst hours of such an event (NASA Space Radiation Analysis Group 2016).

The need to shelter from severe SPEs on a mission to Mars also highlights another technical challenge for the mission—which is to improve on our space weather prediction technologies. For context, the current warning system around Earth provides only 30–60 minutes of notice when a solar event is impending. This notice is provided because satellites and observatories are able to observe the brightening (photons) from the Sun almost immediately when a significant flare or larger event occurs. These photons lead the more dangerous particle flux by anywhere from 20 minutes to several hours before they also arrive at Earth. This provides limited time to shelter electronics on Earth, and is certainly not enough notice to allow astronauts to return to shelter if they are on a longer duration exploratory mission on Mars. As such, a better option is needed.

In 2010, Professor Roger Dube was awarded funding to research options for such a system. His concepts are highlighted in a 2010 Phys.Org website article. A future early warning network will likely incorporate a combination of assets including satellites around Earth, and at the Mars’ poles for continuous observation of the solar surface, in conjunction with existing satellites positioned between the Earth and the Sun. Algorithms are under development that may enable these sensors to predict a storm by as large a margin as three days, and then to relay the warnings to the satellites in orbit at either planet, or to spacecraft in transit (Phys.org 2010).

### **C. IMPROVEMENTS TO MEASUREMENTS OF SPACE RADIATION**

One significant gap in the GCR and SPE data described in this chapter is the fact that all of the measurements summarized are based around Earth. The analysis of comparable radiation “weather” conditions in interplanetary space and on Mars was only

recently undertaken with the incorporation of a state-of-the-art Radiation Assessment Detector (RAD) on the Curiosity Rover mission. According to Donald Hassler's article on the project, this detector has already provided data on the GCR flux levels within the transit vehicle that brought the rover to Mars, and continues to provide radiation measurements from the Martian Surface (2013, 6–9). Further, the mission team's decision to leave the detector powered on for the transit from Earth to Mars was validated when the spacecraft was exposed to a significant solar event in early 2012. This event provided valuable data because the combined solar flare and CME hit not only the spacecraft while it was between planets, but also both Earth and Mars due to their planetary alignment at the time. As such, simultaneous measurements were recorded by multiple instruments at several locations, including: the RAD on the Curiosity mission, multiple satellites including the Advanced Composition Explorer (ACE) around Earth, and the Solar Heliospheric Observatory (SOHO) operating at an orbit that places it at the first Lagrangian Point (L1) between the Earth and the Sun (Hassler 2013, 7–8). This L1 point is a location four times closer to the sun than the distance between the Earth and the Moon, where the gravitational forces on the satellite from the Earth and the Sun balance such that the satellite is able to maintain an orbit in lockstep with the Earth around the Sun.

### **1. Mars Science Lab Space Measurements**

The measurements observed by RAD have been summarized in two more recent publications. In the first, Köhler et al. review the measurements observed in space, including the Solar Particle Events of 2012 (2013, 6–12). This article reviews the placement of the detector on the MSL spacecraft which transported the rover to Mars, which resulted in a mixed shielding environment with densities that vary from  $<10\text{g/cm}^2$  to over  $80\text{g/cm}^2$ . This is similar to the varied shielding found on the ISS, but likely different from a transit module for Mars where the shield design would be more uniform throughout to better protect the crew. This shielding also means that the RAD instruments are measuring a mix of primary and secondary particle radiation as reviewed in Section A of this chapter. The measurements are taken with two types of detectors: a silicone detector and a plastic scintillator. The latter was chosen because it closely mimics the

composition of human tissue. The resulting measurements for the deep space transit from December 2011 to July 2012 are shown in Figure 6. Some gaps in the measurements exist when the detector was powered down to allow for other activity on the spacecraft. Of note are the numbered spikes in dose rate when five distinct SPEs were encountered—two in February 2012, two in March 2012, and one in May 2012. The calculated average for dose rate based on these data was roughly  $481 \pm 80 \mu\text{Gy/day}$  using the silicone detector, which is consistent with the  $461 \pm 92 \mu\text{Gy/day}$  measured with the plastic scintillator. For simplification, the pairs of events that happened within days of each other are treated as a single occurrence for further calculations in this section.

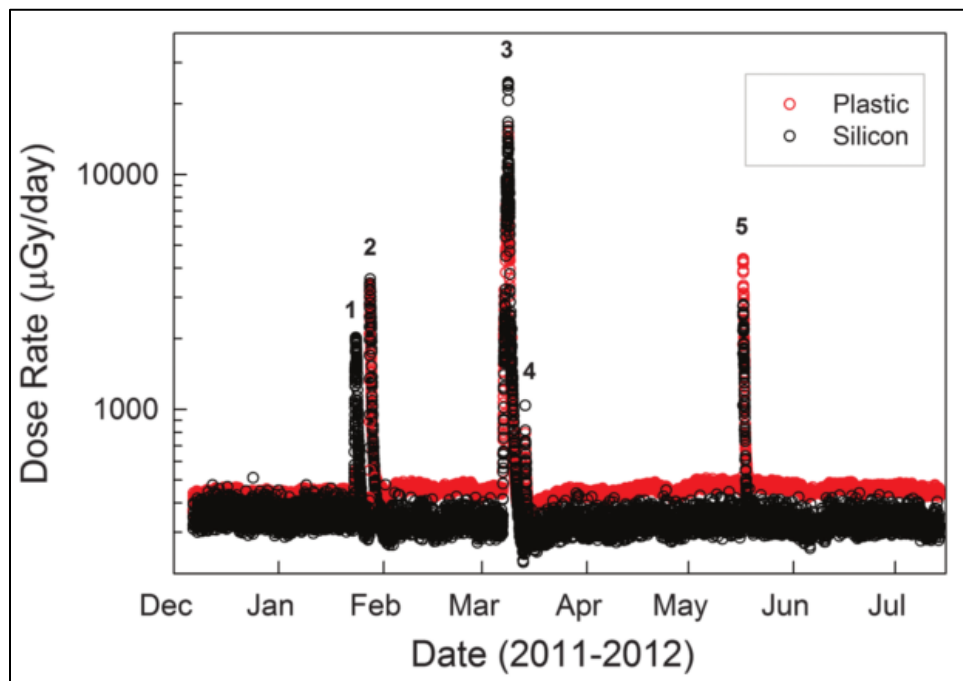


Figure 6. Dose Rate as Measured by the RAD in Deep Space. Source: Köhler et al. (2013).

The team writing this paper was also able to calculate the linear energy transfer (LET) in water of the GCR based on the silicone detector measurements recorded during the final month of the cruise (June–July 2012), during which no solar events occurred. For reference, LET is a measure of energy deposited by a particle radiation flux per unit



of distance. It is commonly used to calculate Quality Factors (a measure of the damage that a particle type/energy is capable of doing) and dose equivalents (a measure of the biological impact of the dose received in tissue), which are further defined in Chapter III of this paper. The result of these LET calculations was an average GCR Quality Factor of  $3.82 \pm 0.25$ , which resulted in an estimated dose equivalent of  $1.84 \pm 0.33 \text{mSv/day}$  (Köhler et al. 2013). For comparison, 2mSv is a dose equivalent roughly equivalent to that received from a single CT scan of the head.

For the Solar Particle Events encountered in space, these calculated dose equivalents also increased, with dose equivalents of 4.0, 19.5, and 1.2mSv measured for each of the three (simplified) events encountered, respectively. The event in March 2012 (which correlates to spikes 3 and 4 in Figure 6) is notable for the high dosage received which would amount to roughly 10 CT scans of the head in just three days' time! A comparison of the dose rates measured by the RAD plastic scintillator as compared to the GOES-11 space weather satellite in orbit around Earth is shown in Figure 7 here. In this figure, the data measured by GOES-11 around Earth is in grey, where the dose measured by the RAD is in black. This data helps us to better understand how Solar Events propagate through the inner heliosphere around the Sun. Köhler et al. note several key points (2013):

- First, that the peak for all events appears to reach the Earth before it does the RAD in transit to Mars.
- Next, that the March 2012 events appear to show the peak of the radiation arriving at RAD a full day after it arrives at Earth. Köhler et al. posit that this may be explained by a combination of differences in the energy sensitivity of the detectors on each spacecraft, and the fact that an early coronal mass ejection (CME) during this event may have distorted the field lines around the sun such that the RAD and GOES-11 were not actually located on the same magnetic propagation line as previously expected.
- The event in May 2012 (which correlates to spike 5 in Figure 6) is of particular interest because it was a “Ground Level” Event (GLE) at Earth—in which the spectrum for the event was particularly energetic or “hard” (meaning the particles encountered were of overall higher energy even though the overall dose for the event measured by RAD was lower). GLE’s are characterized when the spectrum is so energetic that it also

results in the formation of secondary neutron radiation that reaches measurable levels on the Earth's surface. This is further shown by the peak dosage which is higher for GOES than for RAD in Figure 7. The higher energy particles are still capable of doing more damage to biological tissue—which is proven by referring back to Figure 6 where for this SPE alone the red dots for the plastic scintillation detector showed higher (tissue equivalent) doses than those measured by the silicone detector.

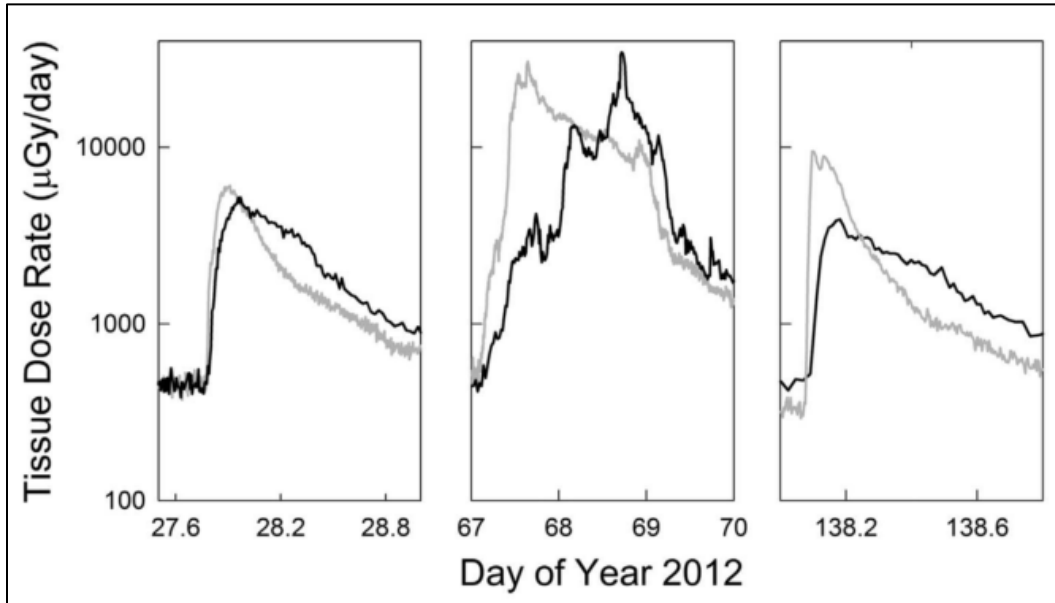


Figure 7. Dose Rate for Solar Particle Events as Compared by the RAD (Black Lines) versus the GOES-11 Satellite (Grey Lines).  
Source: Köhler et al. (2013).

Last, Köhler et al. were able to use the data collected in their study to estimate GCR dose predictions for crew on a Mars mission assuming a 180-day transit in each direction. For the cruise phases alone there and back, this dose estimate came to  $662 \pm 108$  mSv in total, not accounting for the variable spikes in dose rate that could also occur for a Solar Particle Event. Other exposure forecasts are discussed in detail in Chapter III Section F of this paper, but it is relevant to compare this dose estimate to those in Figure 24 in that chapter—where predicted rates with  $5\text{g/cm}^2$  shielding are generally lower than this amount at both solar minimum and solar maximum (approximately 580 mSv and 250 mSv annual estimates, respectively). Comparing this data to the exposure limits reviewed in Chapter III Section D Table 2, we can see that just the cruise phases of the model predicted here would have a high chance of exceeding the 0.6 Sv (600 mSv) career limit set forth for 30-year old, never-smoking females, and would utilize a majority percentage of the career dose limits set forth for males and females of any age. Finally, it is important to note that the data observed by RAD occurred during a weaker than average solar maximum cycle. Unfortunately this also means that crew on a Mars journey could also encounter SPEs with higher event exposures than those described here.

## **2. Curiosity Rover Surface Measurements**

Hassler et al. also published a paper detailing the surface measurements collected by the RAD instruments on the Martian surface from 2012–2013 (2013). During this time the team was also fortunate to observe one hard Solar Particle Event, albeit a weaker one. They also observed several “soft” events, meaning they were not energetic enough to penetrate the Martian atmosphere. During these soft events a decrease in surface dose rate was observed because the lower-energy coronal mass ejections (CMEs) from the sun actually helped to attenuate some of the incoming GCR instead. This phenomenon is known as a “Forbush decrease” and can be seen on Sols 50, 97, 208, and 259 in Figure 8. Also notable in this figure is the hard SPE that was observed on Sol 242.

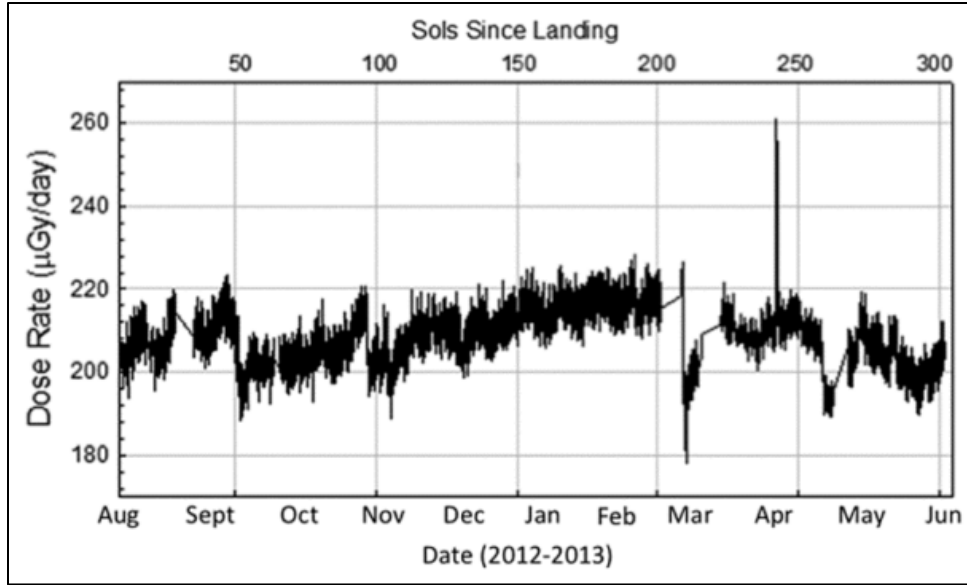


Figure 8. RAD Dose Rate Measurements on Martian Surface. Source: Hassler et al. (2013, 8).

The study team also found a correlation between Martian atmospheric pressure (which would impact atmospheric density over the rover), and dose rate, as shown in this sampling of data in Figure 9. The data reveals that measured dose rates at the rover were lower when atmospheric pressure was higher which in turn caused the denser atmosphere over the rover to attenuate more radiation (Hassler et al. 2013, 8).

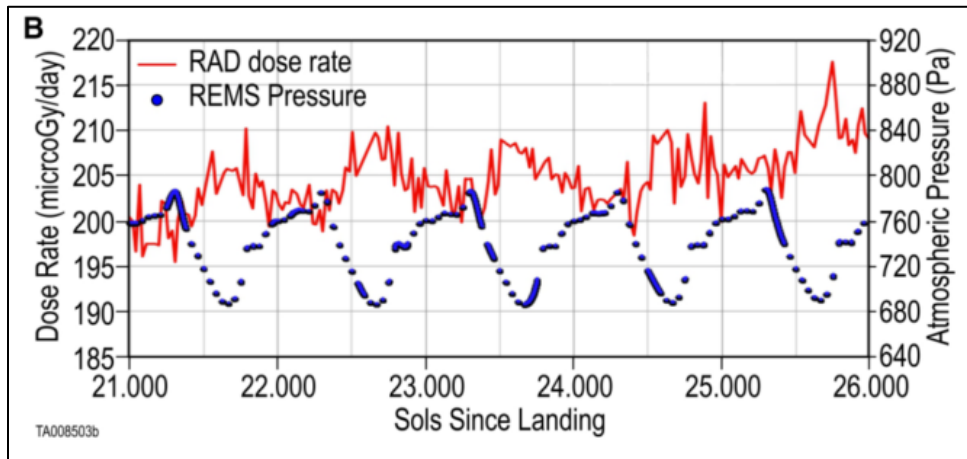


Figure 9. RAD Dose Rate versus Atmospheric Pressure on Martian Surface. Source: Hassler et al. (2013, 8).

The Solar Particle Event observed in April of 2013 also provided a unique comparison to measurements of the same event that were collected at the STEREO observatory in orbit around the sun (which was magnetically aligned with Mars at the time, located at approximately the same Heliospheric longitude), and the GOES-13 satellite in Earth orbit (which was 180 degrees from Mars in Heliospheric longitude at the time). Figure 10 shows this comparison. The following observations from this solar flare can be noted in this chart (Hassler et al. 2013, 3):

- First, plot A shows that the SPE caused an increase in dose rate on the Martian surface of roughly 30% as observed by RAD. It is important to consider that it takes a proton energy of roughly 150MeV to actually reach the surface at Gale Crater where the lander was located.
- Plot B shows that the STEREO-B telescope which was slightly leading Mars orbit saw an increase of nearly four orders of magnitude for this flare, though again one must consider that much of this flux was not energetic enough to reach the Martian surface. Different energy levels of protons as measured by the satellite are depicted in green (for <40MeV), blue (40–60MeV), and red (60–100MeV).
- Plot C shows that the GOES-13 satellite only saw an increase of two orders of magnitude of proton flux, which is consistent with the fact that it was essentially on the opposite side of the sun from this flare at the time.
- While not plotted, the team also noted another interesting observation about the propagation of this flare. The STEREO-A telescope was lagging behind Martian orbit at the time. The flare had a propagation of well over 180 degrees in Heliospheric longitude—which caused the increased measurements seen at STEREO-B and to a lesser extent GOES-13. However, the STEREO-A did *not* see an increase in proton flux from this flare, which shows the limits of propagation more clearly.

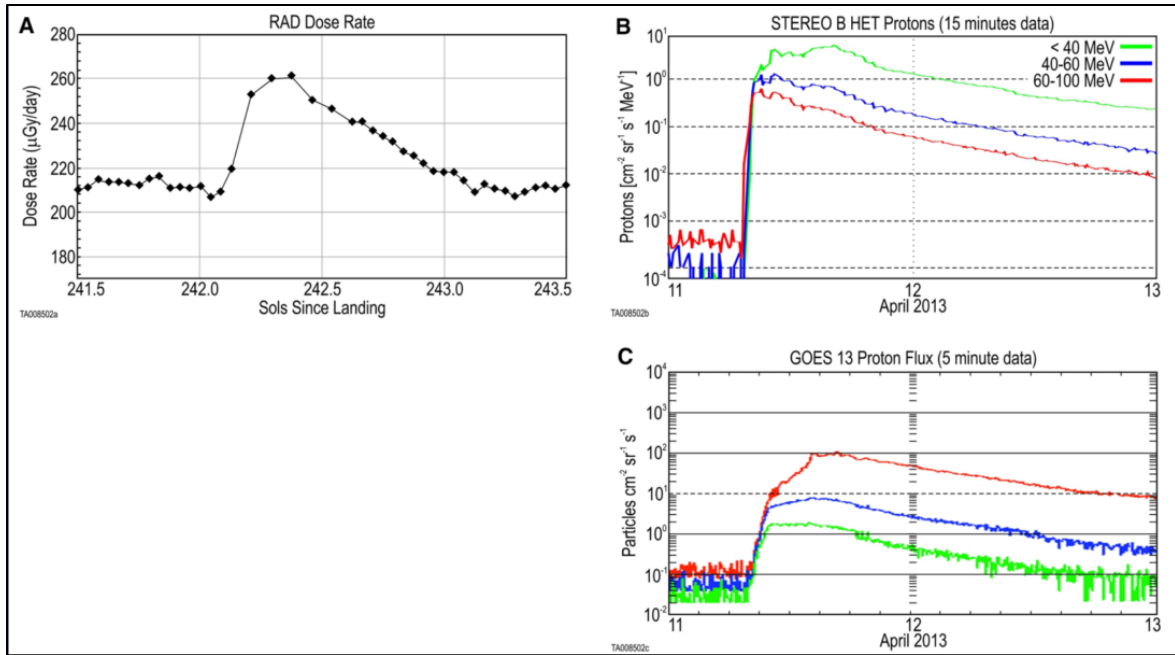
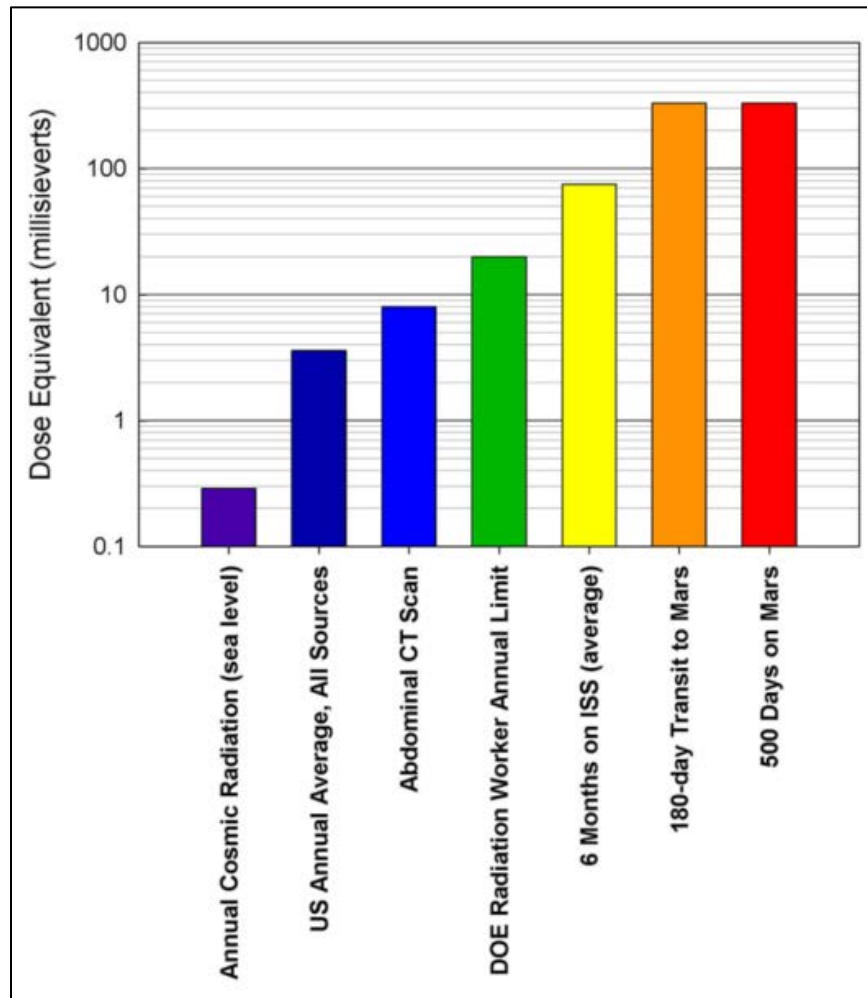


Figure 10. April 2014 SPE as Compared by Various Instruments. Source: Hassler et al. (2013, 10).

Finally, Hassler’s team was able to calculate some helpful/improved comparisons in dose rates and total doses received, as shown in Figures 11–14 here. Figure 11 shows a quick reference in total equivalent doses that would have been received based on RAD calculations for both a Mars transit, and 500-day surface stay as compared to other Earth and ISS based bench-marks in dose levels (for review, dose equivalent is the dose rate multiplied by the Quality Factor for the particle type, which is discussed further in Chapter III Section B).



Note: dose equivalent is providing using a log scale on the vertical axis of this plot.

Figure 11. Comparison of Radiation Dose Equivalents. Source: Hassler et al. (2013, 9).

Figure 12 shows a comparison of particle fluxes encountered, dose rates, Quality Factors, dose equivalent rates, and anticipated human mission dose equivalent totals as compared based on the MSL cruise data and surface data. This data represents the measurements collected for *GCR exposure only*.

<b>RAD Measurement</b>	<b>Mars Surface</b>	<b>MSL Cruise</b>	<b>Units</b>
Charged Particle Flux (A * B)	0.64 ± 0.06	1.43 ± 0.03	cm <sup>-2</sup> s <sup>-1</sup> sr <sup>-1</sup>
Fluence Rate (B)	1.84 ± 0.34	3.87 ± 0.34	cm <sup>-2</sup> s <sup>-1</sup>
Dose Rate (Tissue-like) (E detector)	0.21 ± 0.04	0.48 ± 0.08	mGy/day
Avg. Quality Factor <Q>	3.05 ± 0.26	3.82 ± 0.30	(dimensionless)
Dose Equivalent Rate	0.64 ± 0.12	1.84 ± 0.30	mSv/day
Total Mission Dose Equivalent (NASA Design Reference Mission, DRM)	320 ± 50 (500 days)	662 ± 108 (2x180 days)	mSv

Figure 12. Radiation Environment Measured by MSL/Rover for GCR Only.  
Source: Hassler et al. (2013, 11).



Figure 13 shows a further comparison of GCR and SPEs (here labeled SEP for solar energetic particle) with regard to measured dose rates (GCR) or event-wide doses (SEPs) on both the MSL cruise and the Mars surface. Note that the GCR dose rates on the surface are lower as would be expected, but the SEP doses on the surface are likely artificially low due to the limitations of the data (one weak M Class Flare only) that were measured by the RAD instrument while on the Martian surface.

	<b>GCR Dose Rate (mGy/day)</b>	<b>GCR Dose Equiv. Rate (mSv/day)</b>	<b>SEP Dose (mGy/event)</b>	<b>SEP Dose Equivalent (mSv/event)</b>
MSL Cruise (Zeitlin <i>et al.</i> 2013) (22)	0.464	1.84	1.2-19.5 <sup>a</sup>	1.2-19.5
Mars Surface	0.210	0.64	0.025 <sup>b</sup>	0.025

Figure 13. Radiation Environment Measured by MSL/Rover for GCR Only.  
Source: Hassler et al. (2013, 11).

Perhaps most interesting, Figure 14 shows how the study team was able to approximate anticipated GCR dose rates as a function of depth below the surface, based on the RAD measurements on the Martian surface and a transfer model to estimate the results of shielding beneath Martian regolith. This model makes a strong case for the benefits of using the Martian surface to help reduce overall dose equivalent rate—especially if the regolith can be built up around habitats (or caves can be located) at depths of 2–3m or more.

<b>Depth below Surface</b>	<b>Effective Shield- ing mass (g/cm<sup>2</sup>)</b>	<b>GCR Dose Rate (mGy/yr)</b>	<b>GCR Dose Equiv. Rate (mSv/yr)</b>
Mars Surface (RAD)	0	76	232
-10 cm	28	96	295
-1 m	280	36.4	81
-2 m	560	8.7	15
-3 m	840	1.8	2.9

Figure 14. Radiation Environment Measured by MSL/Rover for GCR Only.  
Source: Hassler et al. (2013, 11).

All of these improvements in Mars transit and surface exposure data will be used in conjunction with the shielding discussion from Chapter V to conduct analytical calculations in Chapter VII.

#### **D. TRAPPED RADIATION**

According to the NASA Space Radiation Analysis Group website, trapped radiation occurs when the Earth's magnetic field traps protons and electrons within the belts extending 10–12 Earth radii from our planet (2016). This includes a region where the trapped protons extend down into typical mission orbit altitudes known as the South Atlantic Anomaly (SAA). While not one of the two dominant radiation types encountered by spacecraft in deep space, trapped radiation must be accounted for on any space mission because astronauts on deep space missions will still receive exposure to it while in Earth orbit, and while conducting maneuvers to leave Earth orbit for deep space. Dose rate assumptions for astronauts in a typical Earth orbit with 28.5 degrees inclination are shown in Figure 15, where flight altitude is compared in nautical miles to the minimum and maximum observed absorbed dose rates for various shuttle mission numbers at both solar minimum and maximum. While these missions are somewhat dated, the variety of altitudes covered provides valuable insight on the minimum and maximum radiation doses measured. Overall this figure shows that trapped radiation dose as a result of the SAA will increase with orbit altitude at any point above 150nm when the spacecraft is passing through this region.

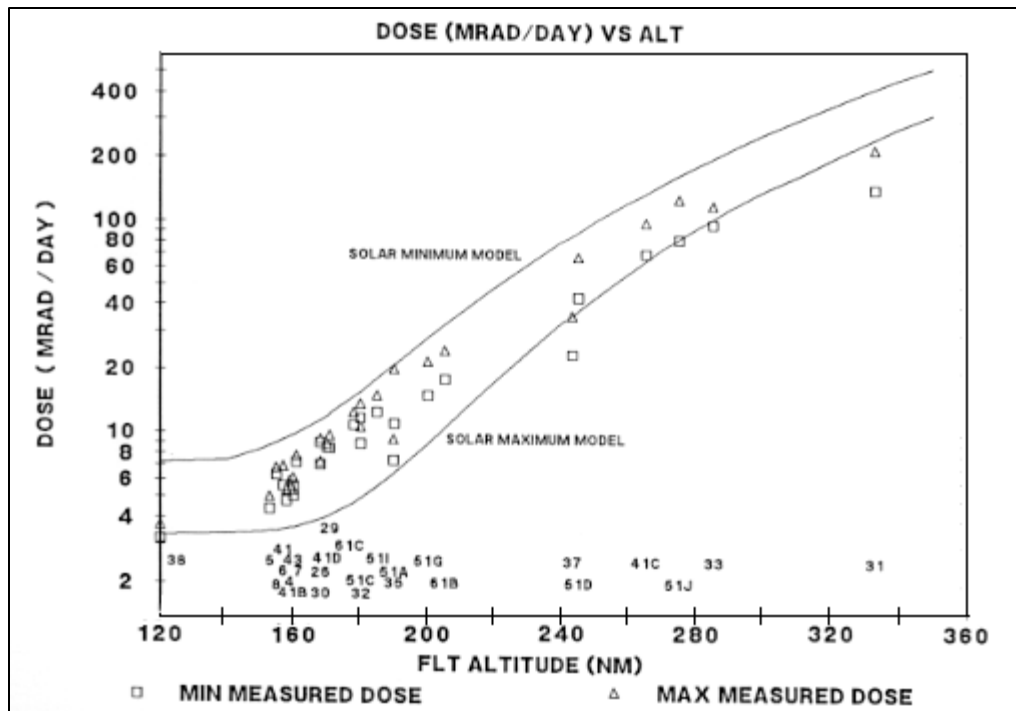


Figure 15. Anticipated Dose Rates for Astronauts in 28.5-Degree Incline Earth Orbit Flights. Source: NASA Space Radiation Analysis Group (2016).

Noteworthy is that the significance of trapped radiation exposure may vary depending on the mission architecture ultimately chosen. According to the “Human Exploration of Mars Design Reference Architecture 5.0 Addendum,” the required Low Earth Orbit (LEO) inclinations for optimal two-phase burn initiation trajectories to Mars range from 28.5 to 50.2 degrees (Drake 2009, 137). The overall dose received would be multiplied when one accounts for any additional days spent in LEO to dock/assemble or otherwise prepare the transit spacecraft for its journey to Mars. Trapped radiation exposure will increase at higher LEO altitudes. Additionally, if one assumes that a typical mission architecture will include an LEO altitude that passes through the SAA, at higher orbit inclinations overall dose rates will actually be lower in spite of the spacecraft passing through the higher flux region of the anomaly, because the time spent in this region will be lower than that spent at a more typical 28.5-degree orbit (NASA Space Radiation Analysis Group 2016).

With the focus of this paper being missions to Mars, the model for such a mission is also simplified because Mars is one of the planets that has no magnetic field. With no magnetic field, the planet is not able to trap charged particles (Wetegrove 2014). Overall, trapped radiation will have a minimal impact on Mars missions when compared to the scale of exposure received from Galactic Cosmic Radiation and Solar Particle Events over hundreds of days in deep space. As such, it is not specifically called out in any calculations or comparisons for the rest of this document.

Now that GCRs and SPEs are understood, the next topic to review is the biological impact of radiation exposure that astronauts will receive. This information is discussed in Chapter III.

### **III. BIOLOGICAL EFFECTS OF DEEP SPACE RADIATION**

Next, we discuss the impacts of the types of radiation encountered on deep space missions on astronauts. Each radiation type has different mechanisms by which it interacts with human tissue. Exposure to different particle types increases the probability of different cancers or organ abnormalities in the long term following low-level exposure; with the added possibility of acute symptoms immediately following high level exposures. This paper reviews how these impacts have been assessed by various organizations to establish the limits for current human space missions, and as the basis for limits that will need to be established in order to support interplanetary missions in the future.

#### **A. TYPES OF RADIATION**

According to Epelman and Hamilton’s article “Medical Mitigation Strategies for Acute Radiation Exposure during Spaceflight,” radiation has two effects on tissue (2006). Excitation is an effect whereby electrons are elevated in their valence level within an atom—raising energy state but still remaining in the atom. Another label for this type of radiation is non-ionizing radiation. Non-ionizing radiation can be damaging as evidenced by phenomena such as UV ray exposure causing skin cancer, and by the acute damage such as burns that can result from exposure to UV or microwave radiation. However—this paper focuses on the effects that result from exposure to GCR and SPE radiation, which fall under the category of ionizing radiation.

Ionization is an effect where electrons are excited to the point of being released from that atom—thus changing its structure into that of an ion with a positive charge versus that of an atom with a neutral charge (Epelman and Hamilton 2006, 130). Ionizing radiation can be broken down into two categories: electromagnetic and particulate.

##### **1. Electromagnetic Radiation**

Electromagnetic radiation consists of photons that are oscillating at different wavelengths/frequencies, which move at the speed of light. The types of electromagnetic

radiation that are energetic enough to ionize human tissue include Ultraviolet Rays, X-Rays, and Gamma Rays (Epelman and Hamilton 2006, 130–131). While it merits mention, electromagnetic radiation does not pose the same hazards to astronauts on a mission to Mars as the particulate radiation discussed in greater detail this chapter, and it is not included in calculations for this paper.

## **2. Particulate Radiation**

Particulate radiation consists of various atomic particle types that are generated either as a primary source (example: Galactic Cosmic radiation), or via secondary interaction which is the result of radiation interaction with nearby shielding or biological matter. Examples of particulate radiation include alpha particles, beta particles (released electrons, encountered mostly in planetary magnetic fields), protons, and neutrons. As reviewed in Chapter II, the chief particulate radiation encountered in deep space comes from GCR, in a mixture of protons, alpha particles, and a small percentage of other heavy ions (Epelman and Hamilton 2006, 130). Significant neutron flux is also generated as a result of the secondary interaction of GCR with spacecraft materials, which causes them to release neutrons and other particles which are energetic enough to damage biological tissue.

## **3. Expansion on Solar Particle Events**

Beyond the background particulate radiation flux discussed for GCR, the two types of ionization radiation discussed here are encountered in succession during significant Solar Particle Events (SPEs). According to Epelman and Hamilton's 2006 article, during large flares or coronal mass ejections, photons from the event travel eight times faster than any particulate radiation released—thus the photon radiation would be encountered by a deep space spacecraft in minutes. This wave of electromagnetic radiation can also signify the strength of the particulate radiation that is yet to come. In worst case scenarios—this particulate increase has yielded increased flux levels on the order of three to five orders of magnitude higher. These rare scenarios could lead to lethal doses of radiation for deep space crew with only nominal shielding in a matter of hours (Epelman and Hamilton 2006, 131). Fortunately, due to scattering processes as the

particulate radiation moves away from the sun, this typically spreads the exposure increase out over one to two days’ timeframe—and allows us to treat that radiation as isotropic versus directional in nature for shielding or shelter designs.

## **B. MEASUREMENT OF RADIATION**

Radiation exposure is measured in units known as Gray (Gy), where one Gray is defined as the absorption and ionization/excitation of one joule of energy per kilogram of tissue (Epelman and Hamilton 2006, 131). Grays are next converted to Sieverts once a “Quality Factor” of the radiation dose received is considered, resulting in a net “equivalent dose.” These factors are dictated by the level of biological damage or impact that can occur once a radiation or particulate type is absorbed within biological tissue. This distinction is important because certain types of radiation (alpha particles for example) are large enough that the particles are easily stopped by barriers such as skin or clothing—but concurrently due to their size they have the potential to cause damage if absorbed into the tissue via other means (ingestion, inhalation). The mechanisms of the damage caused by absorbed ionizing radiation are discussed in Chapter III. A table of Quality Factors for different radiation types from the Nuclear Regulatory Commission (NRC) website may be found in Table 1 (2016).

Table 1. Radiation Quality Factors. Adapted from United States Nuclear Regulatory Commission (2016).

<b>Type of radiation</b>	<b>Quality Factor (Q)</b>	<b>Absorbed dose equal to a unit dose equivalent</b>
X-ray, gamma, or beta radiation	1	1
Alpha particles, multiple-charged particles, fission fragments and heavy particles of unknown charge	20	0.05
Neutrons of unknown energy	10	0.1
High-energy protons	10	0.1

The same website has an excellent breakdown of the more detailed calculation that must be made to determine the equivalent dose for neutron flux based on energy level. A Quality Factor of 10 is a good approximation, but the actual range is anywhere between two and 11.

A final distinction to make is that of unit conversion. Sieverts are an international standard for equivalent dose, but in many U.S.-based dosimetry programs units of Rem (which distinguish equivalent dose or Roentgen Equivalent Man dose) are used. For ease of reference in this document, one Sievert is equivalent to 100 Rem; and one mSv is equivalent to 100mrem.

### **C. BIOLOGICAL IMPACT MECHANISMS**

Biological impact mechanisms of radiation exposure may be described in two categories. First, there is the process by which the dose received impacts cells which can develop into cancers of various organs within the body. Next, radiation exposure can also cause a variety of acute and long-term *non-cancerous* biological effects. These topics are addressed in this section.

#### **1. Mechanisms of Cancer from Radiation Exposure**

Epelman and Hamilton's article neatly summarizes the most common mechanisms by which radiation can impact tissue. First, it can break double strands of DNA and impact cell proliferation, which is especially apparent in tissues such as bone marrow and the lining of the gastro-intestinal organs where cells normally need to see a higher rate of turnover for effective function. Radiation exposure can cause lasting chromosomal alterations in the types of white blood cells that support the human immune system (i.e., lymphocytes)—an effect that has already been validated through its use to verify radiation absorption on long-duration space missions. Finally, radiation can interact with water molecules throughout the tissues of the body, which may result in the generation of free radicals of oxygen (free radicals being atoms that have unpaired valence electrons and are therefore highly reactive). These free radicals may in turn cause subsequent damage to surrounding tissues, and cell death through prolonged exposure (Epelman and Hamilton 2006, 131).



The article “Concepts and challenges in cancer risk prediction for the space radiation environment” reviews many of the challenges in modeling human carcinogenesis predictions in deep space, starting with a discussion of the short-comings of studies in rodents which are helpful but ultimately not infallible due to the fact that rodent tumors are not human tumors (Barcellos-Hoff et al. 2015).

A further challenge in modeling these mechanisms arises because even current cell-culture research underway (detailed below) to model GCR ion impacts on biological tissue is reliant on means to condense such a study to reproduce the possible effects of a three-year mission to a much shorter time period. Thus, higher fluxes are used to simulate prolonged exposure totals. Unfortunately, due to the stages by which cells undergo changes during carcinogenesis (which themselves are not perfectly understood)—such simulations may not be accurate (Barcellos-Hoff et al. 2015, 98). The article goes on to review some of the details that have recently been discovered in this progression whereby cell structures are neo-plastically altered, or DNA is damaged. In the first stage, “Initiation,” occurs when the cell genome develops the “growth potential” that gives it the ability to change. While this stage is thought to be irreversible, the cell’s new potential to change is not actually realized unless the second stage of carcinogenesis, “Promotion,” actually occurs. Promotion then serves as the rate limiting factor in cancer progression as corrupted groups of cells begin to self-replicate, and each population battles the host body which attempts to restore normalcy. If the host body wins, then malignancy is not achieved. If one corrupted cell population breaks through this “extinction barrier” however, then the chances of tumor growth/spread/malignancy greatly increase as the remaining grouping allows less fit cloned cancer cells to be wiped out while concurrently refining the resilience of the population that continues to grow. This phenomenon is known as “Emergence” (Barcellos-Hoff et al. 2015, 98–99).

In reviewing the best attempts to simulate space level exposures for various types of radiation in mice: when exposed to low-linear energy transfer (LET) gamma radiation at three increasing exposure levels, mice showed no increase in tumor incidence for the low and mid-range levels (0.05 mGy/d and 1.1 mGy/d where mGy are milligray per day), but that they did show increases for several tumor types at levels of 21 mGy/d (Barcellos-

Hoff et al. 2015, 100). For review on radiation units, mGy are international units of radiation exposure—which would be converted to radiation dose according to the Quality Factor associated with the energy level of the gamma radiation used (referring to Section B of this chapter, gamma radiation Quality Factor is typically one). According to the same article, when mice were exposed to high-LET neutron radiation at rates 10-fold higher than those encountered in deep space, effects varied by tumor type in the range of tumors being “spared” to tumors occurring at rates comparable to those anticipated for acute exposure. Similar results were observed in fractionized doses of HZE (GCR Heavy Ion) radiation. Overall, the inconsistency of these results again highlights the challenges in reducing uncertainty in models.

## **2. Non-cancerous Impacts from Radiation Exposure**

NASA uses the National Council on Radiation Protection & Measurements (NCRP) publications as a basis for its radiation protocols and exposure limits for space workers. The most recent publication (NCRP Commentary #23) reviews the non-cancer basis for NASA organ-based exposure limits. These topics are summarized here for cross-referencing with the organ based limits that are covered in Tables 3–4 in the next section of this chapter (NCRP 2014, 27–36):

- Central nervous system (CNS) dysfunction and disease—radiation dosage to the CNS can result in a myriad of symptoms ranging from short-term behavioral abnormalities or degraded mental capacity which could potentially compromise a mission to Mars, to long term neurodegenerative diseases that could impact astronauts after they return home.
- Cardiovascular disease—a combination of atomic bomb survivor and animal studies have provided evidence to suggest that even low levels of low-LET radiation dosage may have an impact on the probability of cardiovascular disease. There is limited direct evidence of radiation-induced cardiovascular damage to support this. Research in the form of epidemiological and other studies is still underway to determine whether there is a causal relationship between low-level exposures and cardiovascular abnormalities, and if so what the biological mechanisms and dose-response relationships are.
- Cataracts—exposure limits for the lens of the eye are specified due to the well-documented evidence that space radiation exposure can cause both cataracts and opacities, and especially due to recent research that has

suggested cataracts could be caused by much lower exposure levels than previously estimated.

#### **D. REVIEW AND BASIS OF EXISTING EXPOSURE LIMITS**

According to the “NASA Space Radiation Analysis Group” website (2016), astronauts are classified as Radiation Workers and are required by Presidential Executive Order to comply with OSHA regulations concerning radiation exposure. However, given OSHA has no space-specific limits for exposure, and terrestrial limits have been deemed to be too restrictive for reasonable mission scopes and durations; alternate limits have been adopted per 29 CFR 1960.18 based on the following six requirements:

(1) that its use applies to a limited population, (2) maintenance of detailed flight crew exposure records, (3) pre-flight hazard assessment/appraisal, (4) planned exposures be kept as low as reasonably achievable (ALARA), (5) maintenance of operational procedures and flight rules to minimize the chance of excessive exposure and (6) man-made onboard radiation exposure complies with 29 CFR 1910.96 except where the NASA mission/objectives cannot be accomplished otherwise. (NASA Space Radiation Analysis Group 2016).

These alternate limits were calculated based on the study of terrestrial radiation exposure risks, and with a goal to limit the change in space worker life-time cancer likelihood to only an additional 3% REID (i.e., risk of exposure induced death), within a confidence of 95%. The study data used to calculate these limits were based on research conducted by the National Council of Radiation Protection and Measurements (NCRP), and the resulting limits were vetted by the Nuclear Regulatory Commission (NRC) for approval (Cucinotta 2015, 2).

The most recent calculation of the career space worker permissible exposure limits (PELs) is published in the 2015 *NASA Space Flight Human-System Standard—Volume 1A*; and is shown in Table 2 here. These limits are calculated assuming one-year mission length, and most importantly assume that the space worker has no prior radiation exposure (otherwise, prior exposure must be considered with limits for that astronaut adjusted which may impact mission crew selection or designation for activities that will increase exposure like extravehicular activities or EVAs). Table 2 shows the effective dose limits for workers of various ages, genders, and with comparison to either average

American cancer risks or to that of never-smokers (Williams 2015, 76). For comparison, this 0.1Sv converts to 100mSv or 10Rem of effective dose, which is roughly equivalent to receiving approximately 50 CT Scans of the head in the same period of time.

Table 2. Career Effective Dose Limits. Source: Williams (2015).

Age (yr)	Females		Males	
	Avg. US Adult Population	Never-Smokers	Avg. US Adult Population	Never-Smokers
30	0.44 Sv	0.6 Sv	0.63 Sv	0.78 Sv
40	0.48	0.70	0.70	0.88
50	0.54	0.82	0.77	1.00
60	0.64	0.98	0.90	1.17

The NASA standards also define organ-specific exposure limits with the purpose of mitigating a combination of short term acute effects, and other long term non-cancer impacts. Tables 3 and 4 summarize these limits, with the following notes (Williams 2015, 22).

Table 3. Organ-Specific Exposure Limits for Space Workers. Source: Williams (2015).

Organ	30-day limit	1-Year Limit	Career
Lens*	1,000 mGy-Eq	2,000 mGy-Eq	4,000 mGy-Eq
Skin	1,500	3,000	6,000
BFO	250	500	Not applicable
Circulatory System**	250	500	1000
CNS***	500 mGy	1,000 mGy	1,500 mGy
CNS*** (Z>10)	-	100 mGy	250 mGy

Table 4. Relative Biological Effectiveness Assumptions for Non-cancer Effects. Source: Williams (2015).

<b>Radiation Type</b>	<b>Recommended RBE<sup>b</sup></b>	<b>Range</b>
1 to 5 MeV neutrons	6.0	(4-8)
5 to 50 MeV neutrons	3.5	(2-5)
Heavy ions	2.5 <sup>c</sup>	(1-4)
Proton > 2 MeV	1.5	-

- The limits for the lens of the eye are established to prevent early (<5yr from exposure) severe cataracts, which may be caused by a severe SPE. It is important to distinguish these from less severe cataracts that may be caused by GCR. While these cataracts may progress to a severe state over a longer period of time (>5yrs), they are deemed an acceptable risk to the program.
- Circulatory system doses are calculated as an average over the heart muscle and adjacent arteries, with limits intended to minimize the risk of longer term cardiovascular disease or abnormalities.
- The central nervous system (CNS) limits are calculated at the hippocampus which controls the nervous system from the base of the brain, and are meant to mitigate both acute and long term nervous system abnormalities.
- For review, blood forming organs (BFO) are those responsible for generating white blood cells (lymphocytes) and red blood cells which help to support the body's circulatory and immune systems, and therefore all other organs.
- Table 4 shows relative biological effectiveness (RBE) assumptions which is a term similar to Quality Factor which expresses the amount of damage that a type of radiation particle is capable of doing to a unit of tissue per unit of radiation absorbed (exposure)
- The units in Table 3 are distinguished as milligray equivalent in cases where the RBE for organ types versus non-cancer impacts is relatively well-known.
- However, the central nervous system (CNS) values are expressed as mGy due to the fact that the RBE for CNS non-cancer effects is largely unknown. In this case, an additional exposure limit is noted for particles with a charge (Z)>10.

- In Table 3 the superscripted notes <sup>b</sup> and <sup>c</sup> are expressed in the NASA standard as cases where the understanding of that RBE is also limited due to the fact that data for neutrons at certain energy levels (<1MeV, >25MeV) are not well documented, and the fact that insufficient data exists to conclusively document tissue effects for heavy ions with a  $Z>18$ .

## **E. DOSIMETRY REVIEW AND RESEARCH IMPROVEMENTS**

The NASA Space Radiation Analysis Group website (2016) also highlights the fact that recent re-assessment of nuclear bomb survivor cancer prognoses has necessitated further research into the detailed biological impacts of radiation exposure, in parallel with other improvements that need to be made for passive and active dosimetry. The summary of these efforts may be seen in Figure 16. A review of selected dosimetry improvements and research efforts to improve dose estimates is conducted in sub-sections 1 and 2 of this Section (E) of Chapter III. Radiobiological research is discussed at greater length in Chapter VI of this paper, and shielding optimization is discussed both in Chapters V and VII.

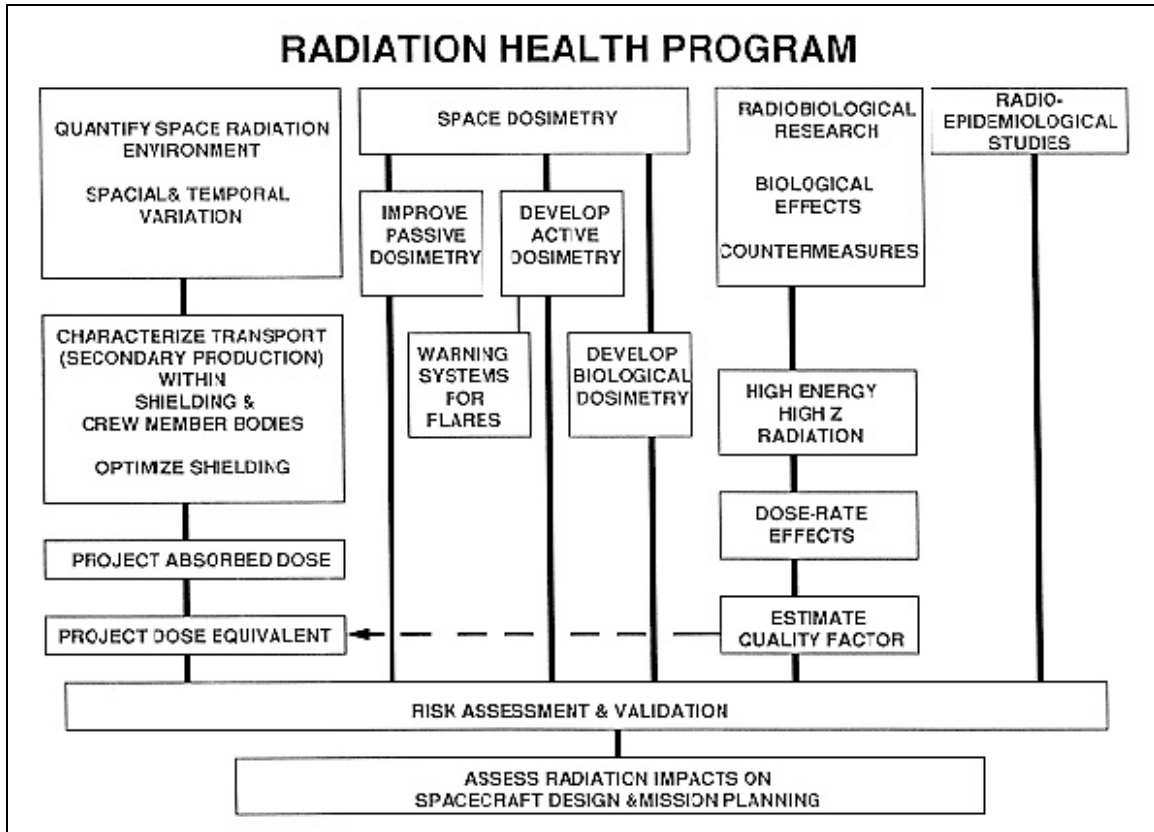


Figure 16. Areas of Investigation within the Radiation Health Program. Source: NASA Space Radiation Analysis Group (2016).

### 1. Dosimetry Review and Improvements

Many advanced passive and active radiation monitors have been developed for use on various space stations, aircraft, and probes to Mars. Passive dosimetry for astronauts on the ISS currently falls under two categories. Personal devices are worn by each crew member to estimate exposure for that individual, and various devices are mounted around the station to help assess the dose distribution based on location within the station (NASA Space Radiation Analysis Group 2016).

One active monitor currently in use is the Tissue Equivalent Proportional Counter (TEPC). This device provides advanced exposure monitoring by measuring the linear energy transfer (LET) as it impacts a small simulated volume of tissue; then combining that measurement with information from other detectors to estimate the Quality Factor of

the exposure received. This detector requires adaptation to adequately estimate the impact of GCR exposure to crews on deep space missions (NASA Space Radiation Analysis Group 2016).

The Charged Particle Directional Spectrometer (CPDS) measures the flux of all trapped, GCR, and secondary particle radiation as a function of time, charge, energy, and direction (NASA Space Radiation Analysis Group 2016). There are both internal and external versions of this instrument in use. Internal devices may be moved to various nodes/modules internal to a spacecraft, while an external detector is used as an assessor for the space radiation environment outside the craft and as a control for the internal instruments.

The newest active dosimeter currently under testing onboard the ISS is the European Crew Personal Active Dosimeter (EuCPAD). This device consists of both a wearable unit and a charging/data transfer station. The data transfer capability will permit astronauts to track radiation exposure daily—and to correlate which locations in a given station/habitat lead to higher levels of types of exposure (Space Daily 2016).

## **2. Research on Dose Estimate Improvements**

Further research is being conducted at Johnson Space Center to determine the specific effects of high-LET radiation (as seen from GCR in deep space) on tissue samples being exposed to various proton/heavy particle accelerators. This research aims to serve as the foundation for the development of biological dosimeters which will provide a much more accurate estimate of the equivalent dose received by crew on deep space missions versus the current systems where biological equivalent is estimated by use of a physical shielding material (NASA Space Radiation Analysis Group 2016).

Other research aims to improve on existing models which use only the concept of Radiological Biological Effectiveness (RBE) to compare initial dose rate slopes for other particle types as compared to gamma radiation, which is then used to develop the Quality Factor (QF) for that type of particle. For review, gamma radiation consists of extremely high energy photons that have resulted from the radioactive decay of other particles. While vastly different from the decayed nuclei/particles that comprise GCR, they are still



used as a baseline value with which the Quality Factors of other radiation particle types are compared.

These existing models (built around a basic comparison to gammas which have a QF of one) do not account for the variability of effects imparted by low linear energy transfer (LET) radiation, and high LET radiation, and the fact that radiation exposure in deep space is a complex mixture of these two (F. A. Cucinotta 2015, 2). In general, dose rate factors do not need to be weighted for high-LET radiation exposure, but for low-LET radiation a dose and dose rate effectiveness factor (DDREF) must be used to correct for the lesser effects that low-dose rate radiation at that energy level impart. This most recent Cucinotta article successfully develops a model to interpolate the QF value between these high-LET (no modification i.e., “max” RBE) and low-LET (DDREF modified i.e., “acute” RBE) cases. The end result of this model has reduced the upper limit of 95% confidence intervals for expected exposure rates by roughly 50% of what it was using the previous simplified RBE-based models (Cucinotta 2015, 3).

A resulting comparison of calculated Quality Factors for selected particle types (protons, alpha, and Carbon/Silicone/Iron ions) versus particle energy level is shown in Figure 17. Note the lower overall Quality Factors calculated once the alternate (“acute”) RBE model is employed.

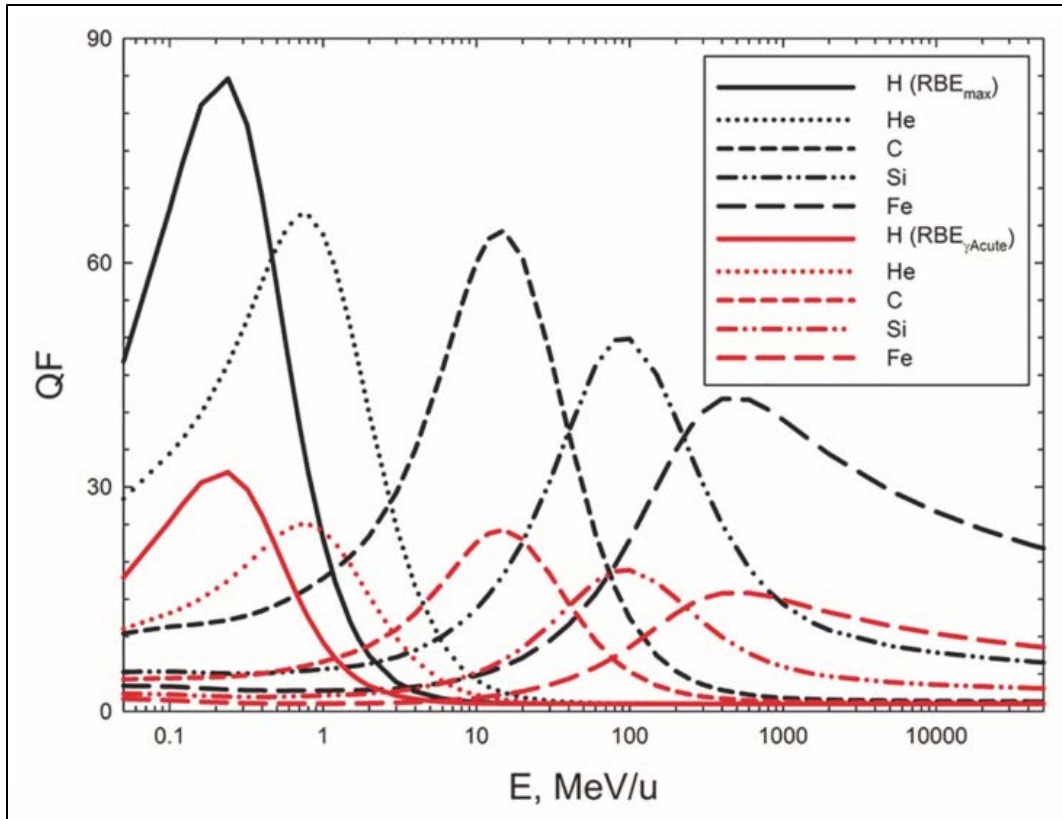


Figure 17. Comparison of Quality Factors Using Both Traditional and “Acute” RBE Models. Source: Cucinotta (2015, 4).

Cucinotta’s study takes this research one step further by developing new models that predict REID based on the adjusted Quality Factors for a one-year deep space mission for both men and women. Figure 18 draws the contrast between the results yielding by using Quality Factors developed by:

- the 2012 Nasa Space Cancer Risk (NSCR) Study
- the RBE “max” assumptions reviewed at the top of this section
- the “acute” RBE alternate model for Quality Factor developed in the 2015 study
- a further adjustment made to the ‘acute’ model by accounting for additional research that demonstrates increased tumor lethality in studies where mice were exposed to highly ionized (high-LET) HZE particles, as opposed to the less lethal tumors induced by low-LET exposure (Cucinotta 2015, 7–11).

Model	%REID	90% CI	95% CI
<b>Male Never-Smokers</b>			
NSCR*-2012	1.54	[0.57, 4.45]	[0.47, 5.85]
RBE <sub>max</sub>	2.05	[0.56, 5.68]	[0.47, 7.58]
RBE <sub>γAcute</sub>	1.2	[0.46, 2.87]	[0.39, 3.76]
RBE <sub>γAcute</sub> with increased high LET** tumor lethality	1.43	[0.62, 5.03]	[0.52, 6.59]
<b>Female Never-Smokers</b>			
NSCR-2012	2.04	[0.64, 6.05]	[0.47, 7.86]
RBE <sub>max</sub>	2.75	[0.64, 7.68]	[0.47, 9.95]
RBE <sub>γAcute</sub>	1.55	[0.51, 3.81]	[0.38, 4.99]
RBE <sub>γAcute</sub> with increased high LET tumor lethality	1.89	[0.72, 6.9]	[0.52, 9.0]

Predictions of different models for %REID, and 90% or 95% confidence intervals (CI) for 45-y old male and female never-smokers on a 1-year space mission using the 2009 solar minimum galactic cosmic ray environment assuming 20 g/cm<sup>2</sup> aluminum spacecraft shielding.

\*NSCR is NASA Space Cancer Risk, RBE is relative biological effectiveness factor

\*\*LET is linear energy transfer.

Figure 18. Predictions of REID over a One-Year Space Mission at Deep Solar Minimum. Source: Cucinotta (2015, 11).

## F. CURRENT EXPOSURE FORECASTS

It is helpful to provide some background data from low Earth orbit missions for context in comparison to what crew will receive in deep space. According to the “Astronaut Health and Safety Regulations: Ionizing Radiation” article, even the time spent on the ISS at solar maximum where the shielding of the solar wind provides maximum deflection of GCR, the dose received in only six months on board averages 80mSv, and at solar minimum, the six-month exposure is 160mSv (Sieffert 2014, 22). These quantities are a significant fraction of the career dose limits reviewed in Section D of this chapter—and again this is within the protection of the Earth’s magnetic field. The following sub-sections further demonstrate how severe the exposure forecasts are both for general predictive models in deep space and for specific Mars mission models. This data is the justification for all other alternatives being reviewed in this paper to mitigate exposure so a human mission to Mars can be feasible from the perspective of radiation exposure.

## 1. General Predictive Models

The NASA paper “Space Cancer Risk Projections and Uncertainties” provides an excellent summary of research that has been conducted by various groups to quantify the doses received and the increases in risk for Radiation Exposure Induced Cancers (REICs) for various organ groups, males versus females, and versus age of exposure on missions in deep space (2011). The document first summarizes some dosing scenarios for each organ group for males in both average GCR conditions in interplanetary space at solar minimum (annual dose) and as would be predicted from a severe Solar Particle Event documented in 1972 (dose for the solar event only). The resulting doses to various organs and as averages to skin and blood forming organs (BFO) are shown here in Figures 19 and 20. These figures call out three types of dose measurement, reviewed here:

- Absorbed dose (D)—in mGy, the measure of the energy absorbed.
- Equivalent dose (H)—in mSv, the measure of anticipated long term radioactive effects from the dose absorbed in biological tissue, as converted by the absorbed dose multiplied by Quality Factor which was discussed in section B of this chapter.
- Effective dose (G)—in mGy-Eq, a measure of the weighted or effective dose as it impacts energy absorbed by different organs, as converted by the RBE discussed in Section D of this chapter.

Organ/tissue	August 1972 SPE			Annual GCR at solar minimum		
	D mGy	G mGy-Eq	H mSv	D mGy	G mGy-Eq	H mSv
Avg. Skin	2692.3	4052.1	4259.7	198.8	375.8	832.3
Avg. BFO	306.9	462.5	442.1	185.7	337.2	614.0
Stomach	112.3	169.6	168.0	182.2	324.4	547.6
Colon	251.4	379.0	363.8	185.6	336.4	606.2
Liver	174.1	262.7	255.0	183.1	327.9	566.6
Lung	205.6	310.1	299.4	184.5	332.9	590.9
Esophagus	195.4	294.8	285.0	184.0	331.3	584.4
Bladder	118.7	179.2	176.8	181.6	322.5	540.8
Thyroid	333.2	502.1	479.0	186.8	341.1	632.7
Chest/Breast	1615.9	2430.6	2323.9	194.1	365.6	770.2
Gonads/Ovarian	748.1	1125.7	1072.2	186.5	339.7	640.9
Front brain	571.7	860.9	816.4	190.6	354.4	696.9
Mid brain	279.6	421.5	403.9	187.7	344.1	640.2
Rear brain	557.5	839.6	796.2	190.5	354.0	695.2
Lens	1959.0	2946.2	2829.4	196.2	372.4	806.3
Gallbladder	118.7	179.2	176.8	181.6	322.5	540.8
Remainder	406.3	611.9	585.9	186.1	338.2	619.5
Point Dose	5389.0	8125.0	8663.0	218.2	434.4	1140.7
E, mSv	$w_T$ (ICRP 1991)		612.3			611.1
	$w_T$ (ICRP 2007)		676.2			620.7

Figure 19. Organ Doses for Males with 5g/cm<sup>2</sup> Aluminum Shielding. Source: Cucinotta et al. (2011, 30).

Organ/tissue	August 1972 SPE			Annual GCR at solar minimum		
	D mGy	G mGy-Eq	H mSv	D mGy	G mGy-Eq	H mSv
Avg. Skin	87.8	132.8	144.0	193.5	342.3	599.8
Avg. BFO	23.4	35.7	42.9	182.0	314.9	494.2
Stomach	12.1	18.6	25.5	179.1	306.4	465.5
Colon	21.0	32.1	39.4	181.9	314.6	491.3
Liver	15.6	23.8	30.7	179.8	308.6	473.6
Lung	18.3	28.0	35.2	180.9	312.0	484.4
Esophagus	17.5	26.8	34.0	180.5	310.9	481.4
Bladder	12.0	18.4	25.0	178.6	305.0	462.2
Thyroid	25.7	39.1	46.5	182.9	317.5	502.5
Chest/Breast	67.2	101.9	107.0	189.0	333.8	558.7
Gonads/Ovarian	37.5	57.0	62.5	182.5	316.1	503.3
Front brain	37.6	57.1	64.8	186.1	326.6	530.5
Mid brain	24.0	36.7	44.8	183.7	319.8	506.9
Rear brain	37.0	56.4	64.0	186.0	326.4	529.8
Lens	76.7	116.1	120.9	190.8	338.4	574.0
Heart*	18.3	28.0	35.2	180.9	312.0	484.4
Gallbladder	12.0	18.4	25.0	178.6	305.0	462.2
Remainder	26.0	39.6	46.5	182.3	315.6	496.3
Point Dose	164.7	248.9	267.8	210.7	384.3	751.4
E, mSv	$w_T$ (ICRP 1991)		45.83			492.48
	$w_T$ (ICRP 2007)		48.45			496.74

Figure 20. Organ Doses for Males with 20g/cm<sup>2</sup> Aluminum Shielding. Source: Cucinotta et al. (2011, 31).

A key take-away from Figures 19 and 20 is that an increase in shielding (and thus spacecraft weight) yields substantial benefit in the reduction of SPE dose received. However, as shown here, the same change in shielding has only minimal effect in the reduction of GCR dose due to the higher energy of these particles. This point helps to support the case that is made later in this paper for a mission architecture that incorporates heavier shielding into a small shelter area to be used in the event of a significant SPE.

The results also highlight the challenges that exist in modeling overall effective dose for SPEs because the skin, thyroid, breast, and gonad effective doses from such events are disproportionately higher than the dose for other organs. This distorts

weighting factors and yields overall effective doses that seem un-realistic as measures of whole-body lethality. Different modeling methods of the same 1972 SPE have also been developed to show more realistic effective doses for four crew members in a simulated module, as shown in the Figure 21 (Cucinotta et al. 2011, 32).

		<b>Organ Dose Equivalent, mSv</b>			
		<b>DLOC1</b>	<b>DLOC2</b>	<b>DLOC3</b>	<b>DLOC4</b>
<b>Al-Eq <math>x_{avg}</math>, g/cm<sup>2</sup></b>		15.18	15.08	15.85	15.33
<b>CAM organ dose</b>	Avg. skin	1266	1211	1041	1086
	Eye	868	844	736	771
	Avg. BFO	169	168	152	159
	Stomach	73.8	73.7	67.7	70.3
	Colon	144	144	130	136
	Liver	104	103	94.1	98.0
	Lung	122	121	110	115
	Esophagus	116	116	105	110
	Bladder	75.4	75.3	69.0	717
	Thyroid	184	183	166	173
	Chest	722	706	619	648
	Gonads	353	347	308	322
	Front brain	295	293	263	275
	Mid brain	162	162	147	153
	Rear brain	289	287	258	270
<b>Effective Dose, mSv</b>		213	210	188	196
<b>Point Dose Eq., mSv</b>		2557	2427	2079	2168

“August 1972 SPE organ dose quantities for males using the fully automated ProE structural distribution model LTV, the computerized anatomical man model (CAMERA), and the BRYNTRN codes. The King spectra for the SPE is used. Calculations are at the location of each crew member in the LTV, designated by dose locations (DLOC) 1-4.”

Figure 21. Organ Dose Quantities/Equivalents. Source: Cucinotta et al. (2011, 33).

Numerous models have been derived from the dose estimates above to attempt to predict the risk of exposure induced cancers (REICs), and the risk of mortality from said occurrence (risk of exposure induced death, or REID). Much of this same research identifies the need to further adjust mission dose estimates for exposure received at low

dose rates because the epidemiology data used to derive all REIC/REID models is based on acute gamma ray doses, which are expected to be more damaging as opposed to the relatively low GCR dose rates that would typically be encountered day-to-day in deep space (~.05Gy/hr). This adjustment is accomplished by reducing the REIC/REID by a dose and dose rate effectiveness factor (DDREF). DDREFs of ~2.0 are typical values that have been used in most cancer predictions before further modification (Cucinotta et al. 2011, 38–39).

“Space Radiation Cancer Risks Prediction and Uncertainties—2010” also derives the Figures 22 and 23, which show comparisons between different REIC/REID models as compared to 2005 U.S. Census data for various tissue type cancer incidences and ratios (2011, 39–41). A DDREF of 1.75 for solid (tumor) cancer estimates and for the linear component of leukemia mortality models is assumed. These models are also compared for age at exposure—which logically show a much larger REIC for the same Sv of dose received at younger ages than at older ages where a larger percentage of the baseline (U.S.) population would be more prone to cancer due to genetic or other lifestyle/career effects. The most dramatic comparison on each of these charts is shown for the total and solid cancer rates for both males and females, for female lung cancers, and for male colon/liver/prostate cancers, where the BEIR VII model shows a drastically higher risk for exposure received at younger ages vs the other two models. This is because this model relies on a quantity known as lifetime attributable risk (LAR) instead of the conventional REID as the basis for its calculations. The LAR model unfortunately ignores survival probability basis on radiation contribution—and has been determined by NASA to over-estimate risk, especially where higher doses are involved (Cucinotta et al. 2011, 36). The key take-away from these charts is that REIC for the same unit exposure of radiation is higher using all models at younger ages—which impacts the discussion that is expanded on in Chapter VI about medical screening and selection as a method to mitigate crew radiation risk.



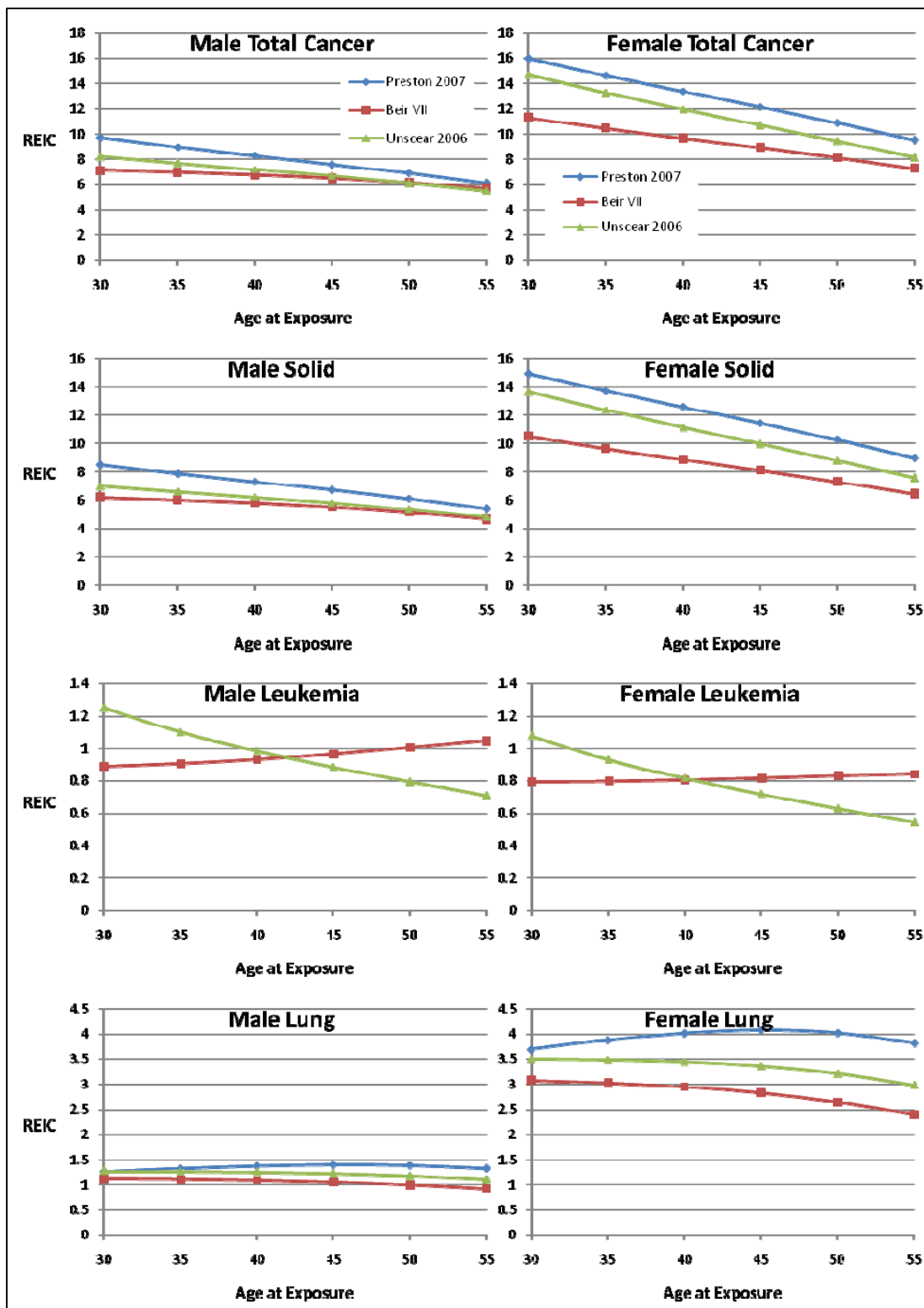


Figure 22. REIC Comparison for Mixed Cancer Types versus Exposure Age per Sv of Dose Received. Source: Cucinotta et al. (2011, 40).

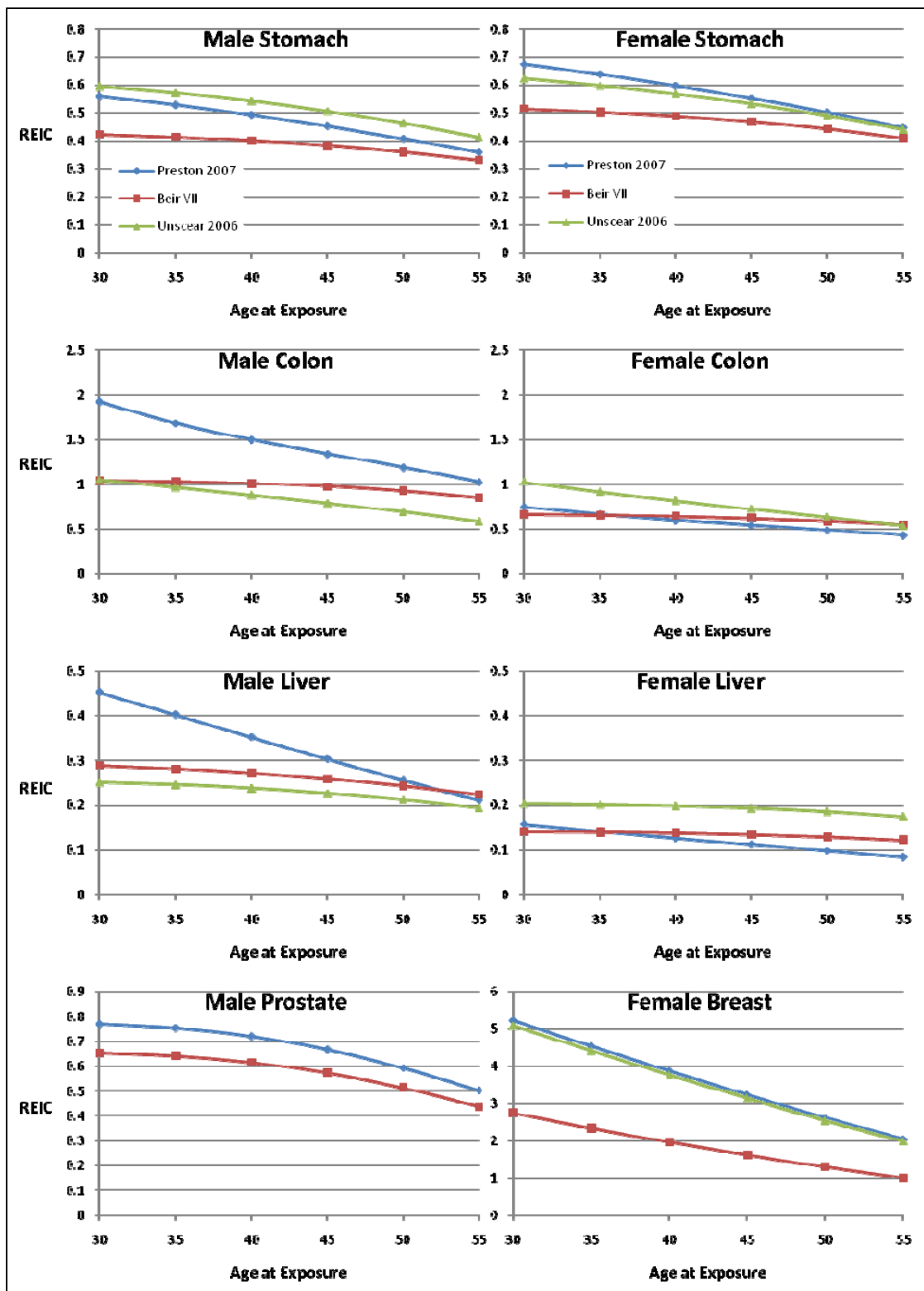


Figure 23. REIC Comparison for Organ-Specific Cancer Types versus Exposure Age per Sv of Dose Received. Source: Cucinotta et al. (2011, 41).

The same study by Cucinotta et al. also reviews the effectiveness of shielding against numerous types of cancer (2011). Figure 24 shows a basic comparison of annual dose received in mSv using two exposure models in deep space versus the depth of shielding used. These calculations are referenced for shielding estimates later in this paper.

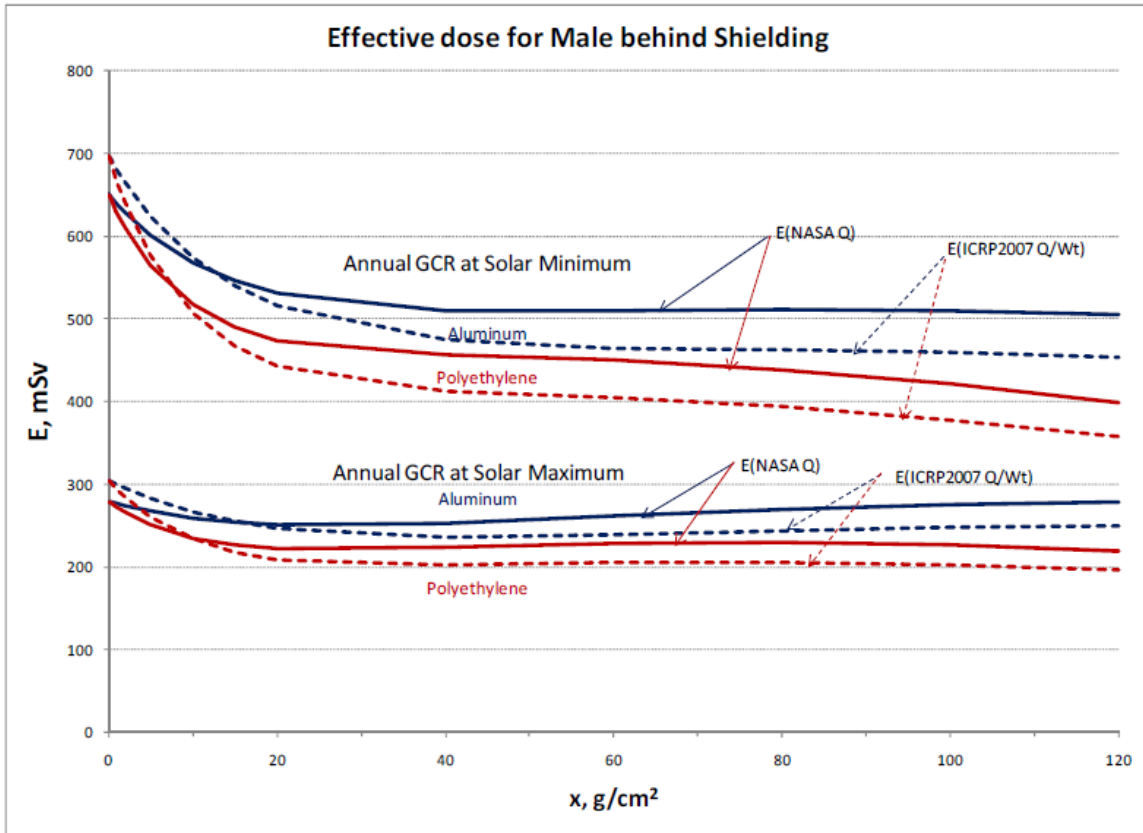


Figure 24. Effective Dose Rates versus Shielding Depth in Deep Space. Source: Cucinotta et al. (2011, 88).

A 2013 study by Cucinotta et al. also leverages the same NASA epidemiology study data to parse out GCR specific annual exposure rates as on the ISS, in deep space, and on the Martian surface as compared to transit vehicle/habitat equivalent aluminum shielding depth ( $X_{Al}$ ). Figure 25 shows relative trends between effective doses impacting both solid and leukemia type cancers (H, shown in blue and green in the figure below), for overall male absorbed dose (D, purple), and for equivalent dose for non-cancer effects

(cardiovascular/organ abnormalities, G, in red). This figure further demonstrates the limitations of increased shielding thickness when it comes to limiting GCR exposure.

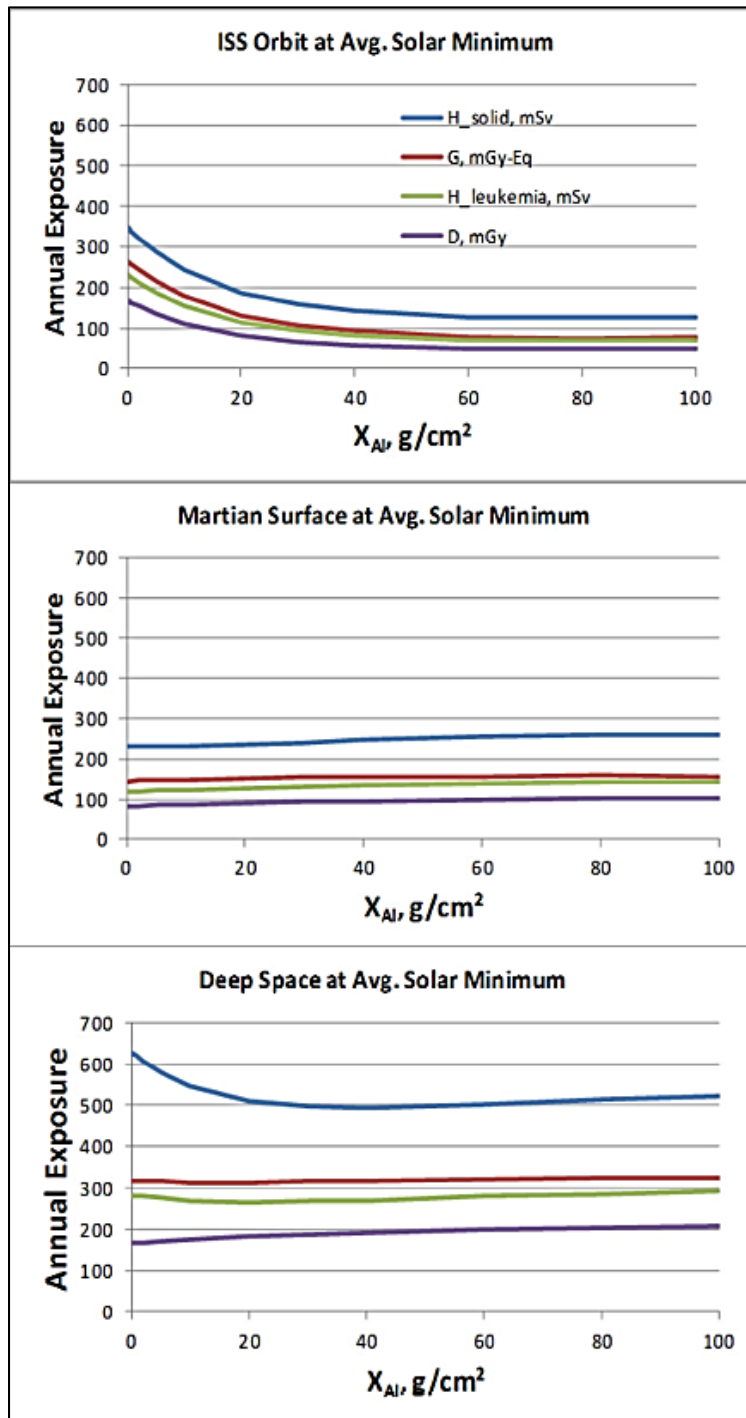


Figure 25. Effective Dose Rates versus Shielding Depth for Multiple Cancer/Organ Effects. Source: Cucinotta et al. (2013, 3).

This GCR specific study also yields a distribution of REID estimates for Mars/Deep Space/ISS as compared to the variation encountered in the particle component of GCR flux. This component can be quantified by the term  $Z^2/\beta^2$ , where  $Z$  is the charge number of the particle encountered and  $\beta$  is the particle velocity. This term has been shown to “describe the density of the ionization of a particle track more effectively than LET and is used in the NASA Quality Factor” (Cucinotta et al. 2013, 2). Figure 26 shows the resulting distribution with the assumptions of  $20\text{g/cm}^2$  nominal shielding for non-smoking males.

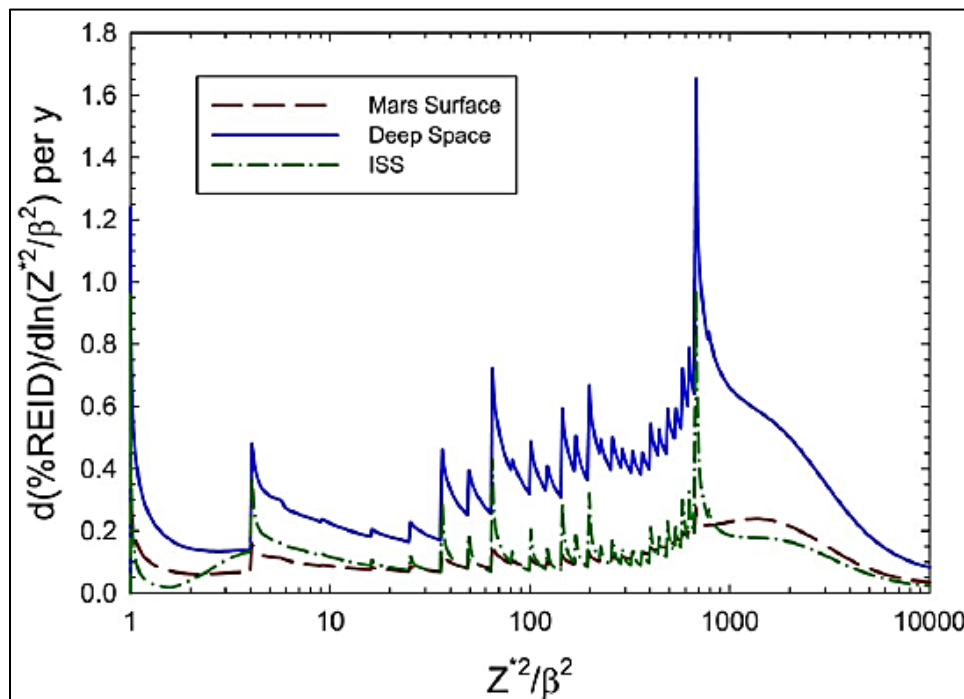


Figure 26. REID Distributions versus Density of Ionization for Particle Tracks.  
Source: Cucinotta et al. (2013, 4).

The same study also derives Figure 27, which summarizes the anticipated annual exposure rates for both solid cancers and total dose at two shielding depths, along with a calculation of the log of the proton fluence on the right axis from various SPEs (vertical lines on chart) which shows early promise as a predictor of SPE specific organ dose.

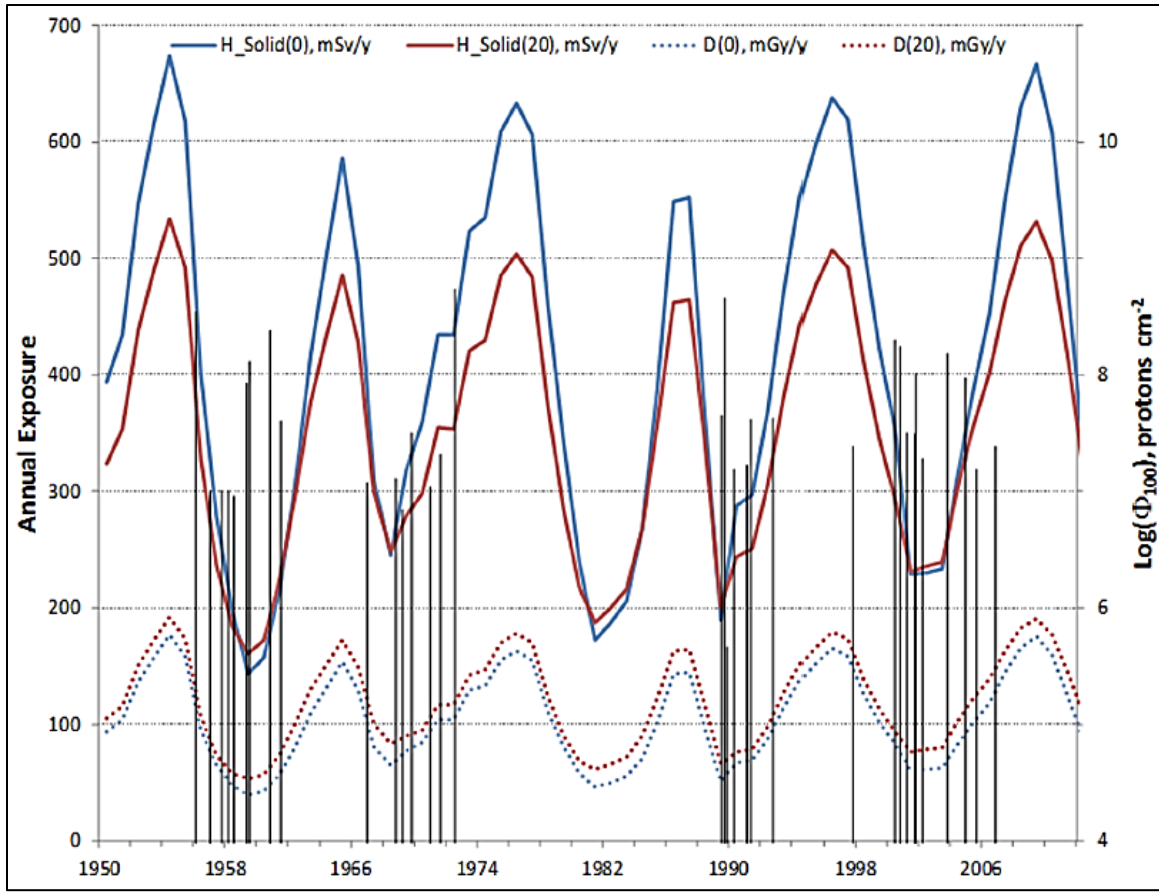
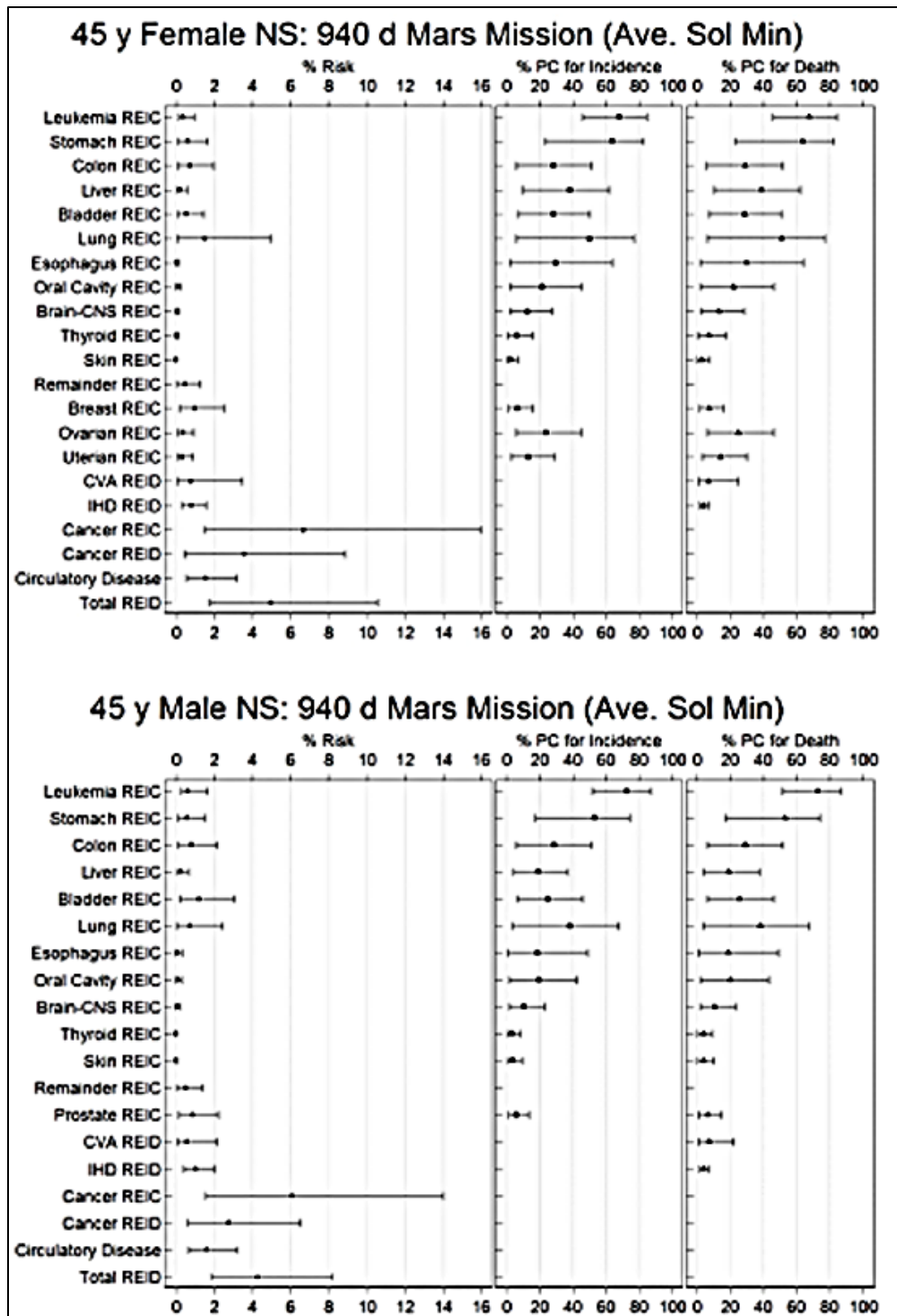


Figure 27. Estimates of GCR Organ Doses over Recent Solar Cycles at 0g/cm<sup>2</sup> and 20g/cm<sup>2</sup> Shielding. Source: Cucinotta et al. (2013, 4).

## 2. Mission-Specific Models

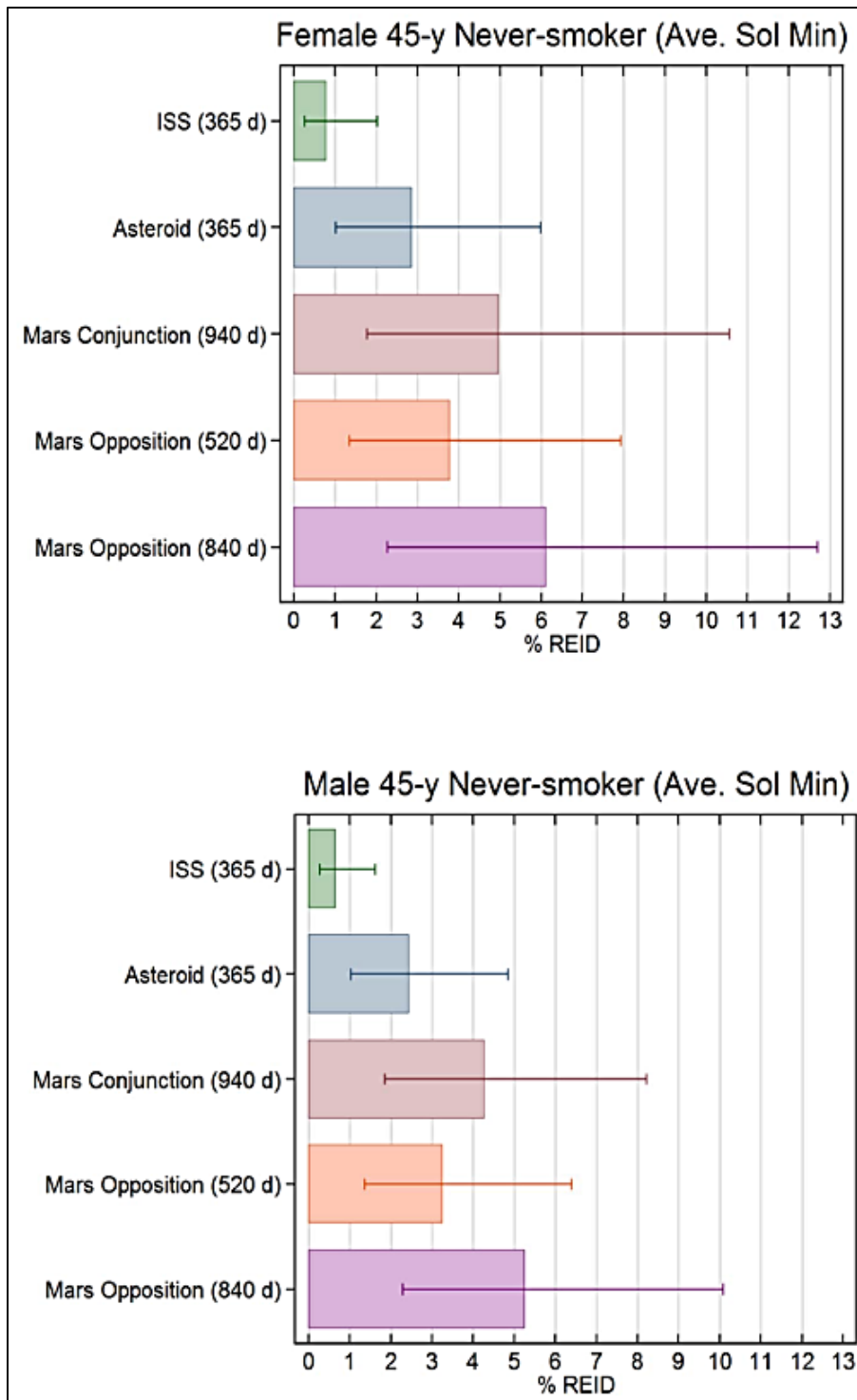
The article “How Safe Is Safe Enough? Radiation Risk for a Human Mission to Mars” provides a detailed review of anticipated total REIC risks from GCR flux and confidence levels for both 45-year-old non-smoking males and females on a typical Mars mission. Both mission timeframe (solar minimum versus maximum) and mission architecture are considered. Mission architectures are reviewed at more length in the next chapter but they may be summarized into two categories here: Conjunction and Opposition Class. Opposition class missions involve launch from opposing orbital position versus Mars, and yield overall architectures with anywhere from 460–780 days of total transit time in deep space to and from the planet, and only 60 days of time on the Martian surfaces (Short-stay) in order to meet optimal return windows. Conjunction Class missions involve shorter deep space travel times (approximately 400 days total), but lend themselves to a Long-stay on the Martian surface (~540 days), thus yielding more mission time total. For the purposes of this study, a 940-day mission timeframe was used (Cucinotta et al. 2013, 1), and mission timing was assumed to fall at solar minimum where GCR flux would be at its strongest. Figures 28 and 29 show the resulting gender and organ specific REICs for such a mission, and the combined cancer/cardiovascular disease REID predictions for both genders with a comparison of a small sample set of mission types/durations (Cucinotta et al. 2013).



Assumptions for this figure: transit and habitat vehicles have 20g/cm<sup>2</sup> and 10g/cm<sup>2</sup> shielding, respectively. PC calculations indicate chance of death by 20 years past-mission, and all brackets denote 95% confidence intervals.

Figure 28. Organ Specific REICs for a Typical Mars Mission. Source: Cucinotta et al. (2013, 6).





Assumptions: transit and habitat vehicles have 20g/cm<sup>2</sup> and 10g/cm<sup>2</sup> shielding, respectively. All brackets denote 95% confidence intervals.

Figure 29. Combined REIDs for Various Mission Types. Source: Cucinotta et al. (2013, 7).

The unfortunate reality revealed by these studies is that if present nominal shielding capabilities are used on missions of this duration, that astronauts will more than double or triple their risk of cancer incidence versus the current 3% limit. For women the risk is even higher than for men. Incidences of cancer from such missions may yield at least a 15-year loss of lifespan—as compared to a typical loss of lifespan of 40 years if a mission results in loss of crew (LOC). The studies also demonstrate clearly that efforts to reduce the very large uncertainty seen in some of the 95% confidence intervals may at least yield better predictions for these missions in the future. The need for further research is also highlighted to better understand phenomena such as impacts to cognitive function and memory that may be caused by GCR within the time-span of some of the longer-duration missions proposed (Cucinotta et al. 2013, 6–8).

Based on the predicted exposure levels and impacts reviewed in this chapter, a mission to Mars may seem untenable for human beings at this time. However, research is also currently in progress on methods to reduce this exposure, or to mitigate the impacts of any exposure received. This paper addresses this research in three key categories: methods to reduce exposure via mission architecture, methods to reduce exposure via improved shielding, and methods to reduce the impact of exposure via medical doctrine. Mission architecture is discussed first, in Chapter IV.

## **IV. REDUCING EXPOSURE THROUGH MISSION ARCHITECTURE**

An overarching theme that backs all formalized human radiation worker programs and limits is the premise that exposure levels should be maintained “as low as reasonably achievable” (ALARA). In order to realize this, three basic tenants are employed: decreased time exposure to the radiation flux, increased distance from the radiation flux, and increased shielding to further attenuate the flux. This chapter addresses the first two topics through a brief review of proposed human Mars mission architectures and the trade-offs in different radiation exposure types and risks that result. The third topic of shielding is discussed further in Chapter V of this paper.

The “Human Exploration of Mars Design Reference Architecture 5.0 Addendum” contains a consolidated comparison of the radiological advantages and disadvantages of different Mars mission types (Drake 2009). The mission types are necessitated because in cases where a more energy efficient outbound orbit is used, orbital alignment (phase angle) upon arrival at Mars is not favorable for an energy efficient return trajectory until a longer timeframe has passed. In cases where less efficient trajectories are used, the conditions at Mars align for an energy efficient return fairly soon after arrival on the surface. Thus, Mars missions fall into two distinct classes: Opposition Class or “Short-stay” Missions with longer deep space transit times (~600 days total) and limited surface stays (30–90 days); and Conjunction Class or “Long-stay” missions with shorter deep space transit times (~400 days total), and longer surface stays (~500 days) (Drake 2009, 50–51).

### **A. OPPOSITION CLASS MISSION ARCHITECTURE**

The Opposition Class or Short-stay Mission Class has a typical mission trajectory profile as shown in Figure 30. This mission class has higher propulsive requirements versus the Conjunction Class, and must use additional deep space propulsion maneuvers or orbital swing-by maneuvers with other planets (Venus) both to reduce total mission energy and fuel weight required, and to help constrain Mars and Earth re-entry speeds.

The most significant feature of this mission class is the requirement for either the outbound or the inbound orbit to pass relatively close to the sun during the longer leg of the transit—typically 0.7 astronomical units or less (where one AU is 149.6 million kilometers, the mean distance from the center of the Earth to the center of the sun). This impacts some of the radiation exposure risks for the mission, as is detailed later in this chapter.

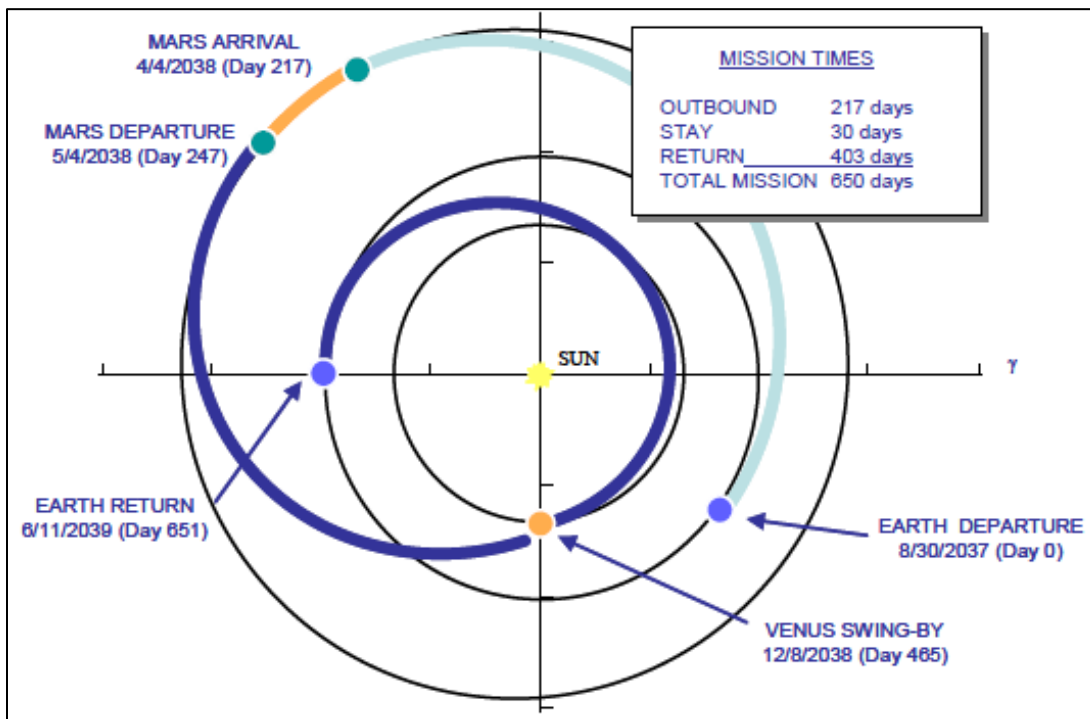


Figure 30. Typical Opposition Class Mission Trajectories. Source: Drake (2009, 50).

Short-stay missions do not have to use a Venus swing-by to succeed. However, the advantage to using this maneuver is a reduction of fuel requirements because the swing-by essentially provides a “free” deep space maneuver to help optimize trajectories and planetary arrival speeds. The trade-off for this savings is the fact that the three planets (Earth, Venus, Mars) must have a very specific alignment for the trajectories to be feasible. Figure 31 shows the mission windows available for different Short-stay mission durations with the Venus Swing-By built in, as compared to the relatively more frequent

availability of the Long-stay mission windows that is discussed in the next section (Drake 2009, 55).

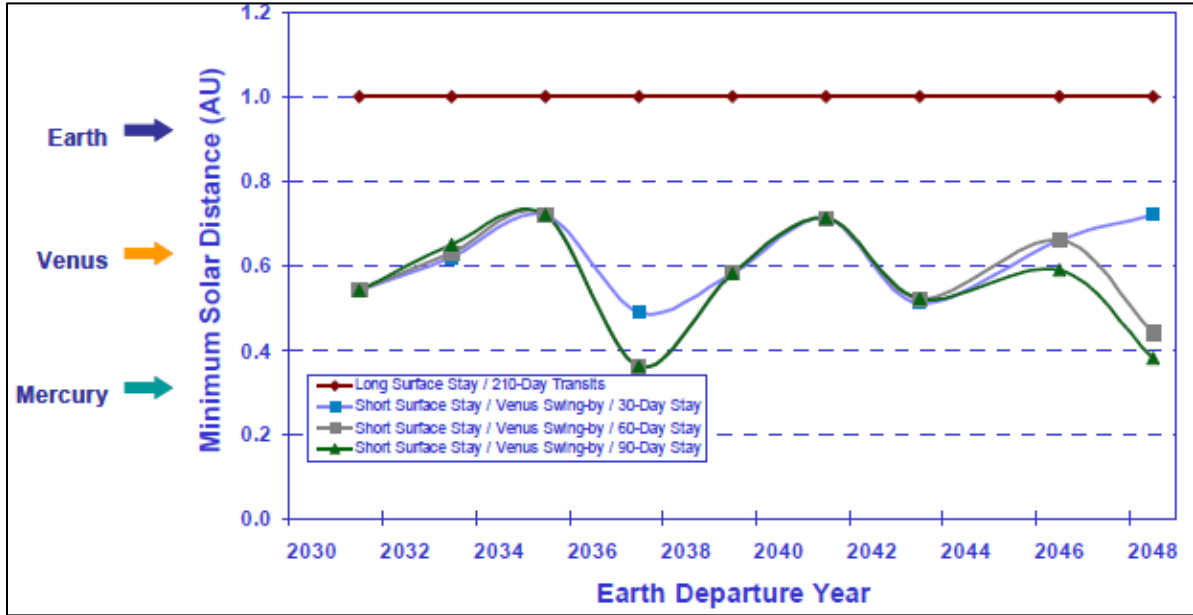


Figure 31. Opposition Class Mission Departure Years with Swing by versus Long-Stay Architecture. Source: Drake (2009, 56).

Figure 31 also highlights the key concern for this mission class. Some mission windows in the near future will involve the crew and transit vehicle spending over 100 days within 1.0 AU from the Sun. From a thermal standpoint, this will require transit vehicle designs to incorporate additional thermal shields, and potentially deployable radiators, cooling loops, and sun-shades to mitigate the heating effects of the perihelion (closest to the sun) passage. Positioning of shields, sun-shades, and solar arrays on the vehicle relative to the sun will also have to be precisely controlled in order to prevent over-heating of critical components (Drake 2009, 56).

From a radiation stand-point, the most significant impact of the perihelion passage necessitated by the Short-stay model is the fact that proximity to the sun will yield significantly larger radiation exposures during SPEs and even throughout longer-duration solar storms. The strength of the radiation dose is proportional to the square of the

distance from the sun ( $1/R^2$ )—so these mission models will likely necessitate a transit vehicle design that has both additional module shielding to protect the crew and components during perihelion passage; and also a heavier shelter to protect the crew from the higher flux that could be encountered during a worst-case SPE (Drake 2009, 56).

## B. CONJUNCTION CLASS MISSION ARCHITECTURE

The Conjunction Class or Long-stay Mission Class utilizes the most energy-efficient trajectories to transit between Earth and Mars when the orbital alignment of the two planets is relatively close. A longer stay on the Martian surface allows the crew to wait for a return of optimal orbital alignment to use a minimum energy trajectory for the return trip as well. Figure 32 shows sample trajectories for a Conjunction Class mission (Drake 2009, 51).

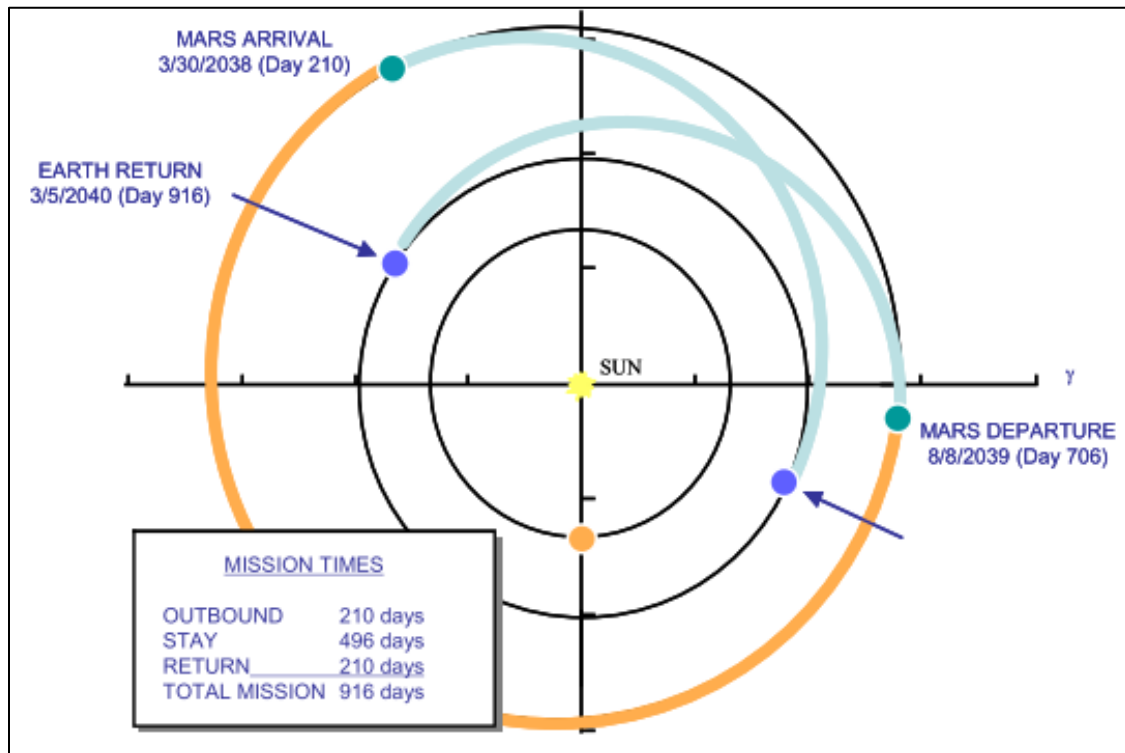


Figure 32. Typical Conjunction Class Mission Trajectories. Source: Drake (2009, 51).

Drake’s 2009 Design Reference Architecture Addendum also makes a distinction between two basic categories of Long-stay missions. First, there are those that use minimal energy trajectories for optimum fuel efficiency. The second is referred to as a “fast transit” Mars mission, where trajectories have been chosen to minimize the time spent in deep space between the two planets. The comparison of these Long-stay mission types, along with a typical Short-stay mission, is shown in comparison to the first European nautical journey to India by Vasco de Gama in Figure 33.

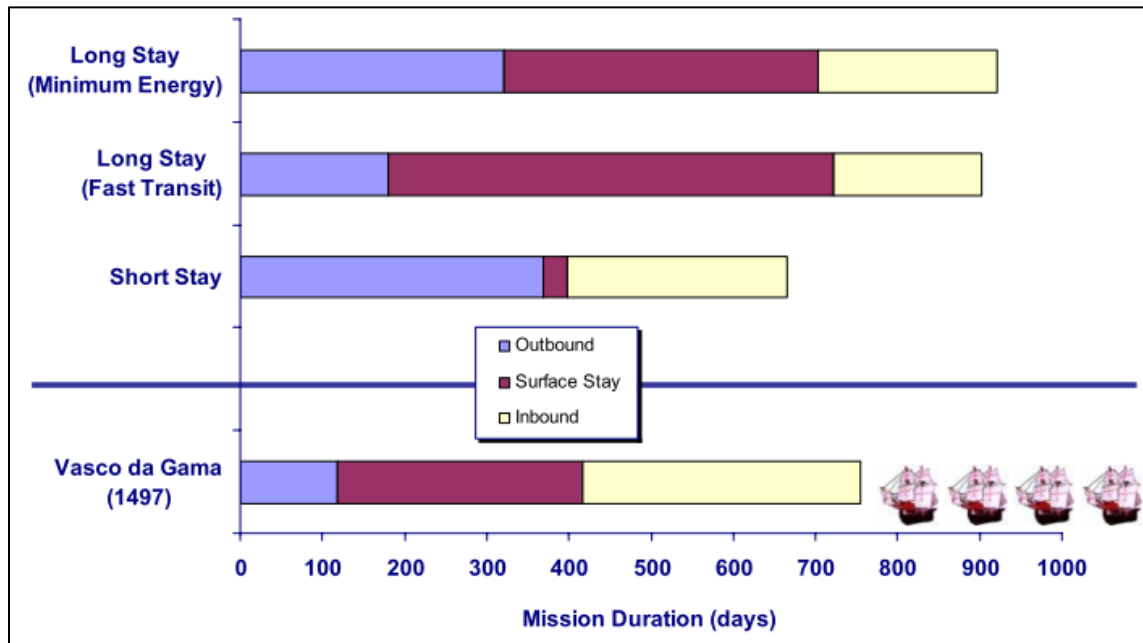


Figure 33. Comparison of Mission Class Transit Times, Stay Times, and Total Durations. Source: Drake (2009, 52).

In general for Long-stay missions, the trade-off of shorter transit times for a longer Martian surface stay time may actually have several advantages, including (Drake 2009, 51):

- Reduced risk due to shorter deep space transit times, thus minimizing isotropic GCR exposure times and chance of a significant SPE occurring while in transit.
- By ratio, a typical Short-stay Mission model will have its crew in transit for over 90% of the total mission duration, whereas a Long-

stay or “fast transit” mission will have the crew in transit for only 30% of the total duration. *Note: more details on anticipated radiation exposure are discussed at length later in this section.*

- More time on the Martian Surface, which permits more time for crew acclimatization to the planet’s conditions after a long zero-G transit, and more exploration time beyond that.
- Greater shielding while on the Martian surface for 70% of the Long-stay mission duration, where a significant portion of the GCR flux is blocked by both the mass of the planet and its thin atmosphere.
  - Specifically, the mass of the planet under the crew and its atmosphere may be estimated to provide 10–20 g/cm<sup>2</sup> Al-equivalent, depending on habitat latitude and the season.
  - Adequate surface stay time to implement further shielding methods including regolith applications for habitat shielding, and potential habitat assembly in caves (see Chapter V for more detail).

## C. COMPARISONS OF MISSION ARCHITECTURES

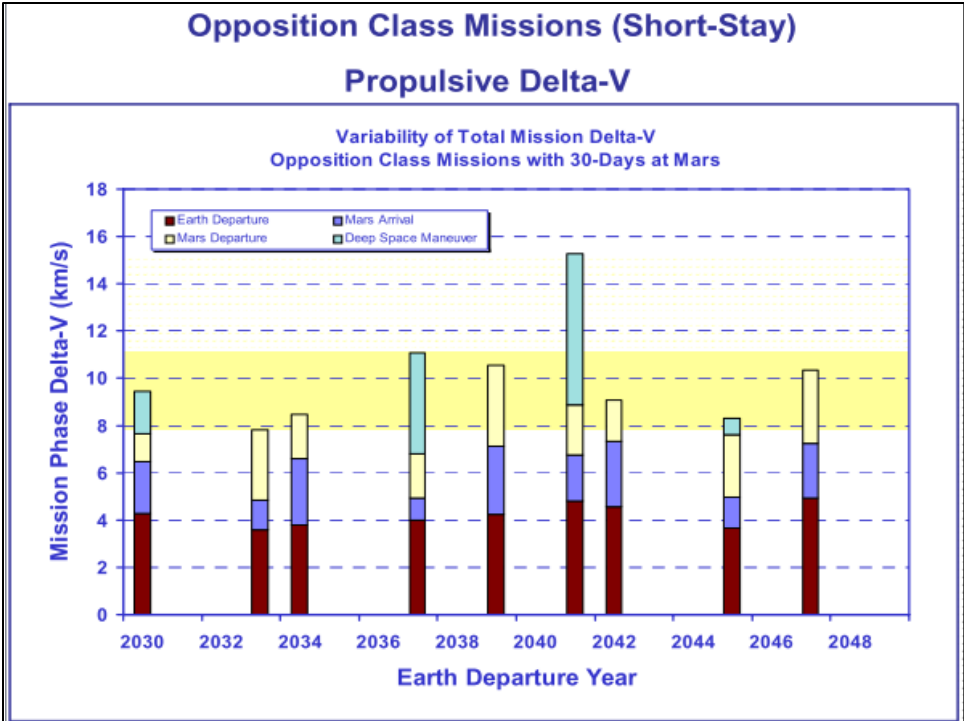
Some of the advantages and disadvantages of the Opposition and Conjunction (Short and Long-stay) mission classes have been reviewed in the first two sections of this chapter. A selection of metrics for comparison between them is discussed in greater detail in this section. These metrics are reviewed again as part of the systems engineering analysis techniques employed to weigh all mission alternatives versus human radiation exposure mitigation in Chapter VII.

### 1. Propulsion Requirements

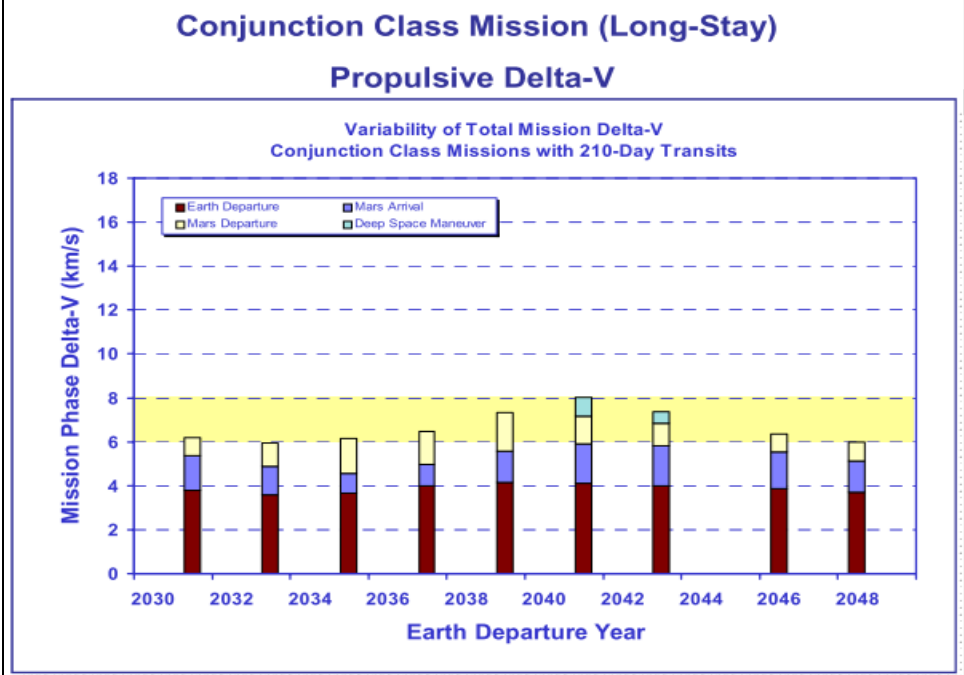
One other key consideration between the Opposition and Conjunction Class mission models involves the concept of Delta-V. In space missions, Delta-V is often expressed as a total of all the propulsive requirements for maneuvers spanning the entire mission and is indicative of total fuel required for the mission. Each maneuver is expressed in terms of the change in velocity (Delta-V) required. Drake’s “Human Exploration of Mars Design Reference Architecture Addendum” reveals that the Delta-V requirements for Opposition Class (Short-stay) missions are in general higher, and in some cases prohibitive enough to potentially impact mission schedule by forcing a decision to skip a launch window (Drake 2009, 57). Figure 34 reveals one such instance



in the year 2041. This figure summarizes the Delta V ratios that will be required for various phases of a mission to Mars (Earth departure, Mars departure, Mars arrival, deep space maneuvering), along with their totals based on the orbital alignments and required trajectories for various launch windows from 2030–2050, for both Long-stay and Short-stay mission models. For each figure, the yellow horizontal band denotes the variation around the average Delta V for that mission type. The upper section of this figure (for Short-stay/Opposition Class Missions) clearly shows one window in 2041 where the Delta V required for deep space maneuvers is such that the total Delta V for that mission window is significantly higher than the Delta V of other comparable missions at different timeframes.



**Note:** Optimized trajectories assuming 407 km circular LEO departure orbit, propulsive capture at Mars into a Mars 1-Sol orbit of 250 km x 33,793 km. 30 sols stay at Mars. Direct entry at Earth with an entry speed limit of 13 km/s.



**Note:** Optimized trajectories assuming 407 km circular LEO departure orbit, propulsive capture at Mars into a Mars 1-Sol orbit of 250 km x 33,793 km. 210 day transits to and from Mars. Direct entry at Earth with an entry speed limit of 13 km/s.

Figure 34. Delta V Comparisons. Source: Drake (2009, 57).

## 2. Scientific Exploration

One of the dominant arguments in the case to send humans to Mars is the added value of scientific investigation that can be conducted there via local human guidance. In comparing the two mission classes, Drake's 2009 "Addendum" breaks each into sub-categories of single-site or multiple-site models—essentially whether subsequent missions in each cycle are planned to re-use the same site time and again, or whether multiple landing/exploration areas should be chosen (Drake 2009, 63).

On the whole, Short-stay/Opposition Class Missions are not favorable from a scientific standpoint due to the limited availability of time on the Mars surface (30–90 days). At the low end, this time frame is not sufficient for the Extravehicular Activities (EVAs) needed to fully explore the landing area, and especially for more challenging operations such as positioning equipment to conduct deep drilling for sampling operations. It also does not allow time for the astronauts to conduct in situ analysis of samples collected on-site so they could adapt future sampling strategy based on initial results; and does not permit enough time to fully grade the samples that are collected to ensure a broad enough sample set is returned to Earth. That said, even on a single-site Short-stay cycle, *some* scientific value is provided given samples will still be returned to Earth. Additional technical challenges that could be met to enhance the value provided in Short-stay missions include (Drake 2009, 64):

- planning for Short-stay missions to take place across multiple mission sites so broader exploration can be accomplished over multiple missions
- developing "fetch" style MERs (Mars Exploration Rovers) to increase efficiency of exploration and sampling while astronauts are present; and potentially analytical MERs to further enhance efficiency of sample collection/processing
- developing autonomous technology to conduct selected operations (drilling) after astronauts from the first mission cycle have departed the planet

In contrast, Long-stay/Conjunction Class Missions allow much more time to maximize the potential for human exploration. It is important to clarify that EVAs comprise higher risk for crew given the nature of venturing outside a spacecraft or habitat

with limited radiation shielding and oxygen/sustenance available. While models for these missions only allocate 25% of astronauts' time to EVA exploration and sample collection, the length of human presence affords much greater opportunity to make more intuition-driven and potentially dramatic discoveries as compared to the current methodical exploration efforts that are underway by remotely controlled MERs. There is adequate time to employ more intensive sampling methods including deeper drilling. Further, even if human EVA time is limited, this model also affords more time for on-planet sample analysis; which in turn will help the crew to optimize the selection of samples returned to Earth (Drake 2009, 64).

The greatest challenge that goes in parallel with the Long-stay model is that astronauts would need to employ either horizontal or vertical "mobility" vehicles in order to fully expand the exploration area (potentially hundreds of kilometers) around the landing site. In this same vein, the full scientific benefits of the Long-stay model are not realized unless subsequent missions with at least three different landing locations are chosen. A single location Long-stay mission plan has actually been deemed to be less preferable to a multiple location Short-stay mission plan because its exploration range will be limited unless a mobility form with a range of thousands of kilometers is developed for on-planet travel (Drake 2009, 64).

### **3. Human Health Hazards**

In keeping with the direction of this paper, the focus of this section is the radiation impacts in comparison between the Opposition and Conjunction mission classes. However, it is worth mentioning several other aspects of these missions that also have human impacts to varying degrees. Table 5 shows assumptions that were made in models comparing the different risks to both human health and performance, and is used for further comparisons in Chapter VII of this study (Drake 2009, 65):

Table 5. Mission Assumptions for Human Health and Performance Assessments

Factor	Short-stay Mission	Long-stay Mission
Travel time in transit to Mars	313 days (~10 months)	180 days (~6 months)
Travel time in transit to Earth	308 days (~10 months)	180 days (~6 months)
Total transit time in deep space % total mission duration	621 days (~21 months) 94%	360 days (~12 months) 40%
Surface stay time % total mission duration	40 days (~1 month) 6%	545 days (~18 months) 60%
Total mission time	661 days (~22 months)	905 days (~30 months)
Closest solar approach – Without Venus swing-by With Venus swing-by	~0.5 AU As close as 0.38 AU	1 AU N/A

AU: astronomical unit (mean distance from the Earth to the sun).

Drake’s 2009 “Addendum” briefly compares human risks from a stand point of medical capabilities, human factors and habitability, and behavioral health/performance. It concludes that medically, a Short-stay mission has a slight advantage given the lesser total mission duration (22 versus 30 months) indicates a lower overall risk of medical situations occurring. For human factors and habitability, the Long-stay mission may be preferred assuming that the mission architecture only allows for a separate surface habitat in this mission class. For behavioral health and performance, a mixed conclusion was reached. While the behavioral stressors of a shorter mission duration (Short-stay Class) may seem preferable versus the Long-stay—the radiation impacts of the close perihelion passage used for Short-stay trajectories may increase the risk of behavioral/performance consequences as well (Drake 2009, 66).

The effects of Zero G space travel during the transits between Earth and Mars were reviewed as another physiological concern. Focusing only on that, the Short-stay model ends up being the less favored option because it places astronauts in space for a length of time that stretches the limits of our human spaceflight experience base. The one exception for this would be a development of artificial gravity (AG) technology for the transit vehicles for the mission (Drake 2009, 65).

Focusing on radiation exposure and risks, Short-stay missions are considered to be slightly less favored for several reasons:

(1) Risk of SPE occurrence during close passage to the sun

The large portion of Short-stay mission trajectories that passes within 0.8 to 0.5 AU to the sun places crew at greater risk for acute radiation symptoms as well as increased cancer risk if an SPE occurs, even with the assumption that the mission transit vehicle (MTV) will have a heavily shielded area (at least  $20\text{g/cm}^2$ ). The Mars surface along with astronaut habitats are assumed to provide sufficient shielding from SPEs, for Drake's study, only deep space transits are considered. Because the probability of a SPE occurring is proportional to the time spent in deep space transit, this translates to a 1.7 times higher likelihood that a Short-stay mission will encounter such conditions when compared to the shorter transit times of the Long-stay model (Drake 2009, 69). For both mission models, Drake's study also reveals the need to further research two topics. The first is SPE radiation impacts for proton events of extremely high energy ( $>150\text{MeV}$ ), because such levels have not been well-researched, and may cause acute crew impacts even with a heavily shielded shelter onboard. The second need is that of improving solar weather prediction and notification systems.

(2) GCR exposure

Overall predicted GCR doses are anticipated to be roughly the same between both Long-stay and Short-stay models when one balances the longer deep space transit periods for the Short-stay model with the overall longer duration of the Long-stay model. However, the Short-stay model is still less favored due to the uncertainty surrounding the fact that a larger fraction of the GCR exposure in this model occurs in deep space, where the proportion of heavy ion flux ( $Z>10$ ) is larger (Drake 2009, 67–68). According to Drake's study, further research is required to determine whether heavy ion exposure is likely to cause a more severe or lesser effect on astronaut cancer risks. However, it is also documented that heavy ion exposure is also a chief cause for heart, circulatory, and digestive diseases; as well as latent motor function, behavior, and neurological effects. Here again, the Short-stay model is less favored.

### (3) Mars surface exposure uncertainties

According to Drake's study, the Martian atmosphere provides approximately  $16\text{g/cm}^2$  of equivalent shielding provided by  $\text{CO}_2$  in a vertical direction, and that shielding increases to nearly  $50\text{g/cm}^2$  at lower zenith angles. While this shielding along with the planet's mass are predicted to greatly attenuate the exposure from both SPEs and GCR, for Galactic Cosmic Radiation there is still a certain degree of uncertainty due to a lack of data for secondary neutron production near the Martian surface. This uncertainty translates to higher risk for the Long-stay mission model due to the longer surface stay time (Drake 2009, 68).

Overall, the research reviewed in this chapter indicates that Long-stay mission models may be more favorable from a radiation exposure standpoint. However, this is balanced by the higher mission risk that is inherent in more time spent away from Earth, and by the fact that there are still uncertainties on how the exposure environment on the Mars surface will impact crew.

Next, this paper reviews the shielding methods assumed for various mission architectures and their effectiveness, along with potential new shielding technologies that will further help to reduce exposure.

THIS PAGE INTENTIONALLY LEFT BLANK



## **V. REDUCING RISK OF EXPOSURE THROUGH MISSION SHIELDING TECHNOLOGY**

Shielding is also a key facet of any human Mars mission design in order to maintain astronaut exposure levels as low as reasonably achievable (ALARA). The NASA web article “Real Martians: How to Protect Astronauts from Space Radiation on Mars” provides an excellent summary of the challenges in this arena (Garner 2015). Focusing on GCR mitigation, there is a trade-space between using more/heavier shielding, using lighter and more efficient shielding, and the consideration of when such shielding benefits are negated by the generation of secondary particle radiation which is equally damaging to crew. This chapter reviews a sample shielding design considered for currently proposed Mars mission models, while also discussing some research for new and novel shielding technologies. These new technologies are considered essential for future human missions to Mars to succeed, given the discussions in both this chapter and Chapter III which conclude that current aluminum-focused shielding technologies will not be adequate versus the current space worker exposure limits.

### **A. INITIAL MISSION DESIGN AND SHIELDING ASSUMPTIONS**

Drake’s publications on the Mars Mission Architecture provide an excellent foundation of assumptions for both transit spacecraft and Mars habitat design. The “Human Exploration of Mars Design Reference Architecture 5.0 Addendum” provides detailed consideration of two key alternatives that underlay the design of these modules (Drake 2009). These are the strategy of sending modules to the planet in either a Pre-Deployed configuration, where items not needed by the crew for initial transit are sent to Mars in advance of the crew; and that of the All-Up configuration, where all modules are sent concurrently. All missions operate under the assumption that the following modules will be required:

- Mars transit vehicle—to travel to and from Mars (MTV)
- descent/ascent vehicle (DAV)—to bring the crew for a given mission to and from the surface of Mars. For Short-stay models, this also doubles as the surface habitat.

- surface habitat (SHAB)–separate module for Long-stay missions only
- additional surface equipment–for Long-stay missions only, sent in the same module as the SHAB

### **1. Pre-Deploy Configuration Summary**

For a short-stay mission model, the only unit to be Pre-Deployed is the descent/ascent vehicle. For the first crew, this module would be sent from Earth to Mars orbit approximately one year in advance, in order to confirm its arrival and stability in orbit before the crew is sent. The lead times for subsequent DAVs to be sent may be longer (~2 years) as future launches are timed to find the most energy-efficient opportunities. The DAV will be designed to operate in a minimal configuration while in orbit around Mars awaiting its crew arrival (Drake 2009, 52).

For a Long-stay mission model, two components are Pre-Deployed. The DAV and the SHAB (housing) are deployed such that they arrive at Mars approximately two years before the arrival of the first crew. The DAV is placed in orbit, and the SHAB is landed safely on the Mars surface before transitioning to their minimal operating states. The window to send a second crew’s Pre-Deployed assets closely aligns with the window to send the first crew on its journey to the planet. While this complicates the launch scenario from Earth due to a concurrent launch plan being required, it also provides a unique opportunity not afforded to any other mission model. The second set of modules launches shortly before the launch of the first crew, although this crew will arrive first due to the fast transit trajectory employed. The arrival of the second DAV and SHAB shortly after this provides redundancy. If either the first crew’s DAV or SHAB has experienced a malfunction during their two-year wait at Mars, the crew may use the second set of modules instead. Again, this redundancy is possible in the short-stay/Pre-Deploy model, but it will not work for either of the All-Up models discussed in subsection 2 (Drake 2009, 52–53).

## **2. All-Up Configuration Summary**

The All-Up configuration entails launching all elements for the same Mars mission within the same launch opportunity. It is important to note that these elements would not be launched as part of the same Earth launch vehicle, or be landed on Mars as part of the same vehicle stack, due to the prohibitive mass of such a configuration. Instead, all modules would depart Earth orbit on the same trajectory in order to arrive at Mars at approximately the same time. For a Short-stay mission, only one separate cargo vehicle would be used to transport the DAV from Earth to Mars. This necessitates a crew transit vehicle rendezvous with the DAV in Mars orbit; and vice versa when the crew prepares to return to Earth (Drake 2009, 54).

For the Long-stay mission model, two cargo modules are required in addition to the transit vehicle: the SHAB and the DAV. While it is theoretically possible for these modules to dock in LEO, again the mass of such a large vehicle is prohibitive in terms of the Delta V that would be required to leave Earth orbit. Instead, it is likely all three modules would depart Earth on the same fast transit Mars trajectory and that they could rendezvous in interplanetary space (Drake 2009, 54–55).

## **3. Mass Reference for Transit Vehicles**

The “Mars Design Reference Architecture–Addendum #2” report contains useful assumptions for nominal vehicle masses that may be applied to calculations in Chapter VII of this paper (Drake and Watts 2014, 368-369). Figure 35 contains one such example. It is important to note that the focus of this model is the Mars transit vehicle (MTV), which would be used for crew transport to/from Mars regardless of whether the All-Up or Pre-Deploy mission configuration are chosen. Figure 35 highlights numerous useful values, including mass break-downs by dry mass (vehicle structure and systems), provisions for both normal and contingency operations, and propellant for vehicle maneuvering (as a further note, this break-out does not include the structure or mass for the necessary propulsion stages that would be used to launch the vehicle from Earth, or to initiate the transfer orbit to Mars). According to the DRA 5.0 Addendum #2, the shielding assumptions included in the figure are based on a “protection” baseline of 20

layers of multi-layered insulation (mostly for thermal purposes and not geared to radiation shielding), and a 5.8cm water wall on the crew quarters will also serve as the protective shelter for SPEs. This water-wall is specifically called out with a mass of 603kg, relative to the total module mass which is over 57,000kg. Finally, Figure 35 also provides useful dimensions for the MTV cylinder which may be used for basic shield density calculations and comparisons in Chapter VII.

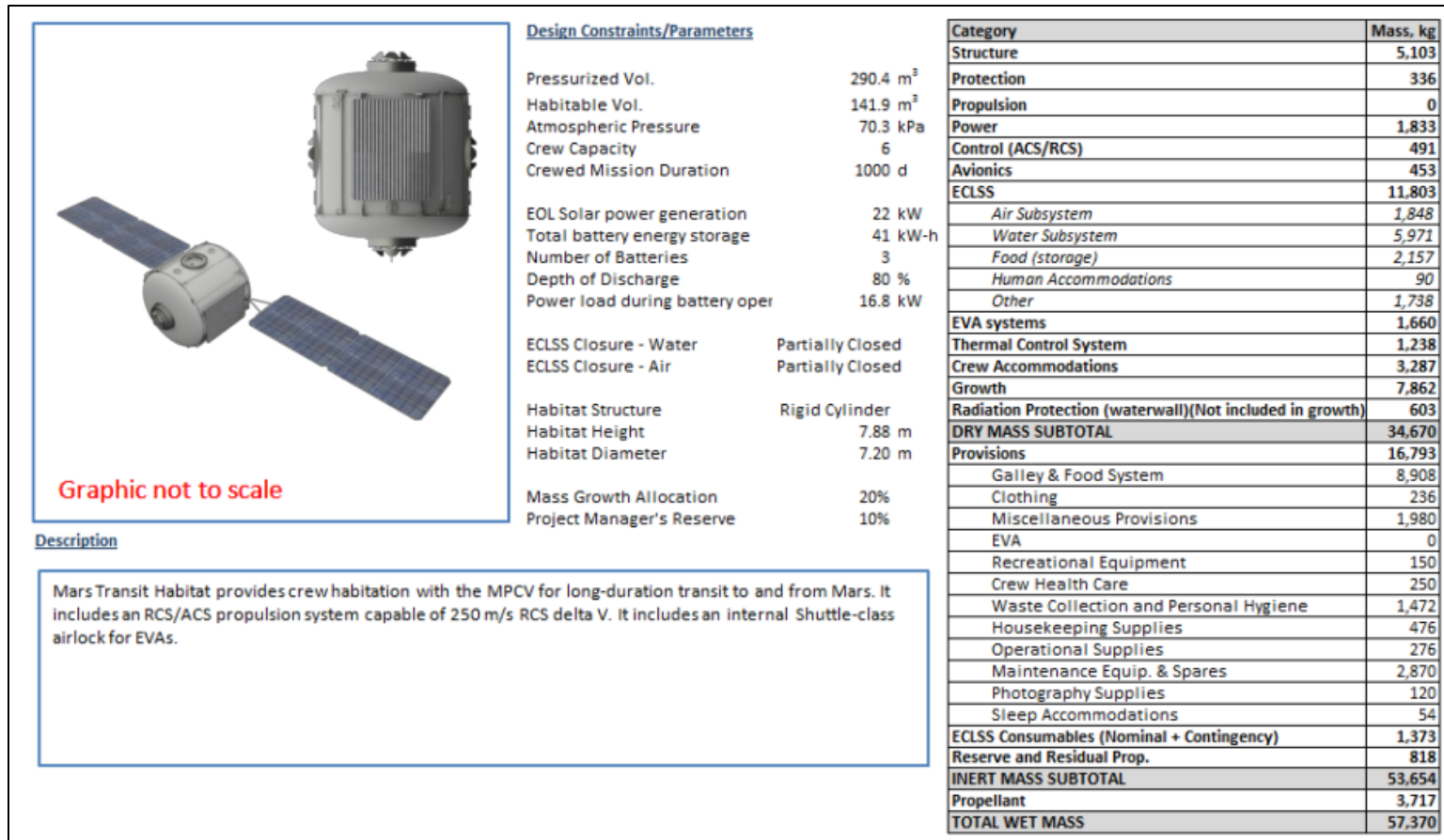


Figure 35. Nominal Six-Person, 1000-Day Duration Mass Allocation Break-Out for Mars Transit Vehicle.  
Source: Drake and Watts (2014, 369).

## B. SHIELDING CONSIDERATIONS FOR MARS SURFACE HABITAT

The Martian atmosphere provides some measure of protection from GCR and SPEs, but operations on the Martian surface also pose additional challenges due to the fact that radiation interacting with the Martian atmosphere, regolith, and even conventional shielding materials like aluminum can also generate secondary neutron radiation, which also poses some level of human risk. Recently, Slaba et al. conducted a study to analyze the thickness at which conventional shielding materials ultimately provide no additional benefit, or even become counter-productive, in mitigating these effects (2013).

The models from this study resulted in the dose comparisons shown in Figure 36. In this figure, the dashed lines denote  $\frac{1}{2}$  free space approximations that demonstrate a simplistic shielding model which assumes that the planet's mass underneath an object or person *on the surface* provides shelter from one half of the radiation flux incoming from space, where that radiation is treated as purely directional with no accounting for back-scatter or the presence of atmosphere or regolith. This simplistic transport model is compared to the solid lines of the Slaba et al. study results which do include atmospheric and regolith scattering effects. Polyethylene is compared to aluminum due to its effectiveness as a neutron attenuator. Equivalent dose rate is shown on the left, as compared to effective dose from the analyzed velocity/energy of the neutron dose received on the right. For review, effective dose may be conceptualized as the biological damage that the dose equivalent is capable of delivering, when scaled by a Quality Factor that is based on radiation particle size and energy. This topic is reviewed at greater length in Chapter III Section B.

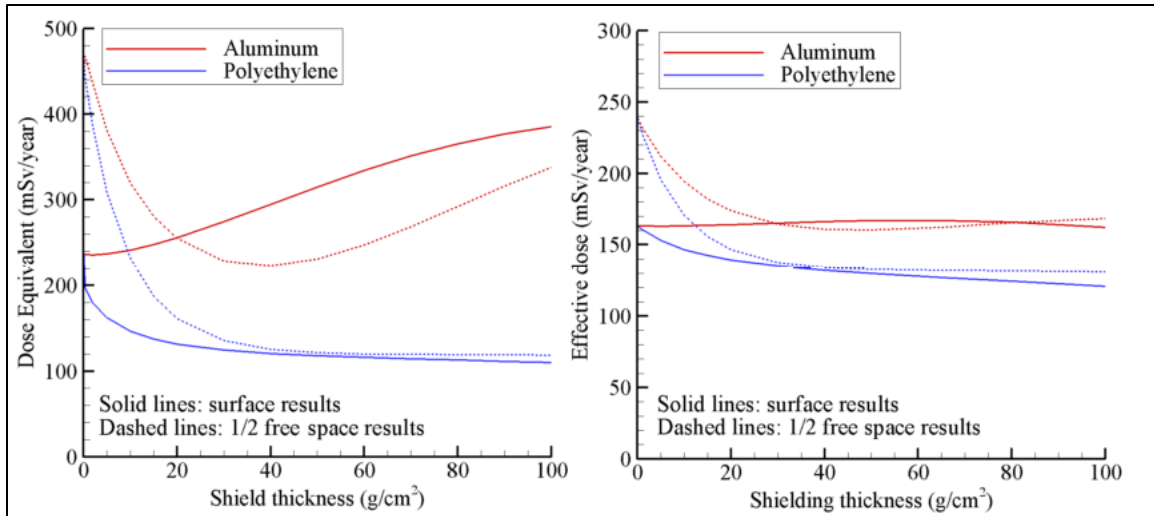


Figure 36. Dose Equivalent and Effective Doses versus Shielding Depth on the Martian Surface Compared to 1/2 Free Space Approximations. Source: Slaba et al. (2013, 6).

The study results highlighted by Figure 36 make two strong cases regarding aluminum shielding. First, in terms of dose equivalent, there is a very clear minimum in free space at 45g/cm<sup>3</sup> shield thickness, and it is clear that some additional shielding benefits may be gained by increasing aluminum shielding thickness in transport vehicles up to that point. Second—while additional aluminum shielding does increase dose equivalent on the Martian surface, ultimately effective dose remains relatively constant. Polyethylene is shown to be slightly more effective than aluminum over comparable thicknesses, but also provides minimal additional benefit at thicknesses over 40g/cm<sup>3</sup>. Slaba et al. conclude that these results indicate that adding or re-arranging shielding masses on the Martian surface will not appreciably reduce effective dose exposure received. They also reveal that even Martian regolith will not provide any worthwhile level of shielding unless several hundred g/cm<sup>2</sup> are used (Slaba et al. 2013, 6). For reference, previous Mars rovers (Pathfinder) determined that the typical density of the regolith was 1.52g/cm<sup>3</sup>, so if one conducts a sample calculation with a required shielding thickness of 300g/cm<sup>2</sup>, the resulting actual regolith thickness would need to be nearly 200cm, or 2m. The study team further suggests that consideration should be given to replacing structural aluminum in the Mars surface habitats with hydrogen-containing

carbon composites, based on the fact that aluminum increases the level of secondary interactions and therefore provides no shielding benefit on the Martian surface. Research on these composite materials is discussed in further detail in Sections C and D of this chapter.

Mars itself may still have some potential to provide in situ use of regolith and other materials for crew and their mission, however. Examples from the Drake “Design Reference Architecture 5.0 Addendum” publication include the generation of additional water, methane, and other propulsion materials (2009). The most relevant counter-point to the study conducted by Slaba et al. is that initial Long-stay missions to the Mars poles may provide the potential use of ice as a shielding material, if the technical challenges of drilling and processing frozen/icy regolith are addressed (Drake 2009, 27). Research has also been conducted on Lunar regolith where samples have been returned to Earth for further study. One study found that Lunar regolith reduces dose by a comparable amount to aluminum for the same shield thickness used (Miller et al 2008). An earlier presentation for the International Lunar Conference predicts that one to two meter thickness of Lunar regolith is an optimal amount to shield from GCR and SPEs while also providing some measure of protection for a habitat from meteorite strikes as well (Lindsey 2003). Further research also shows that Lunar regolith can be utilized in many ways, ranging from sandbags to heat processed ceramic and glass materials, some potentially stronger than steel. Regolith bricks are presented as a means to create not only structures, but also permanent landing pads and roads (Spudis 2011). It stands to reason that many of these same concepts may be attainable in the Martian environment as well.

However, more definitive comparison to the regolith of Mars requires both further testing with simulants created based on the unmanned rover analyses of the Martian soil, along with the eventual return of Martian soil samples to Earth. Current studies are already assessing potential solutions using simulated regolith and polyamide binders (which may also be generated from materials on Mars) in order to generate bricks which could be used to construct habitats or additional shielded chambers on the surface with a minimum of materials being brought from Earth (NASA Science Beta 1998). The use of caves has also been proposed in studies to assess not only the potential of Martian caves



for science and resource utilization, but also as a basis for inflatable habitats which would likely provide better shielding than found on the surface (Boston et al 2003).

Additionally, according to “...Addendum 2.0” of the Drake studies, Martian regolith may also be used to provide direct shielding for radiation sources that the crew may use on the Martian surface, such as a reactor system for power (Drake and Watts 2014, 390). While crew exposure to radiation from reactor-based power systems is not the focus of this paper, it is also worth noting that Drake and Watts account for this by suggesting the placement of significant distance (200m) between any crew habitat and the reactor, in addition to burying the unit in regolith in order to maximize shielding which should keep crew exposure to nominal levels as compared to what they would receive from space (2014, 395-397).

The Drake DRA 5.0 reports also highlight challenges that must be met for a human mission to Mars to be realized. Top among these challenges are the improvements that must be made for health and human factors for both anticipated effects from prolonged low gravity and radiation exposure. Drake summarizes three areas in the sub-topic of radiation exposure that must see improvements in the next 15 years. They are: improved radiation exposure limits, establishment of better space weather forecast systems to shelter from SPEs, and to provide adequate shielding technologies against both GCR and SPEs (Drake 2009, 288). Chapter III reviews the 200-300% margin by which astronauts will exceed existing exposure limits if only existing shielding technologies (chiefly aluminum) are employed. As such, the creative placement of hydrogen-rich mission cargo (water and propellant stores) may be useful to help provide some of this additional shielding; but it is also necessary to consider novel materials that may be used in spacecraft structure, crew garments, and so forth. These novel technologies are detailed in Sections C and D of this chapter.

### C. HYDROGEN-FOCUSED SHIELDING RESEARCH

Garner's web-article also discusses materials under research that have potential applications in spacecraft, in the Martian surface habitat, and even in crew space suits (2015). Hydrogen is an optimal element for such shielding because it works well against particle radiation where the particles are of similar size (protons, neutrons). Hydrogen is also abundant in materials already required for the mission. Water reserves and plastic wastes which are processed into tiles for storage are both examples of materials that could be configured within the spacecraft to provide increased shielding or even a sheltered area for solar events. Maintaining these volumes is challenging, however, as trash is generated over the course of an entire mission, and water is consumed (albeit recycled to a large extent). Polyethylene (also known as high density polyethylene or HDPE) is another hydrogen-rich material that is used for radiation shielding. It is limited by its strength and the fact that it cannot be used for spacecraft structures due to the thermal and launch/landing stresses involved. It is also heavy if added to existing structure (Garner 2015).

Kristina Rojdev and William Atwell completed a study recently for *Gravitational and Space Research* to further analyze different hydrogen-loaded materials for potential shielding benefits (2015). Hydrogen or other gases can be incorporated into lighter-weight shielding materials in multiple ways. First, they can be chemically bonded to the molecules of the material (hydrogenated). Second, they can be "loaded" as stated above, where the gas atoms are incorporated into the molecular structure without the presence of atomic bonds. In this study they compared metal hydrides (MH), metal organic frameworks (MOF), and nanoporous carbon composites (CNT) with the performance of HDPE and more typical spacecraft aluminum shielding as a baseline. An initial study exposed 64 variants of these materials to simulated conditions from the 1989 solar events that are reviewed in Chapter II of this paper. Conditions were chosen to simulate the hardest fluence from these events where the highest fluence and highest energy protons were present. The performance of all materials under these conditions was compared to that of two materials: aluminum which is the traditional shielding material used on older spacecraft, and HDPE which is treated by Rojdev and Atwell as the "standard" of

hydrogen-rich shielding materials for space applications. This study reveals that over 60% of the materials performed better than aluminum—and therefore show promise as multifunctional shields (Rojdev and Atwell 2015, 61).

The next phase expanded the study to 85 materials, and researched the potential of these materials for GCR shielding in addition to SPEs. Also, an additional category was also added to the study—which is that of methane-loaded materials. Methane’s atomic formula is  $\text{CH}_4$ , which means it also possesses enough hydrogen to have potential for shielding. It also has the benefit of being less flammable than hydrogen alone, which is important given these materials will be exposed to significant thermal gradients in a space environment which could cause gaseous materials to come un-bonded from their composites; they could seep into the spacecraft.

Figures 37–39 list the various material formulae tested within each of the categories reviewed at the start of this section, broken down by their loading condition (base or unloaded, hydrogen-loaded, or methane-loaded) along with the density tested and the type(s) of simulated deep-space exposure they received.

MOF			
Loading Condition	Chemistry	Density (g/cm <sup>3</sup> )	Exposure
Base	C <sub>432</sub> H <sub>288</sub> Be <sub>48</sub> O <sub>144</sub>	0.42	GCR
H	C <sub>432</sub> H <sub>1120</sub> Be <sub>48</sub> O <sub>144</sub>	0.46	GCR
Base	Mg <sub>18</sub> O <sub>54</sub> H <sub>18</sub> C <sub>72</sub>	0.91	GCR
H	Mg <sub>18</sub> O <sub>54</sub> H <sub>141</sub> C <sub>72</sub>	0.95	GCR
Base	Al <sub>4</sub> O <sub>32</sub> C <sub>56</sub> H <sub>44</sub>	1.61	GCR
H	Al <sub>4</sub> O <sub>32</sub> C <sub>56</sub> H <sub>96</sub>	1.68	GCR
Base	C <sub>200</sub> H <sub>128</sub>	0.31	GCR
H	C <sub>200</sub> H <sub>325</sub>	0.35	GCR
Base	C <sub>27</sub> H <sub>31</sub> NO <sub>22</sub> Sc <sub>3</sub>	1.03	GCR
H	C <sub>27</sub> H <sub>66</sub> NO <sub>22</sub> Sc <sub>3</sub>	1.07	GCR
Base	Zn <sub>216</sub> C <sub>3132</sub> O <sub>702</sub> H <sub>1242</sub>	0.25	SPE, GCR
H	Zn <sub>216</sub> C <sub>3132</sub> O <sub>702</sub> H <sub>14814</sub>	0.30	SPE, GCR
CH <sub>4</sub>	Zn <sub>216</sub> C <sub>4189</sub> O <sub>702</sub> H <sub>5470</sub>	0.31	SPE, GCR
Base	C <sub>1536</sub> H <sub>864</sub> Cu <sub>96</sub> N <sub>32</sub> O <sub>480</sub>	0.47	SPE, GCR
H	C <sub>1536</sub> H <sub>2734</sub> Cu <sub>96</sub> N <sub>32</sub> O <sub>480</sub>	0.50	SPE, GCR
CH <sub>4</sub>	C <sub>1908</sub> H <sub>2352</sub> Cu <sub>96</sub> N <sub>32</sub> O <sub>480</sub>	0.55	SPE, GCR
Base	C <sub>288</sub> H <sub>96</sub> Cu <sub>48</sub> O <sub>240</sub>	0.95	SPE, GCR
H	C <sub>288</sub> H <sub>531</sub> Cu <sub>48</sub> O <sub>240</sub>	0.99	SPE, GCR
CH <sub>4</sub>	C <sub>362</sub> H <sub>392</sub> Cu <sub>48</sub> O <sub>240</sub>	1.06	SPE, GCR
Base	H <sub>112</sub> C <sub>192</sub> O <sub>128</sub> Zr <sub>12</sub> Ti <sub>12</sub>	1.10	SPE, GCR
H	H <sub>260</sub> C <sub>192</sub> O <sub>128</sub> Zr <sub>12</sub> Ti <sub>12</sub>	1.33	SPE, GCR
CH <sub>4</sub>	H <sub>208</sub> C <sub>216</sub> O <sub>128</sub> Zr <sub>12</sub> Ti <sub>12</sub>	1.17	SPE, GCR
Base	H <sub>112</sub> C <sub>192</sub> O <sub>128</sub> Zr <sub>24</sub>	1.20	SPE, GCR
H	H <sub>260</sub> C <sub>192</sub> O <sub>128</sub> Zr <sub>24</sub>	1.22	SPE, GCR
CH <sub>4</sub>	H <sub>208</sub> C <sub>216</sub> O <sub>128</sub> Zr <sub>24</sub>	1.27	SPE, GCR

\* MOFs are seen as a catch all phrase for periodic nanoporous materials. This is a non-metal, carbon-based framework that does not have the chemical structure of a CNT, has similar properties to MOFs, and large adsorption capacity.

Figure 37. MOF Material Formulas and Densities Used for Radiation Transport Calculations. Source: Rojdev and Atwell (2015, 64).

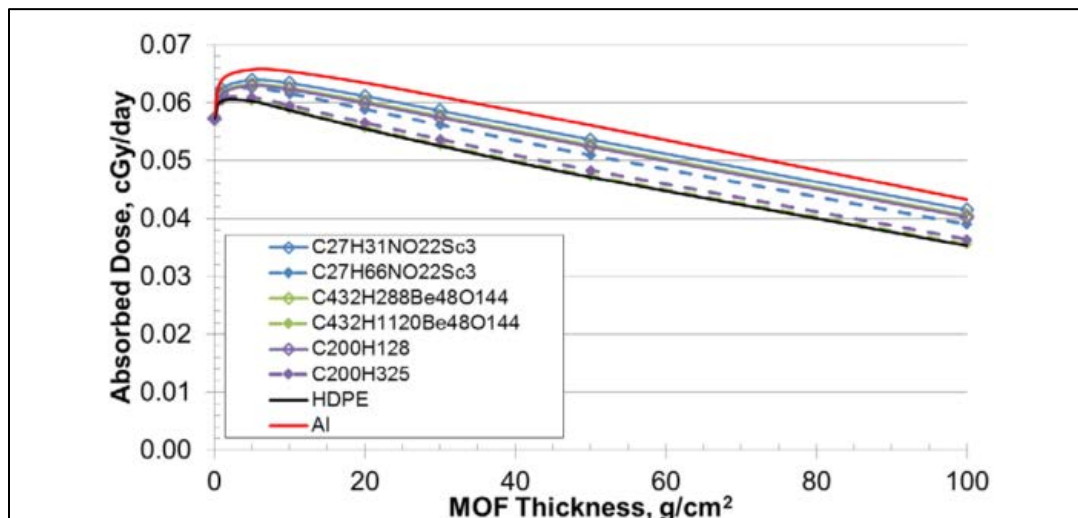
CNT			
Loading Condition	Chemistry	Density (g/cm <sup>3</sup> )	Exposure
Base	C <sub>2</sub> H <sub>4</sub>	0.95	SPE, GCR
Base	(C <sub>2</sub> H <sub>4</sub> ) <sub>97.7</sub> C <sub>2.30</sub>	0.95	SPE, GCR
H	(C <sub>2</sub> H <sub>4</sub> ) <sub>97.7</sub> (CH <sub>3</sub> ) <sub>2.3</sub>	0.95	SPE, GCR
CH <sub>4</sub>	(C <sub>2</sub> H <sub>4</sub> ) <sub>97.7</sub> (CH <sub>4</sub> ) <sub>0.32</sub> C <sub>1.98</sub>	0.95	SPE, GCR
Base	(C <sub>2</sub> H <sub>4</sub> ) <sub>93.27</sub> C <sub>6.73</sub>	0.96	SPE, GCR
H	(C <sub>2</sub> H <sub>4</sub> ) <sub>93.27</sub> (CH <sub>3</sub> ) <sub>6.73</sub>	0.96	SPE, GCR
CH <sub>4</sub>	(C <sub>2</sub> H <sub>4</sub> ) <sub>93.27</sub> (CH <sub>4</sub> ) <sub>0.93</sub> C <sub>5.8</sub>	0.96	SPE, GCR
Base	(C <sub>2</sub> H <sub>4</sub> ) <sub>89.06</sub> C <sub>10.94</sub>	0.97	SPE, GCR
H	(C <sub>2</sub> H <sub>4</sub> ) <sub>89.06</sub> (CH <sub>3</sub> ) <sub>10.94</sub>	0.97	SPE, GCR
CH <sub>4</sub>	(C <sub>2</sub> H <sub>4</sub> ) <sub>89.06</sub> (CH <sub>4</sub> ) <sub>1.51</sub> C <sub>9.43</sub>	0.97	SPE, GCR
Base	(C <sub>2</sub> H <sub>4</sub> ) <sub>79.41</sub> C <sub>20.59</sub>	1.00	SPE, GCR
H	(C <sub>2</sub> H <sub>4</sub> ) <sub>79.41</sub> (CH <sub>3</sub> ) <sub>20.59</sub>	1.00	SPE, GCR
CH <sub>4</sub>	(C <sub>2</sub> H <sub>4</sub> ) <sub>79.41</sub> (CH <sub>4</sub> ) <sub>2.84</sub> C <sub>17.75</sub>	1.00	SPE, GCR
Base	(C <sub>2</sub> H <sub>4</sub> ) <sub>63.16</sub> C <sub>36.84</sub>	1.04	SPE, GCR
H	(C <sub>2</sub> H <sub>4</sub> ) <sub>63.16</sub> (CH <sub>3</sub> ) <sub>36.84</sub>	1.04	SPE, GCR
CH <sub>4</sub>	(C <sub>2</sub> H <sub>4</sub> ) <sub>63.16</sub> (CH <sub>4</sub> ) <sub>5.08</sub> C <sub>31.76</sub>	1.04	SPE, GCR
Base	(C <sub>2</sub> H <sub>4</sub> ) <sub>50</sub> C <sub>50</sub>	1.10	SPE, GCR
H	(C <sub>2</sub> H <sub>4</sub> ) <sub>50</sub> (CH <sub>3</sub> ) <sub>50</sub>	1.11	SPE, GCR
CH <sub>4</sub>	(C <sub>2</sub> H <sub>4</sub> ) <sub>50</sub> (CH <sub>4</sub> ) <sub>6.9</sub> C <sub>43.1</sub>	1.10	SPE, GCR
Base	(C <sub>2</sub> H <sub>4</sub> ) <sub>39.13</sub> C <sub>60.87</sub>	1.16	SPE, GCR
H	(C <sub>2</sub> H <sub>4</sub> ) <sub>39.13</sub> (CH <sub>3</sub> ) <sub>60.87</sub>	1.17	SPE, GCR
CH <sub>4</sub>	(C <sub>2</sub> H <sub>4</sub> ) <sub>39.13</sub> (CH <sub>4</sub> ) <sub>8.4</sub> C <sub>52.49</sub>	1.16	SPE, GCR

Figure 38. CNT Material Formulas and Densities Used for Radiation Transport Calculations. Source: Rojdev and Atwell (2015, 65).

MH			
Loading Condition	Chemistry	Density (g/cm <sup>3</sup> )	Exposure
Base	Li <sub>2,35</sub> Si	1.67	GCR
H	91% Li <sub>2,35</sub> Si and 9% H	0.84	GCR
Base	LiB	1.65	GCR
H	91% LiB and 9% H	0.67	GCR
Base	CaNi <sub>5</sub>	6.60	GCR
H	96% CaNi <sub>5</sub> and 4% H	6.6	GCR
H	CaNi <sub>5</sub> H <sub>6</sub>	5.01	GCR
Base	LaNi <sub>4,7</sub> Al <sub>0,3</sub>	8.00	GCR
H	LaNi <sub>4,7</sub> Al <sub>0,3</sub> H <sub>6</sub>	6.08	GCR
H	96% LaNi <sub>4,7</sub> Al <sub>0,3</sub> and 4% H	7.6	GCR
Base	LaNi <sub>4,8</sub> Sn <sub>0,2</sub>	8.40	GCR
H	LaNi <sub>4,8</sub> Sn <sub>0,2</sub> H <sub>6</sub>	6.38	GCR
H	96% LaNi <sub>4,8</sub> Sn <sub>0,2</sub> and 4% H	8.4	GCR
Base	LaNi <sub>5</sub>	8.20	GCR
H	LaNi <sub>5</sub> H <sub>6</sub>	6.22	GCR
Base	Al <sub>2</sub> Cu	5.83	GCR
H	Al <sub>2</sub> CuH	5.39	GCR
Base	Al	2.70	GCR
H	AlH <sub>3</sub>	2.5	GCR
H	BaAlH <sub>5</sub>	3.30	GCR
H	SrAl <sub>2</sub> H <sub>2</sub>	2.64	GCR
Base	Ti <sub>0,98</sub> Zr <sub>0,02</sub> V <sub>0,48</sub> Fe <sub>0,09</sub> Cr <sub>0,05</sub> Mn <sub>1,5</sub>	7.20	GCR
H	Ti <sub>0,98</sub> Zr <sub>0,02</sub> V <sub>0,48</sub> Fe <sub>0,09</sub> Cr <sub>0,05</sub> Mn <sub>1,5</sub> H <sub>3,3</sub>	5.80	GCR
Base	TiCr <sub>1,8</sub>	5.70	GCR
H	TiCr <sub>1,8</sub> H <sub>3,5</sub>	4.50	GCR
Base	TiFe <sub>0,9</sub> Mn <sub>0,1</sub>	6.50	GCR
H	TiFe <sub>0,9</sub> Mn <sub>0,1</sub> H <sub>2</sub>	5.20	GCR
H	LiAlH <sub>4</sub>	0.92	GCR
H	LiMg(AlH <sub>4</sub> ) <sub>3</sub>	1.80	GCR
H	Mg(AlH <sub>4</sub> ) <sub>2</sub>	2.24	GCR
H	NaAlH <sub>4</sub>	1.81	GCR
H	Y <sub>3</sub> Al <sub>2</sub> H <sub>6,5</sub>	4.10	GCR
Base	V	6.00	GCR
H	VH	5.60	GCR
H	VH <sub>2</sub>	2.30	GCR
Base	Li	0.53	GCR
H	80% Li and 20% H	0.57	GCR
H	85% Li and 15% H	0.56	GCR
H	90% Li and 10% H	0.55	GCR
H	95% Li and 5% H	0.54	GCR

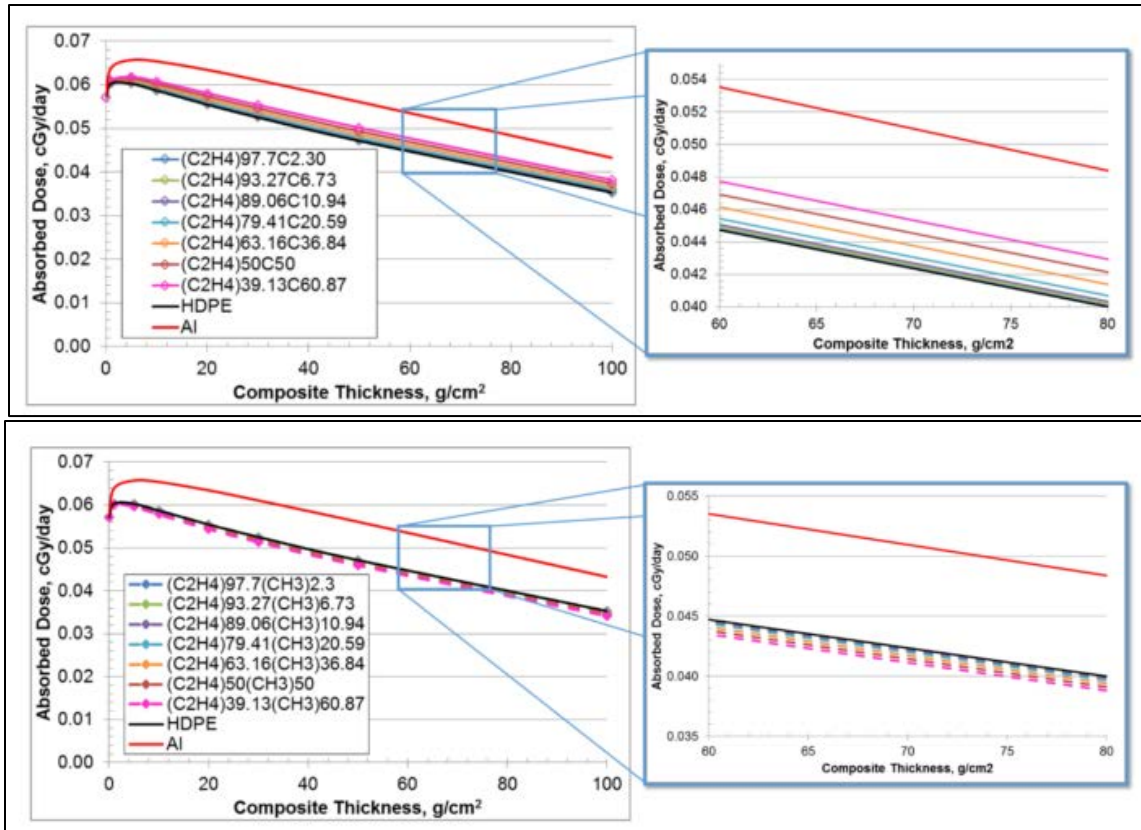
Figure 39. MH Material Formulas and Densities Used for Radiation Transport Calculations. Source: Rojdev and Atwell (2015, 66).

Highlights of the results of this research are shown in Figures 40–42, which compare the absorbed dose curves versus shielding thickness for the materials tested to those of aluminum and HDPE, with hydrogen-loaded variants of each material denoted with dashed lines. For reference, the provided units of centiGray (cGy) per day are equivalent to 10mSv/day. Given most quantities in these figures are on the order of one to ten hundredths of a cGy per day, the overall dose rates are relatively small. One detail to note on all charts is the fact that the net improvement seen in absorbed dose rate between aluminum and all of the composites tested is only approximately one hundredth of a centigray per day—which is relatively small. However, this difference calculated out over a 1000-day mission could still equate to a difference in total dose received of hundreds of Rem. These calculations are considered at greater length in Chapter VII.



Note: selected MOF for further calculation in this paper =  $C_{432}H_{1120}Be_{48}O_{144}$ , the green dot curve just about the black HDPE curve in this chart.

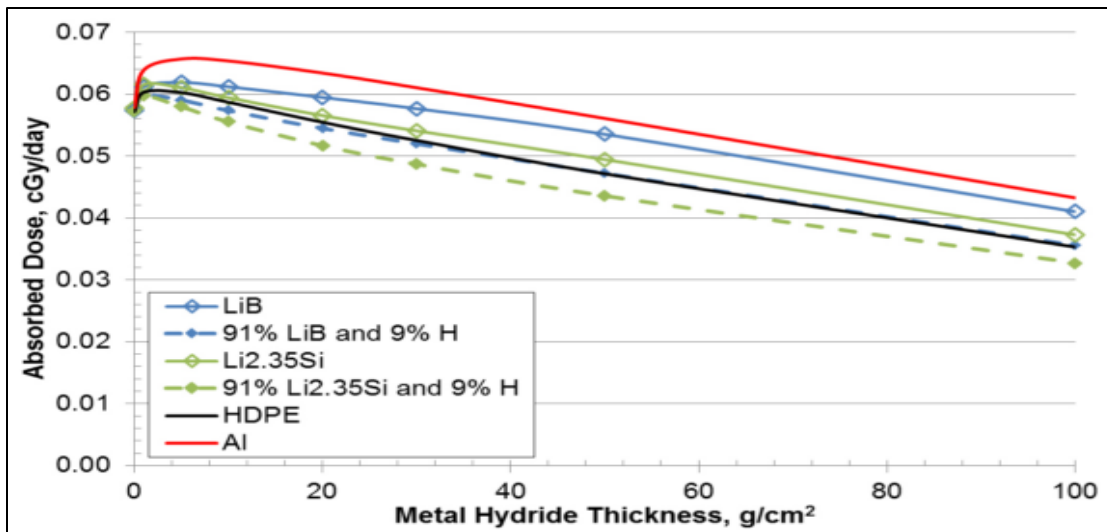
Figure 40. Selected MOF Shielding Effectiveness Results Compared to Conventional Materials for GCR. Source: Rojdev and Atwell (2015, 68).



Note: In this figure, the lower results with the dashed lines are for the hydrogen-loaded variants of the same materials shown in the upper images. The best performing hydrogen-loaded variant (C<sub>2</sub>H<sub>4</sub>)39.13%(CH<sub>3</sub>)60.87% will be used for calculations as needed in Chapter VII of this paper. It is the bright pink dashed line at the bottom of the data displayed.

Figure 41. Selected CNT Shielding Effectiveness Results Compared to Conventional Materials for GCR. Source: Rojdev and Atwell (2015, 69).





Note: these results focuses on lithium-based metal hydrides, which overall showed higher shielding effectiveness than those with other metal hydride bases. The 91%  $\text{Li}_{2.35}\text{Si}$  and 9% H hydride will be carried forward for further assessment in Chapter VII. It is the green dashed line at the bottom of the curves displayed.

Figure 42. Selected MH Shielding Effectiveness Results Compared to Conventional Materials for GCR. Source: Rojdev and Atwell (2015, 70).

Next, Figures 43 and 44 show the results of selected MOFs and CNTs where hydrogen loaded variants (in dashed lines) are compared to their equivalent methane-loaded versions (dotted lines), and to their base versions (solid lines). In this case the materials were subjected to the higher doses that would be encountered in a worst-case (1989-equivalent) series of SPEs. The figures demonstrate that for MOFs, hydrogen and methane loaded materials demonstrate similar performance. However, for CNTs, in many cases hydrogen loaded versions are still superior (for example, the inset on Figure 44, the longer dashed lines in purple and green for the hydrogen loaded versions of two formulae are still the lowest or best-performing curves on the chart when compared to the smaller dotted line curves for their methane-loaded equivalents).

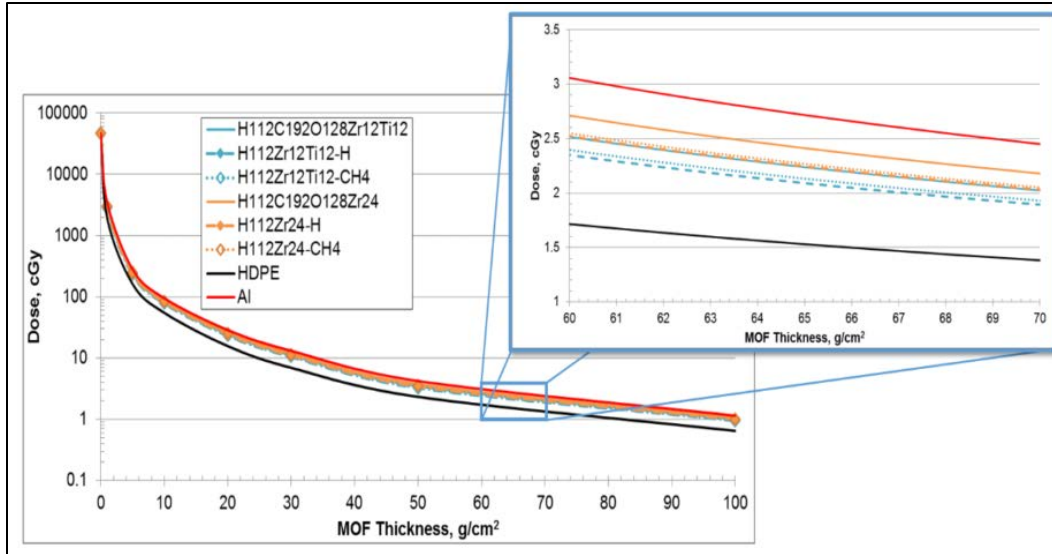
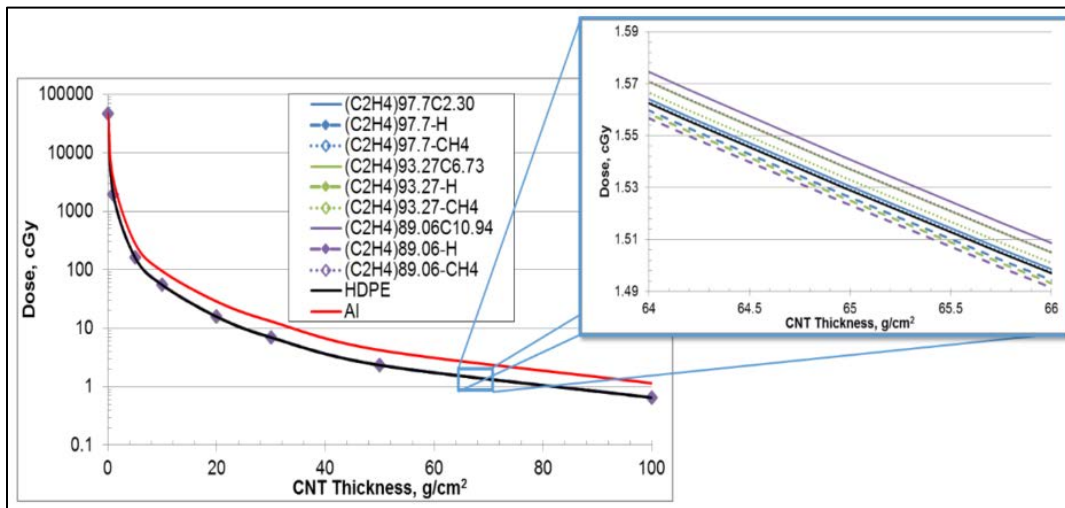


Figure 43. Selected Base, Hydrogen, and Methane-Loaded MOF Shielding Effectiveness Results for SPEs. Source: Rojdev and Atwell (2015, 72).



Note: A methane loaded CNT, (C<sub>2</sub>H<sub>4</sub>)89.06%CH<sub>4</sub>, shows the most promising performance in this figure. It is the purple dotted line on the right inset of this chart.

Figure 44. Selected Base, Hydrogen, and Methane-Loaded CNT Shielding Effectiveness Results for SPEs. Source: Rojdev and Atwell (2015, 73).

While not shown here, equivalent tests were in performed in Rojdev and Atwell's study to compare base, hydrogen-loaded, and methane-loaded materials for shielding performance while exposed to GCR. These tests yielded comparable results, where MOF

materials were largely equivalent between hydrogen or methane-loaded variants; and that for CNTs sometimes hydrogen-loaded versions were still superior.

Overall, while the studies revealed that a majority of the materials tested would out-perform aluminum as a shielding material, many were comparable to HDPE (the CNT category especially)—while a few MH materials were actually superior to it. It was also shown that in most cases, methane-loaded materials had comparable performance to those loaded with hydrogen. Shielding densities from the results of this study are applied in Chapter VII of this paper to further calculate optimal solutions.

#### **D. ADVANCED LIGHTWEIGHT SHIELDING RESEARCH**

The search for lighter weight materials culminates in materials such as hydrogenated boron nitride nanotubes (BNNTs)—which combine the benefits of hydrogen interspersed throughout a nanotube structure along with the benefits of boron which is an excellent absorber of secondary neutrons, and a material which is flexible enough to both be used in structural applications and also in yarn for fabrics (Garner 2015). Boronated materials have been applied in Earth-based shielding technologies for years, with one example being boronated polymer panels which are commonly used for nuclear plants. As discussed in Section B of this chapter, high density polymers (HDPEs) such as these are not strong enough for structural applications, and are also impractical for space use both due to their weight and the fact that they also possess off-gassing and flammability concerns.

Dr. Sharon Thibault et al. recently conducted a study to compare the shielding effectiveness of BNNT to more conventional materials (2012). This study reviewed the additional benefits of BNNTs as compared to other conventional shielding materials such as HDPE. These benefits include (Thibault et al. 2012, 3-4):

- the capacity to be manufactured at structural grade, with potential stability in air at temperatures of up to 800C
- nanotube structure which is favorable for hydrogen-loading
- low density (1.3-1.4g/cm<sup>3</sup>)

- molecular structure which permits them to be incorporated into polymers and as a resin matrix in structural composites

The study focused on two formats for BNNTs. The first are those with hydrogen stored (loaded) into their nanotube structure, in varying percentages. Second are hydrogenated BNNTs, where hydrogen is elementally bonded to the boron or nitrogen in the molecular structure. The results of these studies are extremely promising, as summarized in Figure 45. This figure shows that even a 5% loaded BNNT material will out-perform other conventional shielding materials at reducing GCR dose rate, where all materials are modeled for a 30-cm thickness. Figures 46 and 47 show how 20% loaded BNNTs (referred to as BN+20% wt. H<sub>2</sub>) are shown to outperform all other materials with the exception of liquid hydrogen (which is not a practical shielding material due to liquid state and flammability)—both at reducing GCR dose rate and at minimizing the dose received from a model of the 1972 worst-case Solar Particle Event.

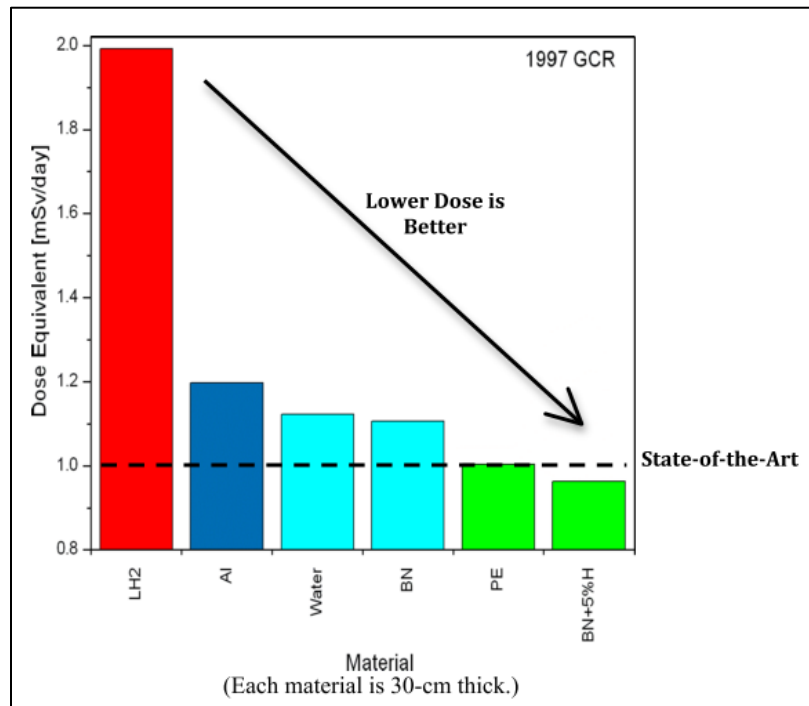


Figure 45. Effectiveness of 5% BNNT against GCR Exposure Compared to Conventional Shielding Materials. Source: Thibeault et al. (2012, 5).

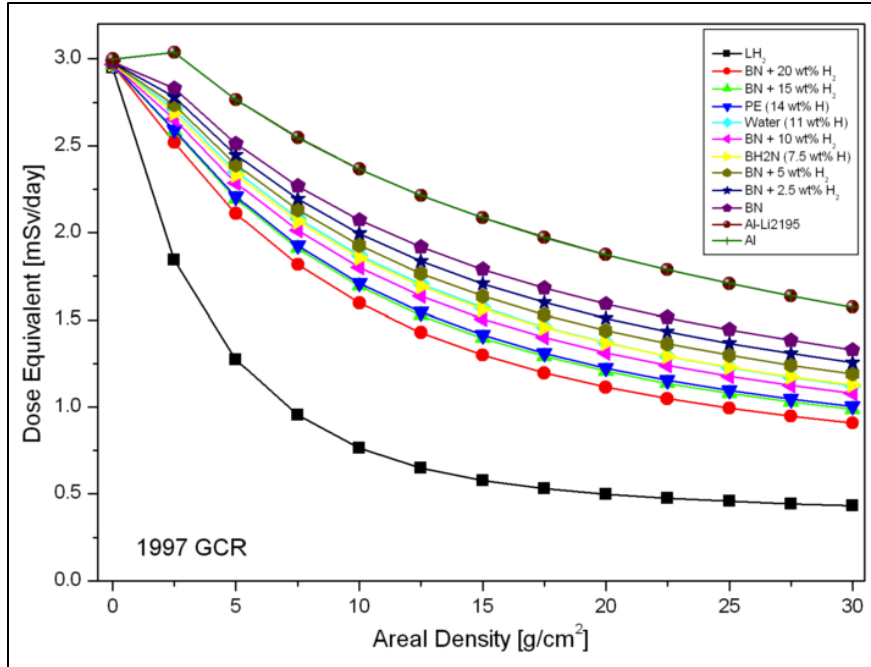


Figure 46. Effectiveness of Selected BNNTs against GCR Exposure Compared to Conventional Shielding Materials. Source: Thibeault et al. (2012, 6).

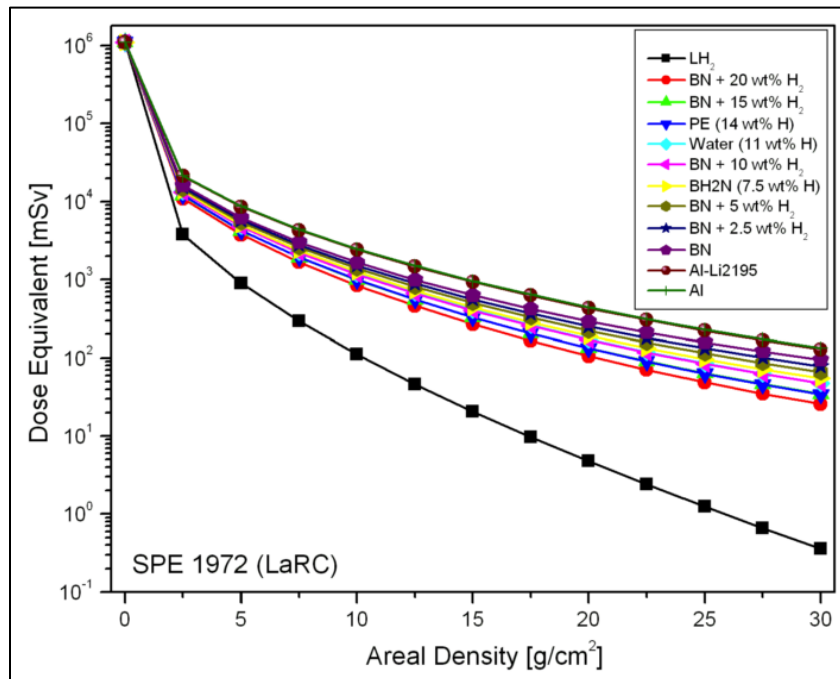


Figure 47. Effectiveness of Selected BNNTs against SPE Exposure Compared to Conventional Shielding Materials. Source: Thibeault et al. (2012, 7).

It is important to note that this study was conducted in 2012, and assessed BNNTs at a technology readiness level (TRL) of 1–2, with a 10-year timeframe for full (TRL 9) capability.

#### **E. FIELD-BASED SHIELDING RESEARCH**

Spacecraft-generated energy fields are also under investigation as a means to deflect radiation, but currently the energy needs for such a system would be prohibitive (Garner 2015). The research for such methods continues but is unlikely to be employed on the 2040-timeframe Mars missions due to the lack of current technical maturity.

While numerous technologies revealed in this chapter show potential to help reduce exposure levels for astronauts, cost factors for some of them are not well documented now. These cost factors are also two-fold, in the sense that additional shielding systems not only have costs of their own, but more significantly that they would add varying degrees to launch mass which impacts mission cost even further due to the fuel mass required to place the extra cargo into orbit. Launch mass from various shielding materials densities is further compared in the trade analysis in Chapter VII. To further control the amount of shielding and therefore mass that will be required for Mars mission spacecraft and habitats; medical technology is also considered as a means to mitigate the impact of radiation exposure. This discussion is continued in Chapter VI.

## **VI. REDUCING IMPACTS OF EXPOSURE THROUGH MEDICAL COUNTERMEASURES**

According to Epelman’s article “Medical mitigation strategies for acute radiation exposure during spaceflight,” medical mitigation of radiation exposure in space is broken into two topics: primary and secondary prevention (2006, 131). Primary prevention includes the selection of astronauts who inherently have lower risk of cancer and other radiation-induced effects. This is reviewed both in Chapter III and in Section A of this chapter, along with the ethical implications of using such methods. Secondary prevention encompasses two areas based on the assumption that astronauts on missions *will* be exposed. Exposure may be reduced with methods like improved shielding and early warning systems combined with storm shelters, as reviewed in Chapter V. Another key topic under study to mitigate astronaut radiation exposure on deep space missions is that of medical countermeasures. This primarily includes the field of radio protective compounds, or prophylactics, where numerous studies are currently underway to determine which medical treatments may help to protect key organs/tissues from the more damaging effects of radiation exposure.

### **A. ETHICAL GUIDELINES FOR SPACE EXPLORATION**

From an over-arching standpoint, NASA Space Worker regulations are developed from the stand point of maintaining these four key principals (NCRP 2014, 48):

- provide a good (beneficence);
- prevent a harm (non-maleficence);
- respect one’s autonomy (autonomy), and
- act fairly (justice)

NCRP Commentary 23 further details the basis of each principal given prioritizing one item from the list over the other is often the biggest challenge. Providing good is an obvious goal of exploration class space missions for the sake of gaining scientific knowledge and advancing ourselves as a species. Preventing harm is the basis for the

existing 3% REID at 95% confidence limit for radiation exposure received by astronauts throughout their mission(s).

The principal of autonomy is a complicated matter because it impacts both NASA as an organization and the individual space worker. On the one hand, NASA is obligated to be transparent with potential space crew about the risks they will be assuming. It also follows that in order for NASA to make informed decisions about crew selection, that potential crew members must be transparent with the organization about factors that may affect their individual health. Revealing family history for cardiovascular disease or cancers, or being open about prior non-NASA radiation exposure are both examples of this point (NCRP 2014, 48-50).

More complicated, however, are other forms of transparency that currently fall within the Genetic Information Non-Discrimination Act (GINA) 2008 prohibition on using genetic screening as a mission selection factor. The NCRP Commentary #23 provides the basis on which GINA was written, which is that genetic susceptibility only provides a small portion of the likelihood that someone may develop a given cancer. Other non-genetic factors can be argued to be more significant than the risks assessed by individual genetic sequence differences overall. However, this report also makes a case that further NASA assessment is required for the potential ethical implications of more advanced phenotypic assays in which researchers can screen for full cellular response to radiation exposure *ex vivo*, i.e., outside the body (NCRP 2014, 42). These screening methods may provide a far more accurate assessment of individual cancer susceptibility in the near future, which again raises the discussion of NASA's responsibility for known risks as follows:

From a stand point of *paternalism*, NASA has a duty to prevent astronauts from making decisions that have the potential to cause themselves greater harm in the long run. As such, it is legal and responsible to screen out a potential crew member who might otherwise prefer to make the autonomous decision to take on higher radiation exposure/risk for the sake of career progression or further scientific pursuit. This decision is also legal from the standpoint of NASA not only being responsible for whether a crew member dies prematurely back on Earth, but for the sake of protecting fellow crew and



mission assets from potential acute effects that could occur mid-mission (NCRP 2014, 51). But such principals may cause further ethical (integrity) issues as they may encourage certain crew to try to “beat the system” by leaving personal dosimetry devices in more heavily shielded areas of a space craft, and so forth. This balance of allowing crew members the autonomy to choose whether to accept a higher level risk versus the paternalism of limiting lifetime exposure is further challenged by the facts reviewed in Chapter III of this paper, where it is currently known that astronauts on a mission to Mars will potentially exceed the current REID limits by 200–300%.

The principal of justice brings further nuance to the ethical debate. On the one hand, it may be assumed that all potential crew should be treated equally, which would seem to contradict outwardly unfair practices such as screening woman of reproductive age out of longer duration space flights in favor of older men. However, from the standpoint of *equitable* treatment this is justified because NASA also has a responsibility to limit the risk of the entire crew for each mission. As such, individual crew risks like those that are increased based on gender and age must be considered. This is what allows the NCRP and NASA to set career exposure limits for both genders that increase incrementally with age. This can further be justified when one considers the premise of *retributive justice* in which NASA is obligated to repay crew or family if a “wrong” is committed. Premature cancers or deaths could be interpreted as a “wrong”—which could require a combination of workman’s compensation or other benefits paid out to a crew-member and their family. Based on this, it can be argued that NASA is therefore correct in discriminating crew selection based on age/gender and tiered exposure limits in order to mitigate this risk (NCRP 2014, 52–54).

## **B. MEDICAL COUNTER-MEASURES**

The *Scientific American* article “Radioactive Omission: Where Are the Anti-Radiation Drugs?” provides further overview of the challenges involved with producing other/better drugs (Harmon and Diep, 2011). Some medicines, such as potassium iodide, have a long history of use in nuclear accidents as a means to “load” certain vulnerable organs like the thyroid with a benign form of iodine in order to mitigate the damaging

effects of radioactive iodide encountered in such an exposure. Still though, methods like this are less optimal for space exposure because (a) they are limited to counteracting the effects of a specific radioactive ion alone, and (b) because they must be given after the exposure is received versus attempting to prevent the potential for damage before. A detailed study by Anzai et al. following the Fukushima-Daiichi accidents helps to describe the three basic categories of radioactive treatment drugs (2016, 6–7):

- *Protectants* are compounds for prophylaxis that are taken in advance of exposure in order to prevent injury from occurring.
- *Mitigators* are compounds that are administered just after exposure in order to decrease the anticipated radiation injury.
- *Treatments* are compounds that are administered after the appearance of radiation injury in order to reduce the symptoms or to help the body heal more effectively.

One example of an existing prophylactic recommended for use in advance of an anticipated acute radiation exposure in space is Amifostine (Epelman 2006, 132). This FDA-approved compound works to reduce ionizing radiation damage to exposed tissues by scavenging the free radicals (again, atoms that have unpaired valence electrons and are therefore highly reactive) that are generated as a result of acute radiation exposure. It is commonly administered to first line responders for radiological emergencies on Earth, and recent randomized studies have shown that it reduces both damage to esophageal/oral/rectal tissues along with bladder toxicity, and also acute effects such as fever or lung inflammation following significant exposure. It has also been used during cancer therapy to help prevent radiation damage to salivary glands. The drug is administered subcutaneously, and will work effectively even if given just minutes before the anticipated exposure. However, it is important to note that this type of counter-measure again requires an early warning system such that the drug may be administered before the exposure occurs.

Further, even FDA approved drugs are not without potentially significant side effects. According to the website “Amifostine - FDA prescribing information, side effects and uses” (Drugs.com, 2016a), there have been serious adverse reactions to the drug including cutaneous reactions (some involving necrosis and fatality), and anaphylaxis.

The page even notes that cutaneous reactions are more frequent in cases where the drug is used as a radiation protectant. Nausea is also a side effect that occurs at a severe level up to 20% of patients during initial use. Side effects such as these may be remedied on Earth where there are hospitals and more supplies available to provide treatment. However, in deep space or on Mars where less medical resources will be available, they must be considered more carefully in terms of the trade-offs of the benefits provided.

Radioactive counter-measures that fall under the categories of *mitigation* and *treatment* must be considered with regard to other damage that results in the event of acute radiation exposure. The chief symptoms of concern include damage to bone marrow which impacts white blood cell and platelet generation, and therefore increase the risk of significant internal bleeding or infection. More severe doses can also impact the lining of the stomach and the central nervous system. In regard to the damage resulting to bone marrow, Harmon and Diep's article reviews the potential of a drug called Filgrastim (branded Neupogen) which stimulates the bone marrow to more rapidly replenish white blood cells (2011). This still fails to address the risks of internal bleeding. According to the web article "FDA Approves Radiation Medical Countermeasure" (U.S. Food & Drug Administration, 2016), in March of 2015 Neupogen was approved for use as a treatment in cases of myelosuppressive radiation doses which cause the symptoms described here. The drug can be administered subcutaneously. Again however, this treatment is not without side effects that could be more difficult to address in space. According to "Neupogen" (Drugs.com, 2016b), significant side effects for this treatment include severe allergic reactions, spleen enlargement with risk of rupture, and capillary leak syndrome.

Harmon and Diep also detail other drugs are also under development for use just before or for the longest safe duration of administration after severe radiation exposure (2011). CBLB502 (also known as Entolimod) is one example, and has shown potential to protect primates from damaging effects for up to 48 hours after exposure. Another drug called Ex-RAD (also known as Recilisib) has shown potential in mice for preventing the damage from radiation if administered either pre- or post-exposure—and may even have potential to mitigate damaging effects if administered with as long as there is a 24-hour

delay after the exposure. Another drug, CLT-008 (also known as Romyelocel-L), also shows great promise for white blood cell regeneration, and it can be given as far as three to five days after an exposure while still being effective. For Long-stay Mars missions, all of these methods potentially could mitigate the risk of crew taking longer trips away from their primary habitat if they were to encounter a Solar Particle Event or some other acute exposure during that time.

All of these drugs are not without their drawbacks however. All three of the delayed options above must be administered by either injection or intravenously in their current forms. It is quite likely that a mission to Mars will require this level of medical care facility as part of the cargo anyway, so in general this should not be a concern. Some of the compounds require refrigeration (Harmon and Diep 2011). In general, storage and dosing for these medicines would be manageable within transit module or surface habitat, but not on longer duration surface exploration missions, which may be a factor in determining how far/long such EVAs could go.

A second and more significant challenge is that of clinical trial so that these medicines can be approved for crew use. For background, the FDA approval process entails years of drug development and then pre-clinical research; and then three phases of clinical trials in which the medicine is trialed first in healthy subjects for side-effects analysis, and then in small and then large groups of subjects who have the condition being treated. Last, the drug must pass an approval process that also takes one to two years. Overall, the entire process from initial development to release may take as much as 25 years.

To date, only Amiphostine and Neupogen have been approved by the FDA for use. A recent press release shows that Entolimod recently passed one Phase I clinical trial, with a second Phase I trial and a double blind Phase II trial currently in progress (Levine 2015). The article “Recilisib (Ex-Rad)” states that this drug has only completed four Phase I clinical trials with both subcutaneous and oral forms of the drug (2016). CLT-008 has also only recently completed Phase I and II developmental studies (Cellerant Therapeutics 2016).

For all of these medicines, a large share of the testing for effectiveness was also conducted on rodents or primates only, given human trials are only permitted for the purpose of determining safety versus side effects alone. Some of them have caused significant side effects for human use as described in this section—and unfortunately their effectiveness for humans versus radiation exposure will never be assessed via large-scale trials because it is unethical to dose humans with radiation intentionally to judge their effects (Harmon and Diep 2011). As such, further long term studies will instead be required to better gauge the effectiveness of each medication versus typical incidence levels of long term cancers or late-onset radiation exposure effects.

While all of these medicines have the potential to provide huge benefit for exposure mitigation for the trade of relatively little cargo space/weight in space, the biggest challenge before a 2040-timeframe mission to Mars will be whether the newer ones can complete trials and review to be approved for use or not. Even if they are, their effectiveness in humans will not be well-quantified which arguably leaves a large level of uncertainty in the risks of their use. For example, even the Phase I and II clinical trials described in the preceding paragraphs were only conducted on small groups of individuals (groups of nine up to 150) who were selected for the trials based on having certain types of cancers or tumors. Thus, for all of these drugs (even those released), the trial results are not entirely conclusive which increases the need for follow-on monitoring, and the potential risks they could pose for astronauts in space if unforeseen side-effects or toxicity from dosing were to occur.

A final complication that merits mention is the fact that all formulated medications are also limited by their shelf life in which they will work consistently as prescribed. The NASA Space Medicine web page overviews further research which is in progress to ascertain whether some medications can be formulated from substrates with longer shelf lives either in space or on Mars. The next step is even more ambitious—to determine whether a core set of substrates could be used by computer and software driven tools to generate new formulae in the event that new medicines are developed on Earth after a mission has already departed.

Even without these technologies, however, for the minimal weight required it should be worthwhile to invest in such capabilities on any future Mars mission as an additional layer of protection. The schedule risk that these medications contribute verses their potential to be viable for the first manned missions in the 2040 timeframe is reviewed in Chapter VII where the trade space of all radiation mitigation strategies is also discussed.

## VII. DETERMINATION OF OPTIMAL SOLUTIONS

This chapter reviews the key costs and benefits in each category of architecture/shielding/medical alternatives discussed in the prior chapters. In any systems trade analysis, the pros of each alternative (chiefly, how effectively each method reduces exposure or impact of exposure) must be weighed against the cons (additional factors to launch weight, cost, technology maturity level versus planned mission time frame, medical side effects, etc.). Given the complexity of the scenarios under assessment, decision matrices are an excellent tool to weigh different methods against the others in order to draw conclusions as to which methods may yield the most promising solutions. These matrices must assess a combination of qualitative data as provided for many alternatives still in their conceptual stages, and some quantitative data which in many cases carries a high degree of uncertainty due to the early stages of such studies and the lack of practical data from actual missions to deep space. This chapter uses a combination of risk method assessments and a decision making tool known as swing weights, which provides the optimum flexibility needed to assess such diverse/varied data, along with the flexibility to adjust the weighted values in the decision matrices in order to better assess the sensitivity of the resulting solutions.

### A. OVERVIEW OF RISK-INFORMED DECISION MAKING METHOD

This work employs the NASA Risk-Informed Decision Making (RIDM) method in order to assess the complex array of exposure reduction alternatives that are outlined in Chapters III through VI. The NASA RIDM Handbook outlines four key mission execution domains that must be considered relative to the potential impacts of each alternative (Dezfuli et al. 2010, 11):

1. **Safety:** in this paper the focus of safety is to lower astronaut radiation exposures below existing limits if possible, and to mitigate exposure risks to the greatest extent possible. This is a dominant goal relative to the others listed here.
2. **Cost:** as outlined in earlier chapters, any alternative under consideration that impacts launch mass which equates to required fuel mass (at a rate of approximately 10x every pound of cargo launched), are the largest drivers

of cost. A secondary consideration may be cost of research and development for less mature medical or shielding technologies.

3. **Technical:** the missions to Mars will likely use a huge variety of new technologies in the context of the shielding and medical countermeasure research outlined here. The newer and less-proven the technology, the higher the risk. Drake's Design Reference 5.0 includes a useful figure (Figure 48) which summarizes the human health specific technology needs going forward. More recent technology area (TA) roadmaps are shown in Figures 49 and 50 which focus on first and second level needs that must be developed in order to realize manned missions to cis-Lunar space, and eventually to Mars. The NASA Office of the Chief Technologist website shows fifteen different technology areas in total for their entire roadmap, but Technology Areas 6 (Human Health), and 7 (Human Exploration Destination Systems) encompass the technology efforts that best match with the radiation protection focus and scope of this paper (2016). Figure 49 also includes third level goals specific to radiation shielding/protection measures, and that for the prediction of significant space weather events.
4. **Schedule:** based on the dates shown in the TA maps in the most recent updates on the NASA "Journey to Mars Overview" website, 2040 is now a more appropriate assumed goal for human missions to the Martian surface. This assumption is made because the current roadmaps only depict humans going to orbit Mars by the mid-2030s, and is used in lieu of the Drake's publications 2030 assumptions when estimating schedule risk for various shielding and medical alternatives for this chapter (2017). Specific examples of these alternatives include: the development of hydrogen loaded and nanotube shielding composites, and completion of sufficient FDA phase 2 trials for newer radiation countermeasure medications in time for application by the 2040 timeframe. Gaps in these technology areas are used to help weigh schedule risks for various options later in this chapter. Of note, some technologies may require fielding capability prior to the first human Mars missions in order to fly with test vehicles and other cis-Lunar human trial missions.



<b>Current Knowledge or Capability Gaps</b>
<ul style="list-style-type: none"> <li>• Determine the effect of long-term stowage in space on food.</li> <li>• Obtain a better understanding of the effects of radiation beyond LEO on the immune system and microbial characteristics, and on overall chemical toxicity (determine whether radiation produces any synergistic, additive, chemical potentiation or chemical antagonism effects).</li> <li>• Obtain a better understanding of the long-duration effects of space flight beyond LEO on the human immune system.</li> <li>• Obtain a better understanding of changes that occur in microorganisms during extended missions beyond LEO.</li> <li>• Obtain a better understanding of the environment of Mars.</li> <li>• Develop a martian Dust Health Standard.</li> </ul>
<b>Technology Needs</b>
<p>Radiation Protection</p> <ul style="list-style-type: none"> <li>• Develop advanced shielding technologies.</li> <li>• Develop radioprotectants and pharmaceutical countermeasures against radiation.</li> <li>• Develop strategies for individual-based risk assessment for crew selection.</li> </ul> <p>Reduced-g Countermeasures</p> <ul style="list-style-type: none"> <li>• Develop the capability to assess the time course of skeletal changes for periods of 6 months and longer.</li> <li>• Develop pharmacotherapeutic monitoring and treatment technologies.</li> </ul> <p>Habitability and Environmental Health</p> <ul style="list-style-type: none"> <li>• Develop emerging technologies in food processing.</li> <li>• Develop an automated acoustic monitoring system.</li> <li>• Develop a technology that promotes autonomy, such as H<sub>2</sub>O remediation systems, contamination-resistant materials, and "smart" medical diagnostic systems.</li> <li>• Develop a technology for monitoring the martian rover for dust (contingent on open or closed rover design).</li> </ul> <p>Life Support Systems</p> <ul style="list-style-type: none"> <li>• Closed-loop life support systems.</li> <li>• Reliable, robust systems that require minimal crew support to operate and maintain.</li> <li>• Systems that are capable of using locally generated consumables including O<sub>2</sub>, H<sub>2</sub>O, and buffer gases.</li> <li>• Systems that operate in both zero-g (transits) and partial-g (surface) environments.</li> </ul> <p>Human Factors</p> <ul style="list-style-type: none"> <li>• Develop risk assessment and monitoring tools that passively detect individual stress and crew cohesion issues.</li> <li>• Construct a Rest and Recreation Center to provide psychosocial support for living and working in space, and tailor it to transit time and surface time.</li> </ul>

Figure 48. Human Health and Performance Challenges. Source: Drake (2009, 293).

<b>6.0 Human Health, Life Support, and Habitation Systems</b>	<b>Goals:</b> Enable long-duration, deep-space human exploration within permissible space radiation exposure limits, minimal resupply consumables, and increased Earth independence.
6.1 Environmental Control and Life Support Systems and Habitation Systems	Sub-Goals: Maintain an environment suitable for sustaining human life throughout the duration of a mission.
6.2 Extravehicular Activity Systems	Sub-Goals: Enable crew operations outside the vehicle or habitat in all mission environments. Protect the crew during launch, entry, and landing, and for the potential events of cabin contamination or depressurization. Protect the crew during ascent/descent transition for planetary excursions.
6.3 Human Health and Performance	Sub-Goals: Maintain the health of the crew and support optimal and sustained performance throughout the duration of a mission as well as terrestrial life, thereafter.
6.4 Environmental Monitoring, Safety, and Emergency Response	Sub-Goals: Ensure crew health and safety by providing the crew early warnings of potentially hazardous conditions and to provide the crew time for effective response should an accident occur.
6.5 Radiation	Sub-Goals: Increase crew mission duration in the free-space radiation environment while remaining below the space radiation permissible exposure limits.
6.5.1 Risk Assessment Modeling	Objectives: Reduce uncertainty in assessing the risk of death due to radiation exposure. Improve risk assessments for cancer and include circulatory and central nervous system (CNS) effects.
	Challenges: Acquiring sufficient ground and flight data on living systems exposed to the relevant space environment. Developing models that accurately predict radiation risks, identifying genetic selection factors, and developing mitigation measures for remaining risk.
	Benefits: Provides well-understood radiation risk assessment and modeling tools with minimal uncertainty to assess astronaut risk due to space radiation exposure for improved mission operations, mission planning, and system design for LEO, deep-space, lunar, and Mars missions.
6.5.2 Radiation Mitigation and Biological Countermeasures	Objectives: Develop biological countermeasures that reduce the risk of adverse effects from radiation by 50% of the mission duration.
	Challenges: One type of BCM will not be sufficient; a suite of BCMs will be needed to address the various health problems expected.
	Benefits: Provides countermeasures for in-flight acute radiation syndrome, in-flight CNS effects, degenerative effects, and cancer. Provides a pharmaceutical interaction tool to evaluate drug response and interactions individually and in combination with other drugs, and an individual sensitivity toolkit to determine effectiveness and toxicity of biological countermeasures for individual astronauts.
6.5.3 Protection Systems	Objectives: Provide reasonable (mass and power) shielding for 365 safe days for near-Earth asteroid (NEA) and 1,000 safe days for Mars, in combination with countermeasures.
	Challenges: Protective shielding cannot completely protect against galactic cosmic radiation (GCR), and shielding options combined with BCMs will be needed for long-duration missions.
	Benefits: Provides lightweight, cost-effective multifunctional materials and structures that can minimize exposure while providing other functionalities, like thermal insulation and micrometeoroid and orbital debris (MMOD) protection. Provides a cross-discipline, integrated systems approach to vehicle design for radiation protective functions. Provides active shielding components, such as lightweight structures and magnets, improved active cooling systems, and high-temperature superconductor technology.
6.5.4 Space Weather Prediction	Objectives: Develop real-time monitoring and forecasting space weather models.
	Challenges: Forecasting the occurrence and magnitude of solar particle events, as well as all-clear periods.
	Benefits: Provides forecasting models that include an all clear forecasting tool, tool for forecasting intensity and evolution, ensemble coronal mass ejection (CME) forecasting, and a high-performance computing architecture.
6.5.5 Monitoring Technology	Objectives: Reduce mass and power, extend battery life, and improve data communications of devices.
	Challenges: Low enough power requirements and be small enough to be distributed throughout and integrated into the spacecraft.
	Benefits: Improves monitoring technologies for exploration missions.

Figure 49. Human Health, Life Support, and Habitation System Goals. Source: NASA Office of the Chief Technologist (2016).

7.0 Human Exploration Destination Systems	Goals: Sustain human presence in space and provide more time for performing core mission activities, while reducing reliance on Earth.
7.1 In-Situ Resource Utilization	Sub-Goals: Leverage in-situ resources to dramatically reduce launch mass and cost of human exploration missions.
7.2 Sustainability and Supportability	Sub-Goals: Establish a self-sufficient, sustainable, and affordable long-duration human space exploration program.
7.3 Human Mobility Systems	Sub-Goals: Enable humans to safely and efficiently perform work or scientific activities outside their primary spacecraft.
7.4 Habitat Systems	Sub-Goals: Develop an autonomously operating spacecraft that promotes crew health and well-being while reducing required crew maintenance and servicing and optimizing resource utilization.
7.5 Mission Operations and Safety	Sub-Goals: Manage space missions from the point of launch through the end of the mission for long-duration missions and over long time delays.
7.6 Cross-Cutting Systems	Sub-Goals: Manage particulate contamination transported by operations, lander plume ejecta, and larger-scale construction and assembly technologies.

Figure 50. Human Exploration Destination System Goals. Source: NASA Office of the Chief Technologist (2016).

These domains may be derived into performance objectives in the later sections of this chapter. Dezfuli et al. also discuss the operational definition of risk as applied with RIDM models. This definition is simplified into three areas (2010, 11):

1. Risk scenarios: the discussion of specific situations or occurrences that may lead to degraded performance or failure of one of the performance measures. Examples here would include radiation events that may cause violation of radiation exposure limits, or on the more extreme, exposure levels severe enough to cause acute symptoms or sickness/death. Cost overruns or schedule slippage are other more simplified results of certain scenarios.
2. Likelihood: a quantitative or qualitative assessment of the chance of the outlined scenarios occurring.
3. Consequences: a qualitative or quantitative assessment of the severity of the performance degradation that could occur as a result of a given scenario.

The chief benefits of this framework are that it can help to distinguish high probability/low consequence risks from those with low probability but high consequences, that it can help to factor out low probability risks with minimal consequences, and that it can help to focus attention on areas of a project that may require additional research or attention in order to reduce uncertainty in the prediction of these risks. The RIDM Handbook also emphasizes that this technique should be used for key decisions involving architecture or design; and in particular for decisions which involve

high stakes, complex alternatives, and high levels of uncertainty. All of these criteria certainly apply to the alternatives being considered in this paper (Dezfuli et al. 2010, 12–13).

Figure 51 shows an overview of the risk informed decision making process. The identification of alternatives has been completed in Chapters II–VI of this paper. Risk analysis of these options and selection of alternatives are completed in the sections that follow.

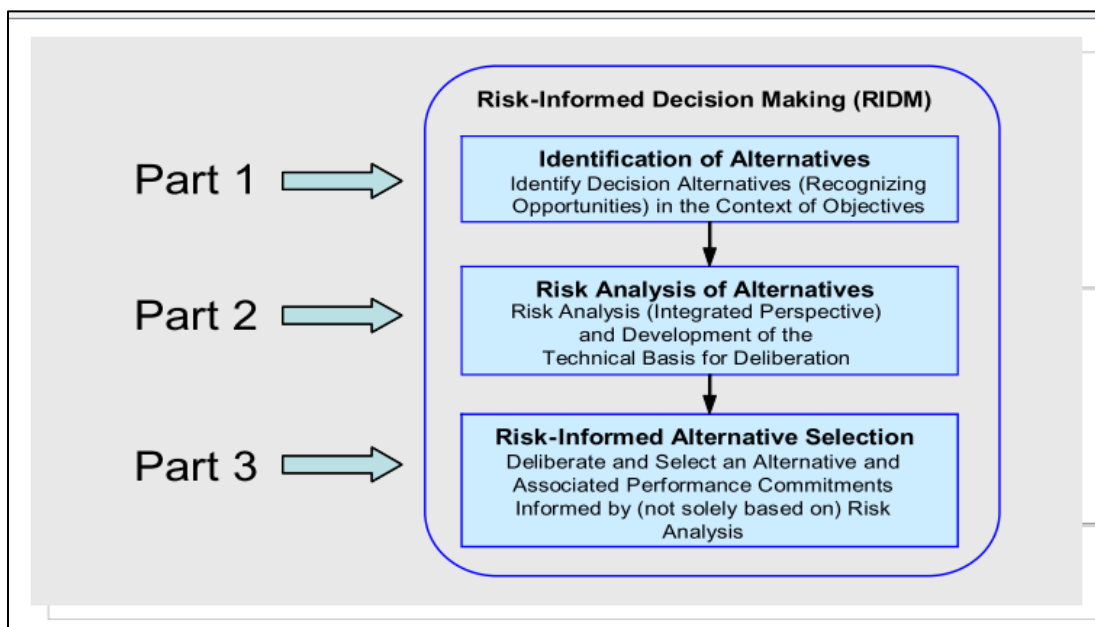


Figure 51. The RIDM Process. Source: Dezfuli et al. (2010, 14).

Risk analysis is conducted by considering two things. First, performance objectives must be defined. These objectives are measured in terms of metrics. For a deep space Mars mission, the objectives/metrics are:

1. **Maintain crew health and safety:** specifically, to maintain crew radiation exposure ALARA through selection of the alternatives laid out. Metrics of measurement include probability of loss of crew, radiation exposure level, and risk of exposure induced death (REID).
2. **Minimize cost:** the primary driver of this is fuel mass required to launch, and therefore to minimize the launch cargo required to achieve other

objectives (crew health) to a satisfactory degree. Therefore, the metric that is used for this comparison is actually mass differences as weighted among the various alternatives. Of note, the development cost of newer technologies is a secondary factor in this objective, where cost in dollars is the metric that is compared.

3. Maximize mission science value: examples include mission models that maximize the opportunities to explore different areas of the Martian surface, and the return of regolith and other geological samples to Earth. Metrics include quantity of samples obtained, value of new science discoveries or technologies developed with cross-application to civilian populations, etcetera. Another consideration in this goal is that of “crew time.” Similar to the ISS, a Mars mission crew will have a large load of routine maintenance to complete on all equipment in order upkeep and test for proper function at all stages of the mission. This maintenance may be a limiting factor in how much time the crew will have for other activities, and in particular how much time they can dedicate to science missions on the Martian surface given some of this maintenance will likely require EVAs to work outside the habitat where the risks of radiation exposure are higher as well.
4. Maintain schedule: new shielding and medical technologies are weighed against the likelihood that they can be ready for use in time for the initial manned missions in 2040. The best metric to measure this would be a relative measure of likelihood that the technologies in question will be at an adequate readiness level to launch in 2040.

The next section defines and hierarchy for the specific goals of this paper in greater detail, leveraging the NASA technology objectives discussed in this section.

## **B. OBJECTIVES HIERARCHY**

One valuable technique to weigh these objectives against each other is that of swing weights. This title is given because the weight assignments in the assessment matrices are calculated in terms of the total of all weights given. As such, the adjustment of any one parameter to carry less or more weight will cause all others in the matrix to “swing” such that their respective weights are higher or lower in response. In this method, mission objectives are weighed on two axes. First, there is the consideration of their importance to the mission’s decision makers. These categories may be simplified from “High” to “Low,” or discussed in terms of threshold objectives (i.e., “Must Have”) verses goal or stretch objectives (“Nice to Have”), and so forth. The second axis assesses

the level of potential impact of variance for the given parameter. A sample table with generic categories is shown in Table 6.

Table 6. Sample Swing Weight Table

		Measure of Importance to Decision Makers		
		Low	Medium	High
Potential Impact of Variance in Parameter	High	C <sub>3</sub>	B <sub>2</sub>	A <sub>1</sub>
	Medium	D <sub>2</sub>	C <sub>2</sub>	B <sub>1</sub>
	Low	E <sub>1</sub>	D <sub>1</sub>	C <sub>1</sub>

Objectives are assigned to different regions of the table based on stakeholder judgement of measure of importance and potential variance. Of note, it is possible to assign multiple performance objectives to the same region if it is determined that their relative weights should be the same. Next, each category in the table is assigned a numerical weight of anywhere from (1–100). Weights are required to be highest for A, and lowest for E, with diagonal precedence that sweeps from the upper right corner to the lower left corner of the table. For example:

- A<sub>1</sub> must be greater than all others.
- B<sub>2</sub> is greater than C<sub>2</sub> and D<sub>1</sub>.
- C<sub>1</sub> is greater than D<sub>1</sub> and E<sub>1</sub>.
- C<sub>2</sub> is greater than D<sub>1</sub>, D<sub>2</sub>, and E<sub>1</sub>.

Once the individual weights are assigned to various objectives, the normalized weight of each ( $w_i$ ) may be calculated by dividing the individual value  $f_i$  (such as, A<sub>1</sub>) by the sum of all values populated in the table, as shown in Equation (VII.B.1):

$$w_i = \frac{f_i}{\sum_{i=1}^n f_i} \cdot \quad (\text{VII.B.1})$$

Once calculated, these weights may be used for each alternative under consideration to determine an overall measure of effectiveness (MOE) by which they can be compared. Each alternative is rated for performance against each objective in the swing weight table. This performance may be calculated via two systems, either a straight numerical comparison (as may be done with shielding performance in this paper where most data is quantitative), or via assignment of numerical values to alternatives that have qualitatively higher/lower performance (as with most discussions of cost and weight and technical/schedule risk). The MOE for each alternative is calculated by multiplying each performance value against the normalized weight for that objective, and summing those products for the assessment of all objectives.

Swing weight tables are also a powerful tool because various weights can be adjusted if future researchers determine that the variance for certain objectives has changed, or if certain objectives prove to be of higher or lower importance. Then the same calculations can be repeated for existing alternatives with relative ease. Weights can also be adjusted to perform a sensitivity analysis demonstrating the impacts of either a change in variance or a change in importance for a given objective.

## 1. Existing Risk Analysis Data and Gap Assessments

To provide context for the set-up of the swing weight table later in this section, it is useful to conduct an overview of the risks/consequence indices associated with certain key objectives. NASA has performed these assessments and reported them on the Human Research Roadmap “Risks” website (2016). Relevant assessments include:

### a. Risk of Radiation Carcinogenesis

Figure 52 summarizes NASA reported estimates for risks of cancers resulting from radiation exposure. Future Mars missions are covered by the Deep Space

Journey/Habitation and Planetary portions of the figure, and the assessments are valued in terms of likelihood and consequence (LxC) where likelihood is scaled from one through three for low to medium to high probability that an event will occur, and consequence is scaled from one through four for very low/low/medium/high consequences which could result. Figure 52 shows that cancer occurrence in the short-term for these mission types is acceptably low, but that the LxC for the long term is much more severe and requires mitigation:

Risk Ratings and Dispositions per Design Reference Mission (DRM) Category					
DRM Categories	Mission Duration	Operations		Long-Term Health	
		LxC	Risk Disposition *	LxC	Risk Disposition *
Low Earth Orbit	6 months	1x1	Accepted	3x2	Accepted Within PELs
	1 year	1x1	Accepted	3x2	Accepted Within PELs
Deep Space Sortie	1 month	1x1	Accepted	3x1	Accepted Within PELs
Lunar Visit/ Habitation	1 year	1x1	Accepted	3x3	Requires Mitigation
Deep Space Journey/Habitation	1 year	1x1	Accepted	3x4	Requires Mitigation
Planetary	3 years	1x1	Accepted	3x4	Requires Mitigation

**Note:** LxC is the likelihood and consequence rating. This risk is mapped to the official (consolidated) HSRB risk "Risk of Adverse Health Outcomes and Performance Decrements resulting from Space Radiation Exposure (Acute, CNS, Degen, Cancer)". The HSRB evaluated the LxC and risk dispositions of this sub-risk for each DRM as part of their review of the consolidated risk.

Figure 52. Risk Assessment for Radiation Carcinogenesis. Source: NASA Human Research Roadmap (2016).



The NASA Human Research Roadmap site highlights the uncertainties already discussed in this paper regarding anticipated radiation exposure and the calculation of risk of exposure induced death (REID) associated with it (2016). Fifteen gaps are identified for future research, with some examples including:

- developing better experimental models for tumor development and carcinogenesis, especially with regard to the quality effects of different types of radiation encountered in deep space
- developing methods to reduce uncertainty of cancer risks for multiple factors, including radiation type, and age/gender/genetic disposition
- developing improved methods to assess the effectiveness of medical countermeasures and to weigh the benefits of their use against the possible mission risks created by certain side effects
- Determination of the most effective shielding methods to mitigate cancer risks, and improvement of shielding analysis to support better spacecraft and habitat design

***b. Risk of Acute Radiation Syndromes Due to Solar Particle Events***

Figure 53 highlights the fact that acute radiation syndrome is a short-term risk. Due to the fact that all future space vehicles are being designed with a heavily shielded area to take shelter from SPEs, this risk is considered acceptable for long-term missions.

Risk Ratings and Dispositions per Design Reference Mission (DRM) Category					
DRM Categories	Mission Duration	Operations		Long-Term Health	
		LxC	Risk Disposition *	LxC	Risk Disposition *
Low Earth Orbit	6 months	1x1	Accepted	Not Applicable	Not Applicable
	1 year	1x1	Accepted	Not Applicable	Not Applicable
Deep Space Sortie	1 month	1x2	Accepted	Not Applicable	Not Applicable
Lunar Visit/ Habitation	1 year	2x2	Accepted	Not Applicable	Not Applicable
Deep Space Journey/Habitation	1 year	2x2	Accepted	Not Applicable	Not Applicable
Planetary	3 years	2x2	Accepted	Not Applicable	Not Applicable

Figure 53. Risk Assessment for Acute Radiation Syndrome Due to SPEs. Source: NASA Human Research Roadmap (2016).

Seven gaps are identified by the NASA Human Research Roadmap team, covering topics that include (2016):

- improving assessment of dosage effects of SPE radiation with the layered complexity of other concurrent deep space effects, and improving the assessment of SPE acute radiation risks
  - optimizing technologies to both predict or detect the start of a Solar Particle Event, and to measure SPE-specific dose received by astronauts
  - optimizing shielding for SPEs
  - optimizing dietary and biomedical countermeasures for SPEs
  - improving risk assessment for SPEs occurring during EVAs
- c. Risk of Cardiovascular Disease and Other Degenerative Tissue Effects Due to Radiation Exposure*

Figure 54 shows how long term mission types have LxC ratings that require mitigation for these risks. The Human Research Roadmap site defines eight gaps requiring further research. These include:

- developing improved models to better predict the effects of space radiation for various tissue effects (cardiovascular, lens, immune, endocrine, respiratory, digestive)
- developing models to better estimate the progression of such conditions both with respect to human factors (age/gender, pre-existing susceptibility) and environmental factors (deep space microgravity, radiation type)
- determining the most effective dietary or biomedical countermeasures to mitigate these conditions, and better understanding the mechanisms by which they work

Risk Ratings and Dispositions per Design Reference Mission (DRM) Category					
DRM Categories	Mission Duration	Operations		Long-Term Health	
		LxC	Risk Disposition *	LxC	Risk Disposition *
Low Earth Orbit	6 months	1x1	Accepted	1x4	Accepted/Low Probability
	1 year	1x1	Accepted	1x4	Accepted/Low Probability
Deep Space Sortie	1 month	1x1	Accepted	1x4	Accepted/Low Probability
Lunar Visit/Habitation	1 year	1x1	Accepted	1x4	Accepted/Low Probability
Deep Space Journey/Habitation	1 year	3x1	Accepted/Standard Refinement	2x4	Requires Mitigation/Standards Refinement
Planetary	3 years	3x1	Accepted/Standard Refinement	3x4	Requires Mitigation/Standards Refinement

Figure 54. Risk Assessment for Cardiovascular Disease and Other Degenerative Tissue Effects. Source: NASA Human Research Roadmap (2016).

*d. Risk of Acute (In-flight) and Late Central Nervous System Effects from Radiation Exposure*

Figure 55 shows the Human Research Roadmap assessment of risks for central nervous system (CNS) effects resulting from radiation exposure in deep space. For long-term space missions the LxC for these risks is moderate but does require more mitigation and data.

Risk Ratings and Dispositions per Design Reference Mission (DRM) Category					
DRM Categories	Mission Duration	Operations		Long-Term Health	
		LxC	Risk Disposition *	LxC	Risk Disposition *
Low Earth Orbit	6 months	1x1	Accepted	1x3	Accepted/Low Probability
	1 year	1x1	Accepted	1x3	Accepted/Low Probability
Deep Space Sortie	1 month	1x1	Accepted	1x3	Accepted/Low Probability
Lunar Visit/Habitation	1 year	1x2	Accepted/Requires Data	1x3	Accepted/Low Probability
Deep Space Journey/Habitation	1 year	2x3	Requires Mitigation/Data	2x3	Requires Mitigation/Data
Planetary	3 years	3x3	Requires Mitigation/Data	3x3	Requires Mitigation/Data

Figure 55. Risk Assessment for Acute Nervous System Effects from Radiation Exposure. Source: NASA Human Research Roadmap (2016).

The basis for this assessment is that initial studies in other animals have shown the potential for neurological effects, including those that could impact motor skills, cognitive function, and behavior in the short term following exposure. In the long term the risks may expand to include the onset of serious conditions such as dementia and Alzheimer's. Overall there is a lack of human study to better understand these risks. The Human Research Roadmap team establishes eight gaps where further research is needed, with topics including (2016):

- improving understanding of how CNS effects develop in space following radiation exposure, and whether there are any biological markers to confirm their development
- researching the potential impact of coinciding conditions (genetic markers or family history for Parkinson's or Alzheimer's, prior CNS injuries including concussions) on the probability that radiation-induced CNS effects could occur
- optimizing shielding technology to help prevent CNS effects
- determining optimal dietary and biomedical countermeasures to help mitigate CNS effects

## **2. Definition of Project-Specific Swing Weight Objectives and Matrix**

Using the objective review from Section A of this chapter, the following key objectives and justifications are established for weighting and assessment. Each category of objectives is assigned a relative weight target which assists in the creation of a swing matrix below. For review, each priority/variance category in the matrix is assigned a value from 1–100 as specified in Section A of this chapter. Multiple objectives may share the same priority/variance rating, which is why the objective category weights are compared to each other to help fine tune the assignment of matrix values:

**Maintain Crew Health & Safety (H&S):** In addition to the detailed crew health radiation exposure risk assessments just reviewed, similar needs are identified in the most recent NASA Technology Roadmaps as shown in Figure 49 in Section A of this chapter (NASA Office of the Chief Technologist, 2016). As such, these objectives are assigned ~40% of the weighting due to the fact that crew health and safety are by far the highest priority from both a stand point of mission success, and from the stand point public

perception and support which are imperative to the backing of future human exploration missions.

- **H&S 1—Maintain radiation exposure ALARA:** Because this is of highest importance along with high potential uncertainty (variance), the weighting must be the highest. This objective is measured on a scale that rewards a range of values based on the percentage of expected dosage reduced (for shielding technologies), and with a maximum value for any instance where radiation dose is predicted to be reduced below existing limits. This optimal goal seems unlikely to be met on the limitations of current research and high uncertainty (potential variance) for existing data. Of note, this comparison of alternatives is concentrated on those that impact GCR exposure since a majority of references studied in this paper assume that SPE exposure is largely mitigated by the use of emergency shelters with high-thickness/water-wall shielding. As an example for the swing weights assigned in Table 7 below, because this objective has a high/high priority and variance rating, it is assigned a swing weight of 37 which gives it a normalized weight of approximately 31% (0.308) of weights assigned in the matrix.
- **H&S 2—Mitigate the effects of radiation exposure:** because it is a given that all astronauts on a human mission to Mars will receive significant exposure to radiation, the next goal is to mitigate the effects of that exposure as much as possible. This includes the prevention of cellular damage from that exposure, and the treatment of symptoms that may result from acute doses. The numerous medical countermeasures discussed in Chapter VI are relevant to this objective. This is treated as an objective of medium importance relative to the more important goal of reducing exposure in the first place. Variance is moderate because many of the medications under study to date are still in preliminary trials, and none have been tested in a deep space environment to assess how well they actually work.

**Minimize Cost & Weight (C&W):** these objectives are assigned ~30% of the weighting due to the fact that weight drives cost which impacts whether NASA (and moreover the U.S. government) will ultimately be able to afford a human mission of this scope on in terms of tax-payer dollars.

- **C&W 1—Minimize weight:** this is of high importance given mission cost is most significantly driven by cargo weight which in turn affects required fuel mass ten-fold. Variance is moderate due to some significant differences in potential shielding designs, and the trades being conducted for mission trajectories and module configurations as discussed in Sections C and D of this chapter.

- **C&W 2—Minimize development costs:** this is also of high importance given the U.S. government/taxpayers must be able to fund the technology roadmap that is needed to make the mission attainable. Variance is still moderate due to the fact that some very new technologies still have a high enough development curves to be prohibitive (example: field based shielding).

**Maximize Science Value (SV):** these objectives are assigned ~20% of the weighting. Discoveries in science due to the exploration and technology development conducted by NASA represent a good return on taxpayer investment and help to advance humankind as a society.

- **SV 1—Maximize Mars surface exploration capabilities:** surface habitats to sustain astronauts on the Martian surface will drive technology development (with potential for cross-application on Earth) in order to physically support those habitats in one of the most isolated and challenging environments. Surface exploration vehicles will further enhance the potential for discoveries that may be made. Initially this objective may be of medium importance, until the first successful missions are complete with only basic experiments and samples conducted. Variance is high due to the variety of surface configurations and capabilities under consideration.
- **SV 2—Maximize sample collection & value:** This objective is of medium importance given the necessity to get samples back to Earth in order to better understand the Martian environment/history and to better-plan future human missions. Variance is moderate due to the decision point of whether more extensive surface based sample analysis technology should be outfitted as part of mission cargo or not. NASA’s current mission to Mars roadmap also includes plans to conduct robotic sample return in advance of human missions.
- **SV 3—Minimize crew maintenance:** “crew time” is a limiting factor in what percentage of time astronauts have available to conduct other research, exploration, and experiments on the Martian surface. This must be balanced against the reality that preventive maintenance is a necessity to adequately mitigate risks to keep crew safe in a location where they depend on habitat and spacecraft technology to survive. As such it may be treated as a low priority with moderate variance which correlates to the complexity of systems outfitted on all modules and vehicles.

**Maintain Schedule (Sked):** these objectives are assigned ~10% of the weighting. While NASA has set rough timeframes in their roadmaps to achieve certain missions, precedent has shown that these dates often move to the right due to the limitations of taxpayer-funded budgets, and in favor of ensuring that all technology levels and risks are at acceptable levels prior to launch. Doing the job “right” verses doing the job quickly is reflected in the lower priority of these objectives.

- **Sked 1–Maximize technical maturity by 2040:** all technology selected for the mission must have sufficient technical maturity in order for human missions to launch “on time.” However, this still remains a relatively low importance objective given the reality that mission time frame will be delayed until all technology is proven and risks are mitigated to the greatest extent possible.
- **Sked 2–Maximize potential for “proving ground” trials:** NASA’s roadmaps already include plans to send trial missions to the Moon, to cis-Lunar Space, and on asteroid capture missions prior to any human missions to Mars. Technologies that favor spiral development such that they can be implemented on these scaled down missions should be favored over those that lack the maturity to use in trials by the 2020 timeframe. This is a medium priority given the reality that even proving ground mission timeframes may slide to the right in order to wait for the desired technologies to be “ready” for testing.

These objectives are visually summarized in the hierarchy chart depicted in Figure 56. The chart breaks the objectives out by category and priority.

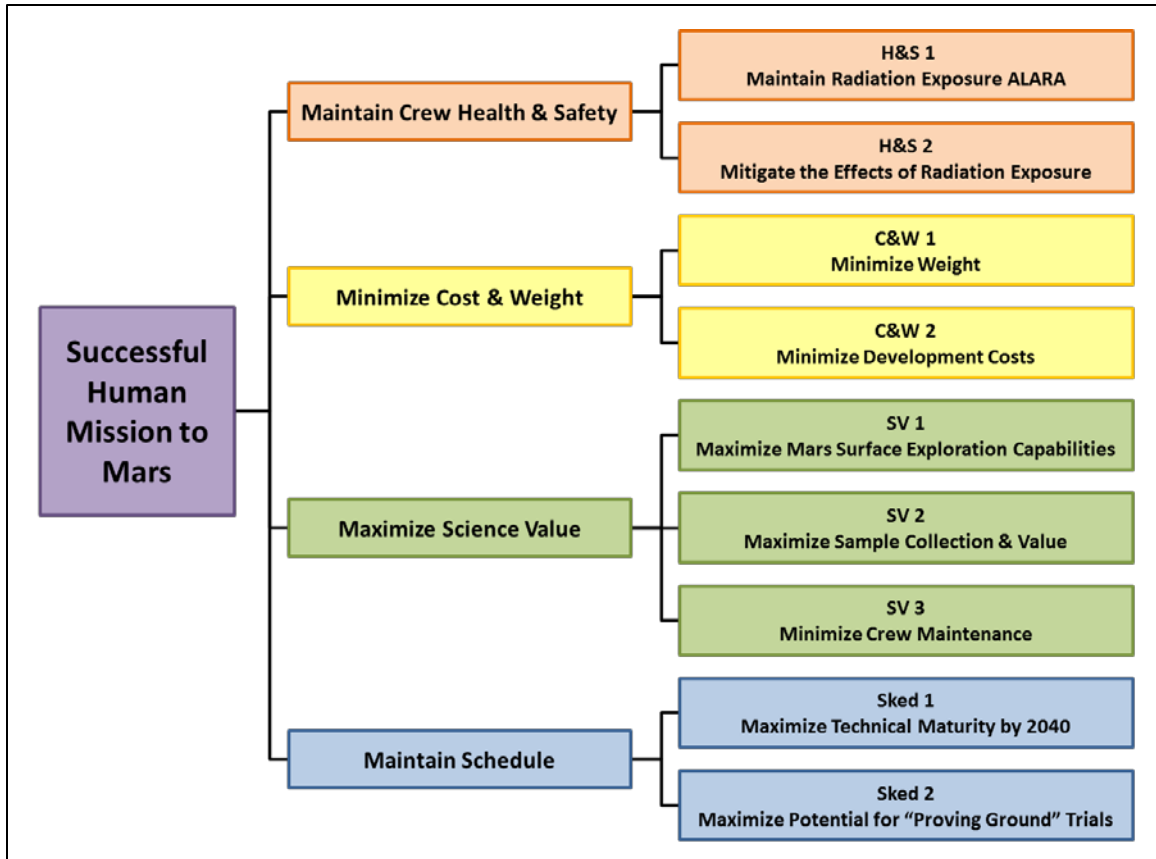


Figure 56. Objective Hierarchy Summary



Based on these objectives, Tables 7 and 8 depict an initial calculation of the overall swing weight matrices that give the weights of each objective category the relative values desired. These tables are manipulated in Section F of this chapter to further analyze the sensitivity of the results. Table 7 shows the initial assigned weights for importance and variance. Again, the swing weights in the top half of the table must be assigned values between 1 and 100. In this case the values are chosen both to maintain a relatively low total for all weights assigned (between 100 and 150, in this case 120). These weights are adjusted to achieve the desired relative weights between categories of objectives as calculated in Table 8. Each normalized value is calculated per Equation (VII.B.1), where the weight assigned to that block is divided by the total of all weights. For example, for high/high,  $37/120 = 0.30833$ .

Table 7. Assigned Swing Weight Matrix and Normalized Values

<b>Swing Weight Matrix (assign numbers 1-100 for each block)</b>						
<b>Importance (Right)</b>	Low	Medium	High			
<b>Variance (Down)</b>						
High	8	13	37			
Moderate	6	11	18			
Low	4	9	14		<b>Total Weights:</b>	120
<b>Normalized Weight Matrix (divide each block by the sum of all)</b>						
<b>Importance (Right)</b>	Low	Medium	High			
<b>Variance (Down)</b>						
High	0.067	0.108	0.308			
Moderate	0.050	0.092	0.150			
Low	0.033	0.075	0.117			

Table 8 uses the normalized weights and the importance/variance assignments for each of the objectives discussed in this section, and calculates their normalized weighting from Table 7. Then all weightings for each category of objectives are summed and compared to the total of all weights to determine what percentage of the overall weight is assigned to that category.

Table 8. Normalized Weights by Objective and Objective Category Weighting

Objective	Importance, Variance	Weight	Subtotals	Total assigned weights*:	1.000
H&S 1	High, High	0.308		Human safety %	40.0%
H&S 2	Medium, Moderate	0.092	0.400	Cost weight %	30.0%
C&W 1	High, Moderate	0.150		Science %	19.2%
C&W 2	High, Moderate	0.150	0.300	Schedule %	10.8%
SV 1	Low, Moderate	0.050		<i>*% calculated based on this total</i>	
SV 2	Medium, Moderate	0.092			
SV 3	Low, Moderate	0.050	0.192		
Sked 1	Low, Low	0.033			
Sked 2	Medium, Low	0.075	0.108		

These weights are used to calculate MOEs for both the shielding alternatives presented in Chapter V, and the medical countermeasures reviewed in Chapter VII. These calculations are conducted in Sections D and E of this chapter.

### 3. Definition of Objective Rating Scales and Assumptions

To evaluate these types of alternatives against the objectives it is important to define a uniform standard by which their measures of effectiveness will be defined. With a swing weight evaluation it is standard to score each alternative against each objective on a scale that rates them zero to one. Table 9 discusses the rationale for ratings that will be assigned for each objective/category.

Table 9. Definition of Objective Rating Scales and Assumptions

Objective	Description of Rationale & Assumptions	Rating Scale
H&S 1	Based on the fact that some shielding data is only measured up to a thickness of 30g/cm <sup>2</sup> , this thickness is used to calculate the effectiveness various materials against each other. In cases where exposure against GCRs could be impacted in all phases of a human Mars mission, exposure for a total duration of 1000 days is estimated for each alternative relative to a baseline of comparable Aluminum shielding. Table 10 reviews the NASA exposure limits. Any alternative that lowers exposure levels less than the existing exposure limits for all ages/genders receive a rating of 1.0. Remaining alternatives are assigned ratings based on their relative effectiveness. Alternatives that do not have numerical data available receive a best estimate of their potential for effectiveness. Alternatives that have no effectiveness on radiation exposure receive a rating of 0.	<ul style="list-style-type: none"> <li>• 1.0 = Exposure limits met</li> <li>• 0.75 = High effectiveness</li> <li>• 0.5 = Moderate effectiveness</li> <li>• 0.25 = Low effectiveness</li> <li>• 0.0 = No impact on exposure</li> </ul>
H&S 2	Any alternative under study that has the potential to mitigate 100% of any exposure effects (either by cellular damage prevention or healing) receives a rating of 1.0. Any alternative that has no impact on exposure mitigation has a rating of 0.0. All alternatives with a moderate level of radiation mitigation receive ratings from 0.1 through 0.9 based on the relative potential for mitigation. For alternatives with the potential for medical side effects, it is assumed that all side effects are acceptable if these drugs are ultimately FDA approved for human use.	<ul style="list-style-type: none"> <li>• 1.0 = 100% mitigation</li> <li>• 0.0 = No impact on mitigation</li> </ul>
C&W 1	Alternatives that have zero/negligible impact on mission weight receive a neutral rating of 0.5. Alternatives that have the potential to increase mission weight (including that of Pre-Deployed cargo) receive ratings from 0.4 to 0.0 based on estimated impact, with 0.0 being the most weight/cost intensive. Alternatives that have the potential to reduce mission weight receive ratings from 0.6 to 1.0.	<ul style="list-style-type: none"> <li>• 1.0 = Highest potential to reduce weight</li> <li>• 0.5 = Weight neutral</li> <li>• 0.0 = Highest potential to increase weight</li> </ul>
C&W 2	Alternatives that carry the highest potential development costs receive a rating of 0.0. Alternatives with no additional development receive a rating of 1.0. All other new technology alternatives are scaled for potential development cost between these two values.	<ul style="list-style-type: none"> <li>• 1.0 = No additional cost</li> <li>• 0.8 = Low cost</li> <li>• 0.5 = Moderate cost</li> <li>• 0.2 = High cost</li> <li>• 0.0 = Highest potential cost</li> </ul>

Objective	Description of Rationale & Assumptions	Rating Scale
SV 1	Alternatives that provide the highest potential for mission tasks that provide science value receive a rating of 1.0. Alternatives that have no impact on the potential for science value receive a rating of 0.0.	<ul style="list-style-type: none"> <li>• 1.0 = Highest potential</li> <li>• 0.5 = Moderate potential</li> <li>• 0.0 = No impact on science gain potential</li> </ul>
SV 2	Alternatives that support in-depth local analysis of samples with the potential to re-sample as needed receive a rating of 1.0. Alternatives that support sample return with minimal analysis receive a rating of 0.5. Any alternative that prevents sample return receives a rating of 0.0.	<ul style="list-style-type: none"> <li>• 1.0 = In-depth analyzed sample return</li> <li>• 0.5 = Basic sample return</li> <li>• 0.0 = Prevents sample return</li> </ul>
SV 3	Alternatives that have no impact on the potential need for “crew time” (maintenance) receive a rating of 0.5. Alternatives that simplify or lessen the need for crew maintenance receive ratings of 0.6 to 1.0 on a relative scale. Alternatives that increase the need for crew maintenance receive ratings of 0.5 to 0.0 where 0.0 is the most time-intensive.	<ul style="list-style-type: none"> <li>• 1.0 = Least time-intensive</li> <li>• 0.5 = Neutral impact on crew time</li> <li>• 0.0 = Most time-intensive</li> </ul>
Sked 1	Alternatives receive confidence ratings based on their potential to have technical maturity to support a human mission to the Martian surface by 2040. The alternatives with the highest confidence or least schedule risk receive a 1.0 rating. Alternatives with the lowest confidence or highest schedule risk receive a 0.0 rating. Alternatives that have no impact on schedule also receive a 1.0 rating.	<ul style="list-style-type: none"> <li>• 1.0 = High confidence of readiness by 2040</li> <li>• 0.0 = Zero confidence of readiness by 2040.</li> </ul>
Sked 2	Alternatives with the highest potential for “proving ground” trials in the 2020 timeframe receive a 1.0 rating. Alternatives with the no potential for proving ground trials receive a 0.0 rating. All other alternatives receive a rating based on an estimate of how soon they may be ready for in-space trials, with alternatives that may be ready sooner receiving higher ratings. Alternatives with no need for proving ground trials also receive a rating of 1.0.	<ul style="list-style-type: none"> <li>• 1.0 = Capable of supporting trials by 2020.</li> <li>• 0.0 = No potential for trials.</li> </ul>

These ratings are used in the assessment of shielding alternatives in Section D subsection 2 of this chapter, and for medical alternatives under consideration in Section E. Other alternatives under consideration (Mission Architecture and Launch Configuration) are simplified in Sections C and D based on the existence of detailed trade studies, and to help narrow the scope of alternatives under consideration in this paper.

### C. EVALUATION OF MISSION ARCHITECTURE ALTERNATIVES

The alternatives for mission architecture may be simplified through the review of trade-offs already completed in the Drake Design Reference Architecture (2009). The trades focus on the key objectives outlined in Section A of this chapter. The summary of these trades is shown in Figures 57 through 59.

	Short Stay	Long Stay
Advantages	<ul style="list-style-type: none"> <li>• 22-month total mission duration is closer to boundary of human experience base (1 Russian cosmonaut flight: 14 months; 6 cosmonauts: 6–14-month flights)</li> <li>• Shorter mission presents far less risk of psychiatric or behavioral condition emerging               <ul style="list-style-type: none"> <li>– Based on Antarctic experience, mission stress curve increases linearly with time</li> <li>– Shorter exposure to and less entrainment required for martian solar day</li> </ul> </li> </ul>	<ul style="list-style-type: none"> <li>• Less time in confined transit vehicle</li> <li>• More EVA opportunities</li> <li>• Less schedule stress during surface period (based on historical considerations)</li> </ul>
Disadvantages	<ul style="list-style-type: none"> <li>• Poorly understood risk of CNS damage possibly leading to cognitive, behavior, learning, and memory changes due to increase exposure to free space, heavy-ion environment</li> </ul>	<ul style="list-style-type: none"> <li>• 30-month total mission duration is outside of human experience base (1 Russian cosmonaut flight: 14 months)</li> </ul>

Figure 57. Advantages and Disadvantages for Behavioral Health and Performance Discipline. Source: Drake (2009, 77).

This review of safety finds that the Short-stay mission model has advantage over the Long-stay because the total length of the Short-stay mission is a dominant factor relative to the human experience base of one 14-month cosmonaut space flight. Because the Short-stay mission will only take 22 months total, this at least is closer to that base as opposed to the Long-stay mission which more than doubles it at 30 months.

Mass roll-up is shown in Figure 58 shows including a comparison for two fuel types, but for the purposes of this discussion we focus on the chemical fuel due to its current technical maturity relative to nuclear thermal (NTR) propulsion.

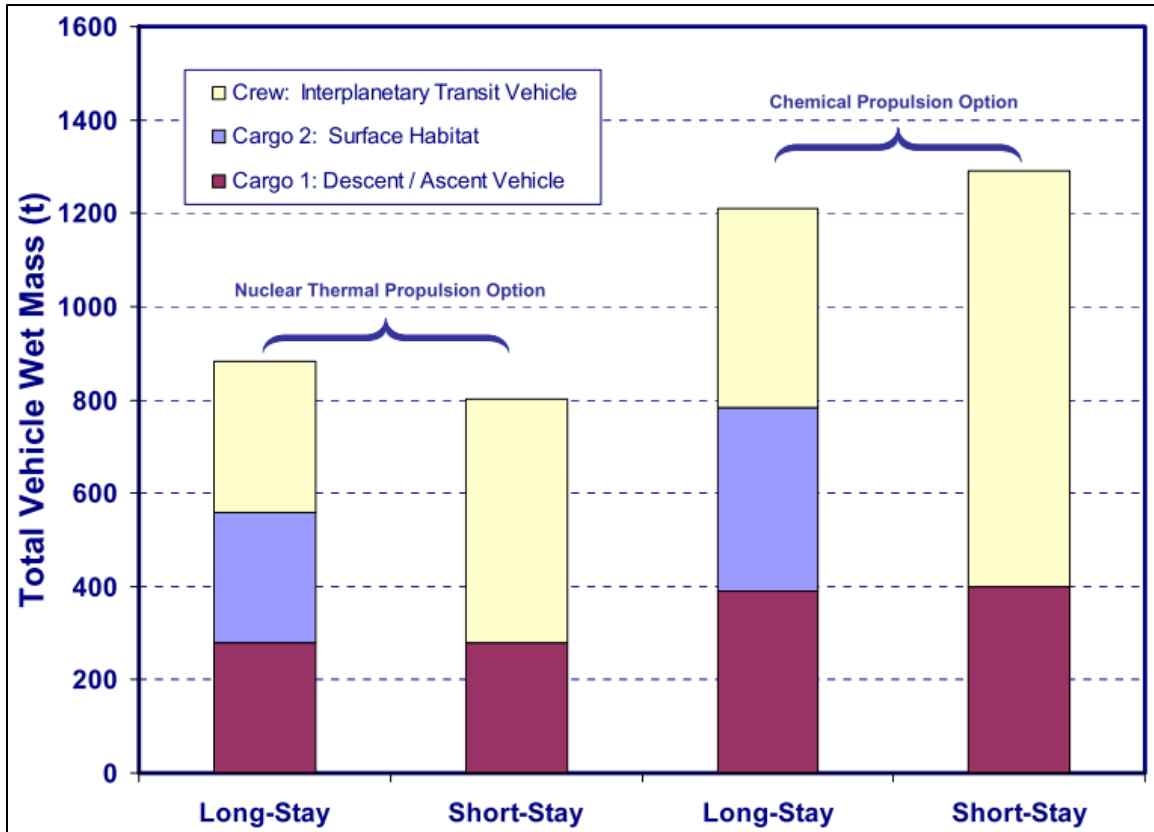


Figure 58. Long and Short-Stay Architecture Mass Comparisons. Source: Drake (2009, 79).

This figure shows clearly how the Long-stay mission has more components (transit vehicle, surface habitat, and ascent/descent vehicle) whereas the Short-stay mission does not need a surface habitat. However, due to the fact that Short-stay mission architectures necessitate less efficient vehicle trajectories going to and from Mars, the significant fuel load required for the transit vehicle results in greater mass required for the Short-stay mission. As such, Long-stay has the more favorable outlook with this objective. It should also be noted that in a further assessment, Drake finds that the Long-stay architecture is still slightly more costly than the Short-stay due to the anticipated costs for the surface habitat and other supporting surface systems, and the additional descent fuel stages required to land them on the Martian surface. Some of these costs may be defrayed in the long term by commonality with systems developed for use on the

Moon, and via re-use as some systems are used by multiple crews via a long-term Long-stay model (Drake 2009, 80).

The overall trajectory architecture trade is summarized in Figure 59. In this figure, the overall comparison of various criteria or Figures of Merit (FOM) lead to an overall conclusion that the Long-stay architecture is favored overall. This was the recommendation put forth by Drake to the NASA Agency Steering Group in 2007 (Drake 2009, 81).

<b>Human Exploration Of Mars</b>		
<b>Long Surface Stay (Conjunction Class)</b>	<b>Figure of Merit</b>	<b>Short Surface Stay * (Opposition Class)</b>
Similar	Total mass in Low-Earth Orbit (mt)	Similar *
45% Smaller	LEO Complexity / Size of Crew Vehicle	Larger
~3100 crew-sols	Expected Useful Crew Sols on Surface (mission return)	~80-500 crew-sols
Best	Exploration Goal Satisfaction (range, depth, frequency)	Lower
3 / 6 kg/kg	Architecture Sensitivity (gear ratios: NTR/Chem)	4 / 13 kg/kg
No Clear Advantage	Probability of Loss of Crew	Somewhat Less
Somewhat Less	Probability of Loss of Mission	No Clear Advantage
950	Total Mission Duration	650 days
500 sols	Mission Flexibility (contingency replanning)	Few sols
Less	Crew Health Risks from Radiation Exposure	More
200 / 500 / 200	Crew Exposure to Zero-G (days out / surface / back)	180 / 30 / 360
Available	Backup Lander and Surface Habitat	None
Somewhat More	Cost Through First Mission	Slight Advantage
Somewhat More	Cost Through Third Mission	Slight Advantage

Figure 59. Summary of Long versus Short-Stay Trade Space. Source: Drake (2009, 81).

It should be noted that current NASA mission plans only include a roadmap up to sending humans to orbit Mars by the mid-2030s, but lack further detail beyond that (see NASA’s Journey to Mars website, <https://www.nasa.gov/content/journey-to-Mars-overview>). It will remain to be seen whether Long-stay or Short-stay concepts are the first ones implemented beyond that, but for the purposes of this paper, Long-stay will be used to support further trade analyses in this chapter.

## D. EVALUATION OF SHIELDING ALTERNATIVES

### 1. Simplification of Decision Regarding Launch Configuration

Drake’s Design Reference Architecture contains a trade analysis summary that weighs the All-Up and Pre-Deploy configurations. The results of this analysis are shown in Figure 60.

Human Exploration Of Mars		
Pre-Deploy Cargo	Figure of Merit	All-Up Mission
Performance		
Slightly lower	Total mass in Low-Earth Orbit (mt)	Slightly higher
Similar	Total Number of Ares-V Launches	Similar
Similar	Total Number of Ares V Launches in Single Window	Similar
Risk		
No clear advantage	Probability of Loss of Mission (Plom)	No clear advantage
No clear advantage	Probability of Loss of Crew (Ploc)	No clear advantage
Higher	Max Cum Time on Systems by End of Mission	Lower by one year or more
Cost		
Slightly higher	Cost through first mission	Slight advantage
Similar	Cost through third mission	Similar
Other		
Available (long stay only)	Backup DAV and SHAB	None
Longer duration	Exploration Goal Satisfaction (longer surface operations)	Shorter duration
Smaller units	LEO Complexity / Size of Elements launched	Large single unit or convoy

Figure 60. Summary of Pre-Deploy versus All-Up Trade Space. Source: Drake (2009, 89).



This figure highlights many of the advantages and disadvantages already discussed in Chapter V Section A. For the All-Up mission, the crew gains some measure of reliability from the likelihood that the mission vehicles (Transit, Descent/Ascent) would likely depart LEO separately but then rendezvous in space. This provides an “Apollo 13” type refuge in the event of an outbound (only) emergency on the transit vehicle. Conversely, the launch mass required to send all vehicles together on a fast transit trajectory to Mars is extremely high due to the increased fuel load required for each vehicle. This model also provides no opportunity for advanced vehicles to arrive, verify proper function, or do advanced ISRU work or robotic exploration on the Martian surface (Drake 2009, 84-85).

For the Pre-Deploy model, the chief advantages are the option to use the most fuel-efficient (albeit slower) trajectories to send the DAV and SHAB to the Martian surface, and the benefits of advance arrival meaning that crews can count on verified status from them prior to their own launch from Earth, and possible advance work being done before their arrival. Further advantages also include lower mass relative to All-Up configurations due to reduced fuel load requirements, and the fact that mission launch intervals will permit for a redundant DAV and SHAB to be on the Martian surface in the event that the crew has an issue with the current vehicles on their mission. However, the counter-point to this is that the vehicles will be required to operate for a longer mission span than they would have to in an All-Up model (in all cases sitting at least a year on the Martian surface before crew arrives) which increases the chance of a system failure during that time. Additionally, there is no redundant vehicle for crew to evacuate to in the event of an emergency during the outbound transit (Drake 2009, 84-85). In spite of this, Drake still concludes that the Pre-Deploy model is the more optimal option which is the assumption moving forward for this paper.

## **2. Analysis of Shielding Alternatives**

The first step in this analysis is to review the alternatives that will be under consideration for their effectiveness at shielding for GCR as discussed in detail in Chapter V. The list includes:

- in situ resource usage (primarily regolith) for shielding on the Martian surface (Ch. V Section B)
- hydrogenated boron nitride nanotubes (BNNTs–Ch. V Section D)
  - specific “best case” example under comparison from Figure 46: BNNT + 20% by weight H<sub>2</sub> (BN is the acronym in the Figure)
- hydrogen-loaded metal organic frameworks (MOFs–Ch. V Section C)
  - specific “best case” example under comparison from Figure 40: C<sub>432</sub>H<sub>1120</sub>Be<sub>48</sub>O<sub>144</sub>
- nanoporous carbon composites (CNTs–Ch. V Section C)
  - Specific “best case” example under comparison from Figure 41: (C<sub>2</sub>H<sub>4</sub>)39.13%(CH<sub>3</sub>)60.87%
- metal hydrides (MHs–Ch. V Section C)
  - Specific “best case” example under comparison from Figure 42: 91% Li<sub>2.35</sub>Si and 9% H
- Field-based shielding concepts (Ch. V Section E)

For reference, NASA exposure limits are reviewed from their discussion in Chapter III here. A helpful unit conversion to review is that of Grays to Sievert, since cGy are a common unit used in some of the shielding data in Chapter V. One cGy is equal to 10mSv, and 1000mSv is equal to one Sv as used in Table 10:

Table 10. Review of NASA Career Effective Dose Limits

Age (yr)	Females		Males	
	Avg. US Adult Population	Never-Smokers	Avg. US Adult Population	Never-Smokers
30	0.44 Sv	0.6 Sv	0.63 Sv	0.78 Sv
40	0.48	0.70	0.70	0.88
50	0.54	0.82	0.77	1.00
60	0.64	0.98	0.90	1.17

Table 11 assesses the radiation shielding effectiveness of each of the six shielding alternatives by conducting sample calculations as compared to Aluminum at a shielding thickness of 30g/cm<sup>2</sup>. A simple density calculation is also conducted to review the physical thickness required for each material to achieve this performance. For all density calculations it is helpful to compare to the density of aluminum which is 2.7g/cm<sup>3</sup>. For the assumed 30g/cm<sup>2</sup> shielding thickness used in these calculations, it would only take an 11cm thick layer of aluminum to achieve the same shielding.

Table 11. Shielding Sample Calculations

Alternative	Shielding Calculation
	Density & Thickness Calculation
Martian regolith shield—refer to Ch. V Section B for details	Comparable to aluminum in effectiveness—extrapolating the Aluminum Curve from Figure 40 yields a dose rate of .043cGy/day at an effective thickness of 100g/cm <sup>2</sup> , and a slope of approximate -.01cGy/day per increase of 40g/cm <sup>2</sup> . It stands to reason that increasing shield thickness to 300g/cm <sup>2</sup> (calculated at a thickness of ~2m of regolith) will reduce absorbed dose rate to negligible levels. Of note, this shielding will only be available for the surface portion of any mission so this is not a full solution.
	Density ~1.52g/cm <sup>3</sup> , ~2m required to be effective against GCR
BNNT + 20% by weight H <sub>2</sub>	Figure 46 shows an equivalent dose comparison of Al verses this composite at a difference of 1.7mSv/day verses 0.9mSv/day: 1.7mSv/day×1000days×1Sv/1000mSv= <b>1.7Sv equivalent dose with Al shielding</b> 0.9mSv/day×1000days×1Sv/1000mSv= <b>0.9Sv equivalent dose with BNNT shielding</b>
	<b>Mission improvement verses aluminum = 0.8Sv</b>
	BNNT Density = 1.4g/cm <sup>3</sup> 30g/cm <sup>2</sup> shield thickness required×1cm <sup>3</sup> /1.4g= <b>21cm thickness required to achieve the calculated shielding density</b>

Alternative	Shielding Calculation
	Density & Thickness Calculation
MOF: $C_{432}H_{1120}Be_{48}O_{144}$	<p>Figure 40 shows an absorbed dose comparison of Al versus this composite at a difference of .061cGy/day versus .053cGy/day:  <math>.061cGy/day \times 1000days \times 10mSv/cGy \times 1Sv/1000mSv = .61Sv</math>  <b>absorbed* with Al shielding</b>  <math>.053cGy/day \times 1000days \times 10mSv/cGy \times 1Sv/1000mSv = .53Sv</math>  <b>absorbed* with MOF shielding</b></p> <p>*We can use the fact that effective dose is equal to absorbed dose multiplied by a Quality Factor (QF) to estimate the equivalent dose of the data for this composite and others below.  <b>1.7Sv equivalent dose with 30g/cm<sup>2</sup> Aluminum shielding</b> ÷  0.61Sv absorbed dose with the same shielding  <b>=an average Quality Factor of ~2.8.</b></p> <p>Converting the MOF data calculated above by Quality Factor:  <math>0.53Sv \times 2.8QF = 1.5Sv</math> <b>equivalent dose with MOF shielding</b></p> <p><b>Mission improvement versus aluminum = 0.2Sv</b></p> <p>MOF Density = <math>0.46g/cm^3</math>  <math>30g/cm^2</math> shield thickness required <math>\times 1cm^3 / 0.46g = 65cm</math> <b>thickness required to achieve the calculated shielding density</b></p>
CNT: (C <sub>2</sub> H <sub>4</sub> )39.13%(CH <sub>3</sub> ) 60.87%	<p>Figure 41 shows an absorbed dose comparison of Al versus this composite at a difference of .061cGy/day versus .052cGy/day:  <math>.061cGy/day \times 1000days \times 10mSv/cGy \times 1Sv/1000mSv \times 2.8QF = 1.7Sv</math> <b>equivalent dose with Al shielding</b>  <math>.052cGy/day \times 1000days \times 10mSv/cGy \times 1Sv/1000mSv \times 2.8QF = 1.4Sv</math> <b>equivalent dose with CNT shielding</b></p> <p><b>Mission improvement versus aluminum = 0.3Sv</b></p> <p>CNT Density = <math>1.17g/cm^3</math>  <math>30g/cm^2</math> shield thickness required <math>\times 1cm^3 / 1.17g = 26cm</math> <b>thickness required to achieve the calculated shielding density</b></p>
MH: 91% Li <sub>2.35</sub> Si and 9% H	<p>Figure 42 shows an absorbed dose comparison of Al versus this composite at a difference of .061cGy/day versus .048cGy/day:  <math>.061cGy/day \times 1000days \times 10mSv/cGy \times 1Sv/1000mSv \times 2.8QF = 1.7Sv</math> <b>equivalent dose with Al shielding</b>  <math>.048cGy/day \times 1000days \times 10mSv/cGy \times 1Sv/1000mSv \times 2.8QF = 1.3Sv</math> <b>equivalent dose with MH shielding</b></p> <p><b>Mission improvement versus aluminum = 0.4Sv</b></p> <p>MH Density = <math>0.84g/cm^3</math>  <math>30g/cm^2</math> shield thickness required <math>\times 1cm^3 / 0.84g = 36cm</math> <b>thickness required to achieve the calculated shielding density</b></p>

Alternative	Shielding Calculation
	Density & Thickness Calculation
Field based shield	No shield performance data available—effectiveness is estimated to be high.
	Density is N/A although it is noted in Chapter V Section E that the weight of cargo needed to generate the power for such technology would be quite high.

Using these calculations, Tables 12–17 review the performance of each alternative relative to the objectives and assigns a rating for each. The bottom row of each table reveals the overall measure of effectiveness (MOE) that is calculated by multiplying the rating for each objective by the normalized weight of that objective and then summing them over all objectives for that alternative.

Table 12. Objective Ratings for Martian Regolith Shielding

Objective	Discussion	Rating
H&S 1	At 2m thickness nearly all exposure is mitigated, but only for approximately half the days of a 1000-day Long-stay mission model because regolith may only be used on the Martian surface. As such a rating of 0.5 is assigned.	0.5
H&S 2	No impact on exposure mitigation	0.0
C&W 1	Regolith shielding requires a 2m thickness to be effective. It also requires additional weight in terms of Pre-Deployed equipment to help move or process the regolith for use at the location of a surface habitat. As such the potential for weight increase is relatively high, and a rating of 0.1 is assigned. It should be noted that the decision to use a “sandbag” system has the potential to reduce this weight, but the trade-off of crew labor and time outside the habitat to shovel-fill the number of bags required could prove to be unreasonable. If automated equipment from prior missions could be used for something like this, this rating would likely improve. Refer to Chapter V Section B for details on this concept.	0.1
C&W 2	The technology to move or process regolith on the Martian surface requires the development of ruggedized moving or brick-forming equipment. Development costs are assumed to be moderate and given a rating of 0.5.	0.5
SV 1	Regolith shielding has the potential to increase Martian surface stay times in the future based on the fact that it would reduce crew exposure to negligible levels while in the habitat. Its potential to add science value to future missions by allowing greater human exploration is extremely high. A rating of 0.9 is assigned.	0.9
SV 2	Regolith shielding provides the potential for longer surface stays which will enable collection of a greater variety of samples from more locations, and the time to analyze them in greater depth. This potential for improved sample value dictates a rating of 1.0.	1.0
SV 3	It is uncertain whether regolith shielding would require more crew time to assemble because the potential for automated technology to complete some or all of the work prior to crew arrival exists. That said, once in place it should require relatively little inspection and maintenance relative to hydrogen and methane based composites where off gassing may always be a concern. A rating of 0.6 is assigned with the assumption that crew time may be slightly reduced.	0.6
Sked 1	Regolith usage requires additional cargo and infrastructure on the Martian surface. Given in situ resource usage is part of the roadmap on the NASA “Journey to Mars Overview” website within the 2030 timeframe, it is reasonably likely that such technology may be ready for use by 2040 (2017). A 0.9 rating is given.	0.9
Sked 2	While some regolith information has already been collected thanks to prior missions to the Moon, sample return from Mars is not planned until the late 2020s (“Journey to Mars Overview” 2017). Further, the “Journey to Mars Overview” roadmap does not show any planned surface missions on the Moon. As such, this technology is not likely to achieve an early proving ground use. A rating of 0.2 is assigned.	0.2
MOE	<i>Sample Calculation–See Table 17 for reference:</i> $(0.5 \times 0.308 + 0.0 \times 0.092 + 0.1 \times 0.150 + 0.5 \times 0.150 + 0.9 \times 0.050 + 1.0 \times 0.092 + 0.6 \times 0.050 + 0.9 \times 0.033 + 0.2 \times 0.075) = 0.456$	<b>0.456</b>

Table 13. Objective Ratings for BNNT Shielding

Objective	Discussion	Rating
H&S 1	BNNTs are by far the most effective of the potential vehicle shielding technologies under consideration, with an estimated 1000-day equivalent of 0.9Sv. However, this still exceeds the career dose limit for all but the oldest male and female never-smoker categories. As such we assign it a rating of 0.8.	0.8
H&S 2	No impact on exposure mitigation	0.0
C&W 1	BNNTs require a shield thickness of 21cm to match the shielding density of 11cm of aluminum—that said their performance is much higher. It is assumed that a thicker composite shield will require more structural material to help encase and support it however. As such this material receives a rating of 0.4 for its likelihood to cause a minor increase in vehicle weight.	0.4
C&W 2	BNNTs are a very new composite technology and it is assumed that their complexity is higher than MOHs, CNTs, and MFs based on the fact that nanotube production is involved. As such, their development costs are assumed to be somewhat high. A rating of 0.3 is assigned.	0.3
SV 1	Composite shielding technology yields science gains in the sense that composites not only enable greater potential for space exploration, but also potential for cross-application on Earth. BNNTs arguably have higher potential than the other composites due to the strength of nanotube technology. A rating of 0.6 is assigned.	0.6
SV 2	All composite shielding technologies are assumed to improve performance over aluminum alone, but none of them reduce exposure levels below the existing limits. That said, a chief goal of human missions to Mars is to enable improved basic sample return, so it is assumed that these technologies support that goal. A rating of 0.5 is assumed.	0.5
SV 3	All composite shielding technologies require some level of increased crew maintenance to inspect and ensure that the composites are not degrading over time. It is assumed that BNNTs may be more stable than the other composites under consideration due to the nanotube technology, but hydrogen off-gassing will still be a significant concern. A rating of 0.4 is assigned.	0.4
Sked 1	Because BNNTs are an extremely new technology, they are assumed to have further technological development to complete in order to be ready for fielding. In the absence of discrete schedule data, they are given a moderate rating of 0.5 which is slightly lower than the other composites under research will receive.	0.5
Sked 2	Based on the same reasoning as Sked 1, BNNTs are assigned a rating of 0.5 for their likelihood to be ready for proving ground trials on cis-Lunar missions in the 2020s.	0.5
<b>MOE</b>		<b>0.502</b>

Table 14. Objective Ratings for MOF Shielding

Objective	Discussion	Rating
H&S 1	MOF data yields the smallest improvement in equivalent dose (1.5Sv) relative to baseline aluminum shielding (1.7Sv)—but it is still an improvement. A “low” rating of 0.2 is assigned.	0.2
H&S 2	No impact on exposure mitigation	0.0
C&W 1	MOHs require by far the greatest thickness for a 30g/cm <sup>2</sup> shield of all the composite vehicle materials under consideration at 65cm. As such their impact on weight increase is assumed to be relatively high (but lower than regolith). A rating of 0.2 is assigned.	0.2
C&W 2	MOHs are a relatively new composite technology (roughly equivalent to CNTs and MFs) and as such their development costs are assumed to be somewhat higher than moderate. A rating of 0.4 is assigned.	0.4
SV 1	Composite shielding technology yields science gains in the sense that composites not only enable greater potential for space exploration, but also potential for cross-application on Earth. A rating of 0.5 is assigned.	0.5
SV 2	All composite shielding technologies are assumed to improve performance over aluminum alone, but none of them reduce exposure levels below the existing limits. That said, a chief goal of human missions to Mars is to enable improved basic sample return, so it is assumed that these technologies support that goal. A rating of 0.5 is assumed.	0.5
SV 3	All composite shielding technologies require some level of increased crew maintenance to inspect and ensure that the composites are not degrading over time. Hydrogen off-gassing will be a significant concern. A rating of 0.3 is assigned.	0.3
Sked 1	All other composites under research are still relatively new technology, but little schedule data was provided as far as when they will achieve sufficient technological readiness to field. They are assigned a moderate rating of 0.6 for this objective.	0.6
Sked 2	Based on the same reasoning as Sked 1, MOFs are assigned a rating of 0.6 for their likelihood to be ready for proving ground trials on cis-Lunar missions in the 2020s.	0.6
<b>MOE</b>		<b>0.303</b>



Table 15. Objective Ratings for CNT Shielding

Objective	Discussion	Rating
H&S 1	CNTs yield a slightly better equivalent dose than MOHs (1.4Sv verses 1.5Sv). A slightly better rating of 0.3 is assigned.	0.3
H&S 2	No impact on exposure mitigation	0.0
C&W 1	CNTs require a 26cm thickness for the shielding calculations done in Table 11, which is roughly equivalent to the 21cm thickness for the BNNT materials. An equivalent rating of 0.4 (still likely to increase weight slightly higher than aluminum alone) is assigned.	0.4
C&W 2	CNTs are a relatively new composite technology (roughly equivalent to MOHs and MFs) and as such their development costs are assumed to be somewhat higher than moderate. A rating of 0.4 is assigned.	0.4
SV 1	Composite shielding technology yields science gains in the sense that composites not only enable greater potential for space exploration, but also potential for cross-application on Earth. A rating of 0.5 is assigned.	0.5
SV 2	All composite shielding technologies are assumed to improve performance over aluminum alone, but none of them reduce exposure levels below the existing limits. That said, a chief goal of human missions to Mars is to enable improved basic sample return, so it is assumed that these technologies support that goal. A rating of 0.5 is assumed.	0.5
SV 3	All composite shielding technologies require some level of increased crew maintenance to inspect and ensure that the composites are not degrading over time. Hydrogen off-gassing will be a significant concern. A rating of 0.3 is assigned.	0.3
Sked 1	All other composites under research are still relatively new technology, but little schedule data was provided as far as when they will achieve sufficient technological readiness to field. They are assigned a moderate rating of 0.6 for this objective.	0.6
Sked 2	Based on the same reasoning as Sked 1, CNTs are assigned a rating of 0.6 for their likelihood to be ready for proving ground trials on cis-Lunar missions in the 2020s.	0.6
<b>MOE</b>		<b>0.363</b>

Table 16. Objective Ratings for MH Shielding

<b>Objective</b>	<b>Discussion</b>	<b>Rating</b>
H&S 1	MHs yield a slightly better equivalent dose than CNTs (1.3Sv verses 1.4Sv). A slightly better rating of 0.4 is assigned.	0.4
H&S 2	No impact on exposure mitigation	0.0
C&W 1	MHs require a 36cm thickness for the shielding calculations done in Table 11, which is slightly higher than the 26cm thickness for CNT materials. A rating of 0.3 based on the fact that they have the potential for a higher increase in weight required.	0.3
C&W 2	MHs are a relatively new composite technology (roughly equivalent to MOHs and CNTs) and as such their development costs are assumed to be somewhat higher than moderate. A rating of 0.4 is assigned.	0.4
SV 1	Composite shielding technology yields science gains in the sense that composites not only enable greater potential for space exploration, but also potential for cross-application on Earth. A rating of 0.5 is assigned.	0.5
SV 2	All composite shielding technologies are assumed to improve performance over aluminum alone, but none of them reduce exposure levels below the existing limits. That said, a chief goal of human missions to Mars is to enable improved basic sample return, so it is assumed that these technologies support that goal. A rating of 0.5 is assumed.	0.5
SV 3	All composite shielding technologies require some level of increased crew maintenance to inspect and ensure that the composites are not degrading over time. Hydrogen off-gassing will be a significant concern. A rating of 0.3 is assigned.	0.3
Sked 1	All other composites under research are still relatively new technology, but little schedule data was provided as far as when they will achieve sufficient technological readiness to field. They are assigned a moderate rating of 0.6 for this objective.	0.6
Sked 2	Based on the same reasoning as Sked 1, MHs are assigned a rating of 0.6 for their likelihood to be ready for proving ground trials on cis-Lunar missions in the 2020s.	0.6
<b>MOE</b>		<b>0.379</b>

Table 17. Objective Ratings for Field-Based Shielding

<b>Objective</b>	<b>Discussion</b>	<b>Rating</b>
H&S 1	Field based shielding data is extremely preliminary but it is assumed to have the potential for a very high level of effectiveness. A rating of 0.9 is assigned.	0.9
H&S 2	No impact on exposure mitigation	0.0
C&W 1	Field based shielding is considered to be prohibitive at present in part due to the large weight that would be required to house equipment on a transit vehicle capable of generating the power required. A rating of 0.0 is assigned for highest potential impact on weight increase.	0.0
C&W 2	Field based shielding is also the newest technology under consideration out of all of the alternatives discussed in this chapter. It is assumed that the potential development costs would be extremely high. A rating of 0.1 is assigned.	0.1
SV 1	Field-based shielding has the potential to increase Martian surface stay times in the future based on the fact that it would reduce crew exposure to very low levels while in the habitat. Its potential to add science value to future missions by allowing greater human exploration is extremely high. A rating of 0.8 is assigned.	0.8
SV 2	Field-based shielding provides the potential for longer surface stays which will enable collection of a greater variety of samples from more locations, and the time to analyze them in greater depth. This potential for improved sample value dictates a rating of 1.0.	1.0
SV 3	Field based shielding necessitates more equipment in the form of shield generators, power supplies, coils and wiring, etc. It is assumed that this will be very maintenance-intensive, and a rating of 0.1 is assigned.	0.1
Sked 1	Based on the review in Chapter V, field based shield technology is an extremely new concept and has a very low likelihood of being ready to field by 2040. It is assigned a rating of 0.1	0.1
Sked 2	It is assumed that field based shielding technology has virtually no chance of being ready to implement for the earliest proving ground trials. A rating of 0.0 is given.	0.0
<b>MOE</b>		<b>0.433</b>

Table 18 provides a summary of the calculations conducted to determine the MOEs described in the Tables 12–17.

Table 18. Summary of MOE Calculations

SHIELDING TRADE STUDY								
Objective	Importance, Variance	Weight	Regolith Ratings	BNNT Ratings	MOF Ratings	CNT Ratings	MH Ratings	Field based Ratings
H&S 1	High, High	0.308	0.5	0.8	0.2	0.3	0.4	0.9
H&S 2	Medium, Moderate	0.092	0.0	0.0	0.0	0.0	0.0	0.0
C&W 1	High, Moderate	0.150	0.1	0.4	0.2	0.4	0.3	0.0
C&W 2	High, Moderate	0.150	0.5	0.3	0.4	0.4	0.4	0.1
SV 1	Medium, High	0.050	0.9	0.6	0.5	0.5	0.5	0.8
SV 2	Medium, Moderate	0.092	1.0	0.5	0.5	0.5	0.5	1.0
SV 3	Low, Moderate	0.050	0.6	0.4	0.3	0.3	0.3	0.1
Sked 1	Low, Low	0.033	0.9	0.5	0.6	0.6	0.6	0.1
Sked 2	Medium, Low	0.075	0.2	0.5	0.6	0.6	0.6	0.0
		<b>MOE:</b>	0.456	<b>0.502</b>	0.303	0.363	0.379	0.433

The summary reveals that overall; BNNT composites have the highest MOE and are therefore the most promising of the vehicle-based alternatives for shielding. Regolith receives relatively high score in spite of the fact that it can only be used for the surface-based phases of a mission, which indicates it should be considered as a parallel solution to any vehicle-based shields. It is worth noting that field-based shields also received a relatively high MOE, indicating it is well worth studying them as a promising alternative in the longer term.

#### E. EVALUATION OF MEDICAL COUNTERMEASURES

The assessment of various medical countermeasures is greatly simplified by the fact that all of them take up a miniscule amount of weight relative to the rest of the vehicle and cargo. This analysis aims to show which option(s) may be the most promising, but ultimately all of them may be worth sending on a human mission to Mars

if they achieve FDA approval in time. The following list reviews the options discussed in Chapter VI Section B of this paper:

- **Amifostine:** A protectant which reduces radiation damage to tissue if taken even minutes before radiation exposure. FDA approved for use.
- **Neupogen:** A mitigator taken after exposure which stimulates the bone marrow to more rapidly replenish white blood cells. FDA approved for use.
- **Entolimod:** can be given before or after exposure and shown to protect primates from damaging effects for up to 48 hours after exposure. Currently in Phase II clinical trials.
- **Recilisib:** tested in mice and shown to mitigate damaging effects if administered either before or up to 24 hours after exposure. Currently in Phase I clinical trials.
- **Romylocel-L:** improves white blood cell regeneration and has the potential to mitigate damage even if administered 3-5 days after exposure. Developmental studies have been completed but no formal clinical trials.

The rating assessment for all of these options is detailed in Tables 19–23.

Table 19. Objective Ratings for Amifostine

<b>Objective</b>	<b>Discussion</b>	<b>Rating</b>
H&S 1	Medical countermeasures have no impact on exposure reduction, and are assigned a rating of 0.0.	0.0
H&S 2	Because it must be taken in advance of radiation exposure to prevent damage, but because it is a protectant that actually stops that damage from occurring, Amifostine receives a relatively high rating of 0.8 for exposure mitigation.	0.8
C&W 1	All medical countermeasures are assumed to have negligible impact on weight, and receive a weight neutral 0.5 rating.	0.5
C&W 2	Because Amifostine is already FDA approved for use, it receives an optimal 1.0 rating for no further development costs being required.	1.0
SV 1	All medical countermeasures for radiation exposure are assumed to have cross application for radiation incidents on Earth. A rating of 0.5 is assigned.	0.5
SV 2	While medical countermeasures could be perceived as a justification for higher risk acceptance in terms of sending crew on longer-duration EVAs to collect a greater range/variety of Martian samples, it is unlikely that missions would ever be designed such that the crew must depend on such medications for survival. A neutral rating of 0.5 is assigned.	0.5
SV 3	Medical countermeasures are assumed to have a negligible impact on crew time. A rating of 0.5 is assigned. It is noted that future technologies such as devices to remotely synthesize medications on Mars would change this rating.	0.5
Sked 1	Because Amifostine is already FDA-approved for human use, it receives a rating of 1.0 for this objective.	1.0
Sked 2	Because Amifostine is already FDA-approved for human use, it receives a rating of 1.0 for this objective.	1.0
<b>MOE</b>		<b>0.503</b>

Table 20. Objective Ratings for Neupogen

<b>Objective</b>	<b>Discussion</b>	<b>Rating</b>
H&S 1	Medical countermeasures have no impact on exposure reduction, and are assigned a rating of 0.0.	0.0
H&S 2	Because it is only taken after exposure to help the body recover from damage done by radiation, Neupogen receives a moderate rating of 0.5 for exposure mitigation.	0.5
C&W 1	All medical countermeasures are assumed to have negligible impact on weight and receive a weight neutral 0.5 rating.	0.5
C&W 2	Because Neupogen is already FDA approved for use, it receives an optimal 1.0 rating for no further development costs being required.	1.0
SV 1	All medical countermeasures for radiation exposure are assumed to have cross application for radiation incidents on Earth. A rating of 0.5 is assigned.	0.5
SV 2	While medical countermeasures could be perceived as a justification for higher risk acceptance in terms of sending crew on longer-duration EVAs to collect a greater range/variety of Martian samples, it is unlikely that missions would ever be designed such that the crew must depend on such medications for survival. A neutral rating of 0.5 is assigned.	0.5
SV 3	Medical countermeasures are assumed to have a negligible impact on crew time. A rating of 0.5 is assigned. It is noted that future technologies such as devices to remotely synthesize medications on Mars would change this rating.	0.5
Sked 1	Because Neupogen is already FDA-approved for human use, it receives a rating of 1.0 for this objective.	1.0
Sked 2	Because Neupogen is already FDA-approved for human use, it receives a rating of 1.0 for this objective.	1.0
<b>MOE</b>		<b>0.475</b>

Table 21. Objective Ratings for Entolimod

<b>Objective</b>	<b>Discussion</b>	<b>Rating</b>
H&S 1	Medical countermeasures have no impact on exposure reduction, and are assigned a rating of 0.0.	0.0
H&S 2	Because Entolimod can be used to mitigate the effects of exposure if taken either before or up to 48 hours after exposure, it receives a moderately high rating of 0.7.	0.7
C&W 1	All medical countermeasures are assumed to have negligible impact on weight and receive a weight neutral 0.5 rating.	0.5
C&W 2	Because Entolimod is already in Phase II clinical trials, it can be assumed that some further investment in development will be required. It is assumed that NASA will not incur the bulk of these costs given this medication is already in development for Earth-based use. A rating of 0.8 is assigned.	0.8
SV 1	All medical countermeasures for radiation exposure are assumed to have cross application for radiation incidents on Earth. A rating of 0.5 is assigned.	0.5
SV 2	While medical countermeasures could be perceived as a justification for higher risk acceptance in terms of sending crew on longer-duration EVAs to collect a greater range/variety of Martian samples, it is unlikely that missions would ever be designed such that the crew must depend on such medications for survival. A neutral rating of 0.5 is assigned.	0.5
SV 3	Medical countermeasures are assumed to have a negligible impact on crew time. A rating of 0.5 is assigned. It is noted that future technologies such as devices to remotely synthesize medications on Mars would change this rating.	0.5
Sked 1	Because this alternative is already in phase II clinical trials, there is a reasonable confidence that it will be FDA approved by 2040 pending the results of more advanced clinical trials. This necessitates a relatively high 0.7 rating.	0.7
Sked 2	Based on where it stands in clinical trials, Entolimod is assigned a moderate rating of 0.5 for its likelihood to be ready for proving ground trials on cis-Lunar missions in the 2020s.	0.5
<b>MOE</b>		<b>0.416</b>



Table 22. Objective Ratings for Recilisib

<b>Objective</b>	<b>Discussion</b>	<b>Rating</b>
H&S 1	Medical countermeasures have no impact on exposure reduction, and are assigned a rating of 0.0.	0.0
H&S 2	Because Recilisib can be used to mitigate the effects of exposure if taken either before or up to 48 hours after exposure, it receives a moderate rating of 0.6 (slightly lower than Entolimod).	0.6
C&W 1	All medical countermeasures are assumed to have negligible impact on weight and receive a weight neutral 0.5 rating.	0.5
C&W 2	Because Recilisib is only in Phase I clinical trials, it can be assumed that further investment in development will be required. It is assumed that NASA will not incur the bulk of these costs given this medication is already in development for Earth-based use—however potential investment may still be higher than Entolimod. A rating of 0.7 is assigned.	0.7
SV 1	All medical countermeasures for radiation exposure are assumed to have cross application for radiation incidents on Earth. A rating of 0.5 is assigned.	0.5
SV 2	While medical countermeasures could be perceived as a justification for higher risk acceptance in terms of sending crew on longer-duration EVAs to collect a greater range/variety of Martian samples, it is unlikely that missions would ever be designed such that the crew must depend on such medications for survival. A neutral rating of 0.5 is assigned.	0.5
SV 3	Medical countermeasures are assumed to have a negligible impact on crew time. A rating of 0.5 is assigned. It is noted that future technologies such as devices to remotely synthesize medications on Mars would change this rating.	0.5
Sked 1	Because this alternative is the second-least mature of all the medical countermeasures under consideration, there is a chance it may not be FDA approved by 2040 pending the results of more advanced clinical trials. This uncertainty necessitates a moderate 0.6 rating.	0.6
Sked 2	Based on how early it is in trials, Recilisib is assigned a reduced rating of 0.4 for its likelihood to be ready for proving ground trials on cis-Lunar missions in the 2020s.	0.4
<b>MOE</b>		<b>0.381</b>

Table 23. Objective Ratings for Romyelocel-L

Objective	Discussion	Rating
H&S 1	Medical countermeasures have no impact on exposure reduction, and are assigned a rating of 0.0.	0.0
H&S 2	Because it has the potential to both speed healing from damage that has occurred, and also to mitigate some damage for up to 3-5 days following exposure, Romyelocel-L receives a relatively high rating of 0.8 for this objective.	0.8
C&W 1	All medical countermeasures are assumed to have negligible impact on weight and receive a weight neutral 0.5 rating.	0.5
C&W 2	Because Romyelocel-L is only in developmental trials, it can be assumed that even more investment in development will be required relative to the other alternatives. It is assumed that NASA will not incur the bulk of these costs given this medication is already in development for Earth-based use—however potential investment may still be higher than Recilisib. A rating of 0.6 is assigned.	0.6
SV 1	All medical countermeasures for radiation exposure are assumed to have cross application for radiation incidents on Earth. A rating of 0.5 is assigned.	0.5
SV 2	While medical countermeasures could be perceived as a justification for higher risk acceptance in terms of sending crew on longer-duration EVAs to collect a greater range/variety of Martian samples, it is unlikely that missions would ever be designed such that the crew must depend on such medications for survival. A neutral rating of 0.5 is assigned.	0.5
SV 3	Medical countermeasures are assumed to have a negligible impact on crew time. A rating of 0.5 is assigned. It is noted that future technologies such as devices to remotely synthesize medications on Mars would change this rating.	0.5
Sked 1	Because this alternative is the least mature of all the medical countermeasures under consideration, there is a chance it may not be FDA approved by 2040 pending the results of more advanced clinical trials. This uncertainty necessitates a moderate 0.5 rating.	0.5
Sked 2	Based on how early it is in trials, Romyelocel-L is assigned a reduced rating of 0.5 for its likelihood to be ready for proving ground trials on cis-Lunar missions in the 2020s.	0.3
<b>MOE</b>		<b>0.373</b>

A summary of the MOE calculations for medical countermeasures is shown in Table 24.

Table 24. Summary of MOEs for Medical Countermeasures

<b>SHIELDING TRADE STUDY</b>							
<b>Objective</b>	<b>Importance, Variance</b>	<b>Weight</b>	<b>Amifostine Ratings</b>	<b>Neupogen Ratings</b>	<b>Entolimod Ratings</b>	<b>Recilisib Ratings</b>	<b>Romylocel-L Ratings</b>
H&S 1	High, High	0.308	0.0	0.0	0.0	0.0	0.0
H&S 2	Medium, Moderate	0.092	0.8	0.5	0.7	0.6	0.8
C&W 1	High, Moderate	0.150	0.5	0.5	0.5	0.5	0.5
C&W 2	High, Moderate	0.150	1.0	1.0	0.8	0.7	0.6
SV 1	Medium, High	0.050	0.5	0.5	0.5	0.5	0.5
SV 2	Medium, Moderate	0.092	0.5	0.5	0.5	0.5	0.5
SV 3	Low, Moderate	0.050	0.5	0.5	0.5	0.5	0.5
Sked 1	Low, Low	0.033	1.0	1.0	0.7	0.6	0.5
Sked 2	Medium, Low	0.075	1.0	1.0	0.5	0.4	0.3
		<b>MOE:</b>	<b>0.503</b>	<b>0.475</b>	0.416	0.381	0.373

The results are not surprising in that the two alternatives (Amifostine and Neupogen) that already have FDA approval are the most favored for use. That said, given how little weight medical countermeasures take up, it will likely be beneficial to include any medication that has FDA approval on future missions in order to optimize the variety of treatment available to the crew. As these medications are actually used in space, some may reveal themselves as more effective in the future, but it is difficult to ascertain this at present given the ethical boundaries that limit human studies on Earth.

## **F. REVIEW OF SOLUTIONS AND SENSITIVITY ANALYSIS**

The optimal shielding and medical countermeasure technologies revealed by the analyses in this chapter are relatively straight-forward. It is important to note that a change in some assumptions could have an impact on the overall results. For example, if we change our assumed mission architecture to Short-stay instead of Long-stay, the benefits of regolith shielding are largely negated due to the very short span of time spent

on the Martian surface. Rather than expanding at length on every possible permutation of mission factors that could occur, it is more beneficial to conduct a sensitivity analysis to determine which mission alternative have the potential to experience drastic shifts in their MOEs in the event that the weighting for certain objectives should change.

### **1. Explanation of Sensitivity Analysis for Swing Matrices**

In this method, one objective is assigned a new normalized weight of 1.0 while all other objectives/categories are assigned a normalized weight of zero. This simulates an optimized “what if this objective is given priority over all others” scenario. A set of alternatives to compare is plotted such that each alternative forms a slope connecting its original MOE to its “optimized” one. MOEs are plotted on the y axis so it follows that whichever alternative is the highest on the plot at a given point is the superior one. The sensitivity of the alternatives to changes in that objective is then tested by observing the plots over a small range surrounding the original objective normalized weight (typically  $\pm 0.1$ ). If any of the lines cross each other within that smaller range, we determine that the alternatives are sensitive to change over relatively small changes in that objective’s priority. This indicates further study of that decision may be necessary as time progresses.

The next sub-section demonstrates this sensitivity analysis for a small subset of objectives and alternatives using the following guidelines:

- A subset of three shielding alternatives are compared to simplify the demonstration: Regolith, BNNTs, and Field Based Shielding.
- Three objectives will be optimized to determine their impact on alternative selection:
  - H&S 1: what would happen if maintaining the lowest exposure possible took priority over cost, schedule, and science value?
  - C&W 1: what would happen if the lowest cost/weight possible took priority over all other objectives?
  - Sked 2: what if the importance of proving ground trials in the immediate future significantly limits whether alternatives would be considered for first human missions to the Martian surface?

## 2. Sensitivity Analysis Results

Figure 61 reviews the original normalized weights and MOEs calculated for each shield type under this analysis. Figure 62 shows the modification of the MOE results once each of the three objectives listed above is optimized to 1.0. The results of these calculations are better demonstrated by line graphs in Figures 63–65. All explanations for these charts are discussed in the paragraphs that follow them.

<b>SHIELDING TRADE STUDY</b>					
<b>Objective</b>	<b>Importance, Variance</b>	<b>Weight</b>	<b>Regolith Ratings</b>	<b>BNNT Ratings</b>	<b>Field based Ratings</b>
H&S 1	High, High	0.308	0.5	0.8	0.9
H&S 2	Medium, Moderate	0.092	0.0	0.0	0.0
C&W 1	High, Moderate	0.150	0.1	0.4	0.0
C&W 2	High, Moderate	0.150	0.5	0.3	0.1
SV 1	Medium, High	0.050	0.9	0.6	0.8
SV 2	Medium, Moderate	0.092	1.0	0.5	1.0
SV 3	Low, Moderate	0.050	0.6	0.4	0.1
Sked 1	Low, Low	0.033	0.9	0.5	0.1
Sked 2	Medium, Low	0.075	0.2	0.5	0.0
<b>ORIGINAL MOE:</b>			0.456	0.502	0.433

Figure 61. Normalized Weights and MOEs for Selected Shield Alternatives

<b>OPTIMIZED H&amp;S 1:</b>					
<b>Objective</b>	<b>Importance, Variance</b>	<b>Weight</b>	<b>Regolith Ratings</b>	<b>BNNT Ratings</b>	<b>Field based Ratings</b>
H&S 1	High, High	1.000	0.5	0.8	0.9
H&S 2	Medium, Moderate	0.000	0.0	0.0	0.0
C&W 1	High, Moderate	0.000	0.1	0.4	0.0
C&W 2	High, Moderate	0.000	0.5	0.3	0.1
SV 1	Medium, High	0.000	0.9	0.6	0.8
SV 2	Medium, Moderate	0.000	1.0	0.5	1.0
SV 3	Low, Moderate	0.000	0.6	0.4	0.1
Sked 1	Low, Low	0.000	0.9	0.5	0.1
Sked 2	Medium, Low	0.000	0.2	0.5	0.0
<b>ADJUSTED MOE:</b>			0.500	0.800	0.900

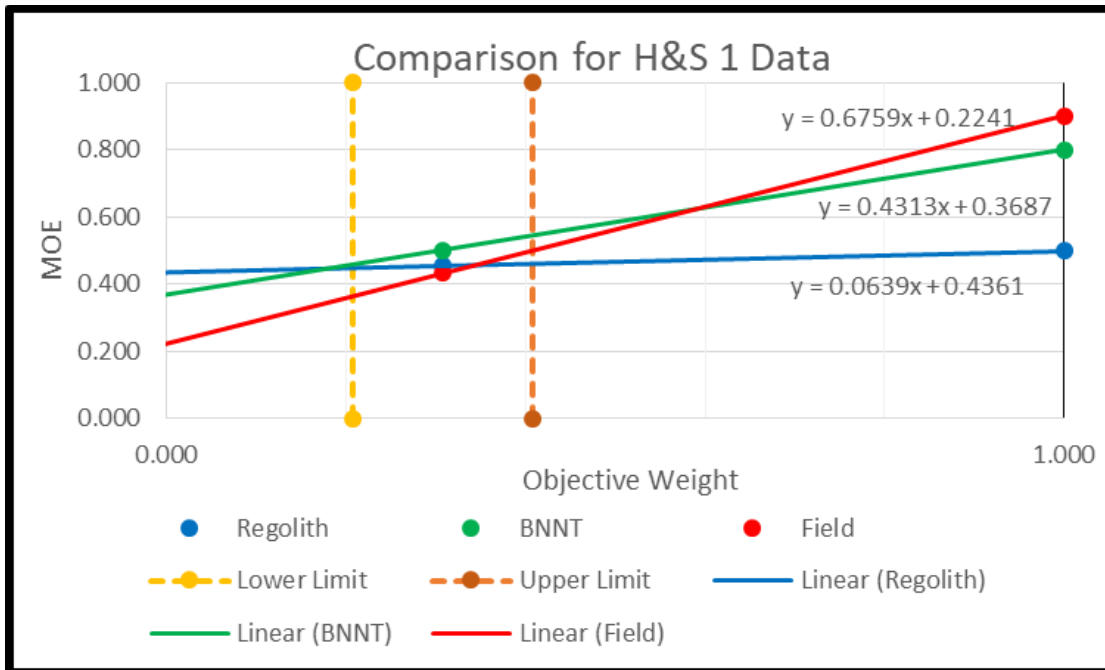
  

<b>OPTIMIZED C&amp;W 1:</b>					
<b>Objective</b>	<b>Importance, Variance</b>	<b>Weight</b>	<b>Regolith Ratings</b>	<b>BNNT Ratings</b>	<b>Field based Ratings</b>
H&S 1	High, High	0.000	0.5	0.8	0.9
H&S 2	Medium, Moderate	0.000	0.0	0.0	0.0
C&W 1	High, Moderate	1.000	0.1	0.4	0.0
C&W 2	High, Moderate	0.000	0.5	0.3	0.1
SV 1	Medium, High	0.000	0.9	0.6	0.8
SV 2	Medium, Moderate	0.000	1.0	0.5	1.0
SV 3	Low, Moderate	0.000	0.6	0.4	0.1
Sked 1	Low, Low	0.000	0.9	0.5	0.1
Sked 2	Medium, Low	0.000	0.2	0.5	0.0
<b>ADJUSTED MOE:</b>			0.100	0.400	0.000

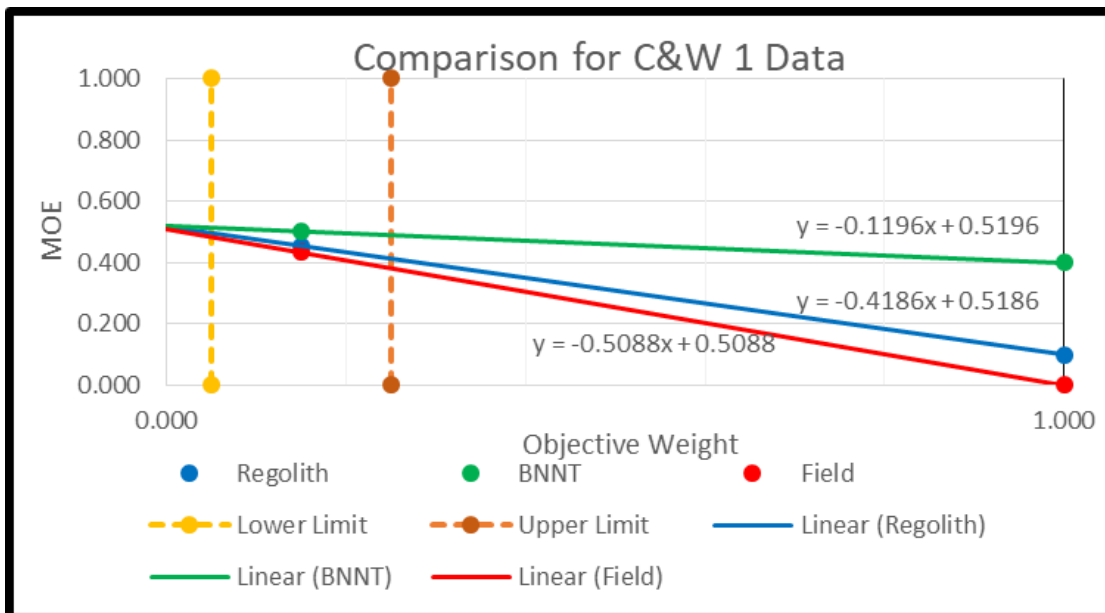
<b>OPTIMIZED Sked 2:</b>					
<b>Objective</b>	<b>Importance, Variance</b>	<b>Weight</b>	<b>Regolith Ratings</b>	<b>BNNT Ratings</b>	<b>Field based Ratings</b>
H&S 1	High, High	0.000	0.5	0.8	0.9
H&S 2	Medium, Moderate	0.000	0.0	0.0	0.0
C&W 1	High, Moderate	0.000	0.1	0.4	0.0
C&W 2	High, Moderate	0.000	0.5	0.3	0.1
SV 1	Medium, High	0.000	0.9	0.6	0.8
SV 2	Medium, Moderate	0.000	1.0	0.5	1.0
SV 3	Low, Moderate	0.000	0.6	0.4	0.1
Sked 1	Low, Low	0.000	0.9	0.5	0.1
Sked 2	Medium, Low	1.000	0.2	0.5	0.0
<b>ADJUSTED MOE:</b>			0.200	0.500	0.000

Figure 62. Optimized Weights and MOEs for Selected Objectives



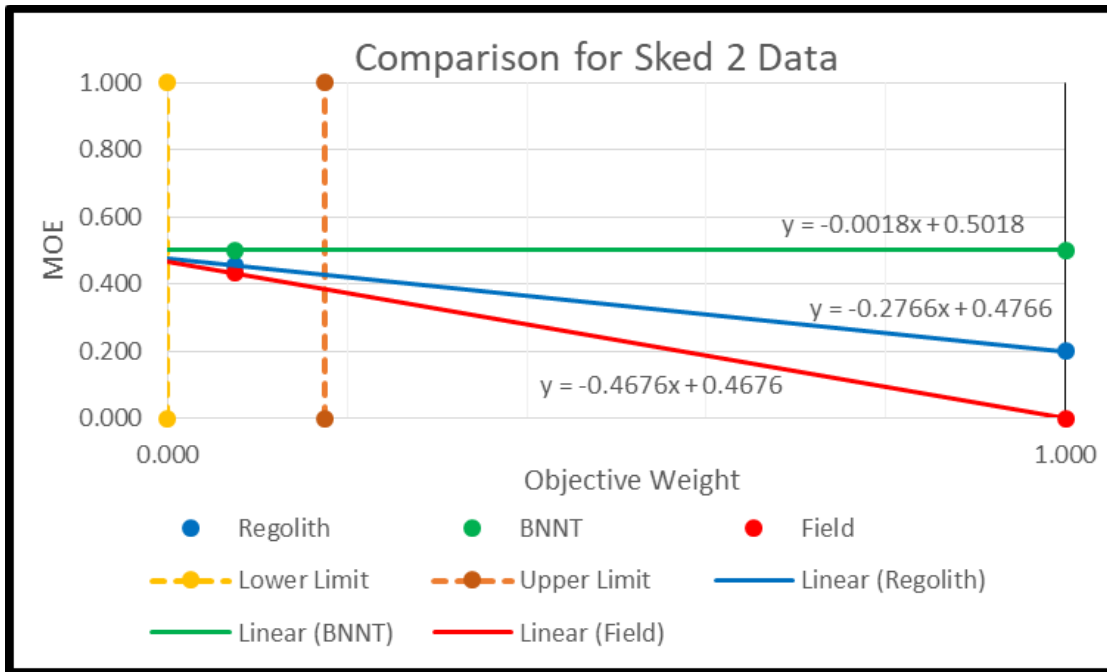
Note: Lower and upper range represent a  $\pm 0.1$  range around the original objective weight over which the degree of change of the MOEs is measured as the objective weights change.

Figure 63. MOE Response to H&S 1 Objective Weight Adjustment



Note: Lower and upper range represent a  $\pm 0.1$  range around the original objective weight over which the degree of change of the MOEs is measured as the objective weights change

Figure 64. MOE Response to C&W 1 Objective Weight Adjustment



Note: Lower and upper range represent a  $\pm 0.1$  range around the original objective weight over which the degree of change of the MOEs is measured as the objective weights change (here, the lower range reaches 0.0 and cannot go lower than that).

Figure 65. MOE Response to Sked 2 Objective Weight Adjustment

To interpret the results in Figures 63-65, we focus on the blue, green, and red lines that are created for each alternative MOE when the normalized weights are adjusted from their original value to 1.0 for the given objective. Then we look at these lines specifically between the lower and upper ranges to see if any of the alternative lines cross within that range.

Figure 63 shows that field based shielding rapidly starts to out-class other shielding systems as reducing exposure becomes a dominant priority. It crosses regolith within the lower and upper limits, but given its relative technical lack of maturity at present, and the fact that it is considered to be a parallel solution to regolith shielding while on the Martian surface, this should not cause us to question our analysis at present. It is worth noting that in the future, if/when field based shields become more viable, these results would seem to indicate that field based shielding may render most other types of



shielding redundant, given that the red field line also crosses the green BNNT line further to the right.

Figure 64 shows that the performance of all alternatives takes an overall downward trend as cost is shifted to dominance as a priority. However, none of the lines for the alternatives cross as they trend downward through the lower and upper limit region. Based on this we can conclude that the relative performance of these alternatives is not sensitive to changes in cost/weight priority. Figure 65 shows the same trend, which demonstrates that the relative performance of the shielding options is also minimally impacted by changes in schedule - although increasing schedule as a dominant priority again causes an overall downtrend in performance.

These are just three examples that show how alternative performance can be impacted as the priorities for mission objectives are shifted. It is important to note that medical countermeasures were not included in these examples due to the fact that a large portion of their objective ratings remain the same across all alternatives. One could posit that out of these objectives, conducting the analysis with a shift of weight to H&S 2, C&W 2, or both Sked objectives would be the only analyses where some change in relative outcomes might be observed.

This creates a powerful analytical tool that can be used by future researchers in combination with the option to vary the weights themselves in the original Swing Matrix setup from Section B of this Chapter. These tools can help to demonstrate or confirm the potential for alternative technologies to change such that they become superior or inferior to other options—as exemplified by the potential that field based shields have to outperform all other leading alternatives if other objectives (namely cost and schedule) are sacrificed to make exposure reduction a priority. This type of analysis can also identify the need to further re-weigh alternative decisions if it turns out that their relative performances are impacted in this way.

THIS PAGE INTENTIONALLY LEFT BLANK

## VIII. CONCLUSIONS

This paper conducts a thorough review of the mechanisms of human radiation exposure in space, and of the alternatives available in multiple technology areas to help reduce/mitigate radiation exposure for astronauts on missions beyond the protection of the Earth's magnetic field. In this case a mission to Mars is used as the basis for this analysis, with multiple simplifications made to control the scope of the alternatives available.

Based on trade studies conducted in the Drake Mars Mission Design Reference Architecture documents, we determine that a Long-stay mission in which the astronauts spend approximately 500 days each in transit and on the Martian surface (1000 days total) is a preferable model to maximize mission science value while also using orbital trajectories that minimize the crew's time in space and in closer proximity to the Sun where the risk of acute exposure from solar storms is potentially higher.

Other Drake trade studies are used to determine that a Pre-Deploy mission model is preferable - in which all necessary surface habitat, return vehicle, and other heavy cargo are sent to the Martian surface in advance of the crewed vehicle. This preference stems largely from the capability of this model to both minimize the weight of separate vehicles sent for the transit which is logistically simpler and less costly than sending an extremely large vehicle with all cargo; and from the fact that advance arrival of the surface habitat and other cargo provides a safety margin for the crew because they would not begin their journey to Mars until they have confirmation that all the necessary equipment arrived safely and is in working order.

Shielding alternatives for human missions to Mars present the greatest challenge for analysis because of the fact that at present, crew is predicted to exceed all existing career exposure limits on such a mission by a factor of 200-300%. Several assumptions are made to simplify this analysis for the purposes of this paper. The first is that all transit and habitat vehicles will include the design of a crew sleeping area/emergency shelter with water wall shielding to sufficiently mitigate acute exposure from any SPEs. Second and related to this, it is assumed that adequate sensors and space weather forecast

technology will be implemented as needed in space around the inner solar system such that crews can receive reliable advance warning to take shelter if such an event occurs.

In the attempt to drastically reduce crew radiation exposure from GCR over a 1000-day Long-stay mission, aluminum shielding alone is not sufficient—but there are a number of promising composite material and in situ resource options that may help to improve performance. A detailed swing weight analysis reveals that out of all composite alternatives, boronated nitride nanotubes (BNNTs) are the most promising option, due to the fact that they have potential for use both as part of vehicle/habitat structures and in yarns for clothing; and because they are extremely lightweight for the level of shielding provided. Regolith shielding is also found to have high promise for the surface portion of Long-stay missions, providing that resources are invested to design the tools and equipment needed to facilitate its use (ideally Martian excavation equipment or even advance robotics that could generate bricks from the material). Manual “sand bag” labor by crew is also an option, though it will incur significant use of astronauts’ time to pile up meters of regolith around their habitat. In the long run, field-based shielding has been shown to have high potential, and should be given a high priority for development by the 2040 timeframe, in parallel with the development of composite shields which would still be needed as a “backup” for shielding in the event of a field-based system maintenance shutdown or failure.

A swing weight analysis is also conducted to compare different options for medical countermeasures which may help to prevent damage from crew radiation exposure, or to help heal damage in the aftermath. Of all options, the two that are already FDA-approved (Amifostine and Neupogen) are shown to be preferable; though three other options currently in various stages of developmental or clinical trials also show high potential. With medications, it is important to remember that these are designed to be used as a failsafe in the event that something goes wrong (for example, crew receiving an acute radiation dose due to unexpected conditions on the Martian surface or being unable to get to shelter before an SPE). Further, due to the minimal weight involved, it may be logical to bring “any and all” options that are FDA approved as part of cargo, at

least until practical application in space determines whether certain options are superior for human use or not.

Overall, this paper also finds that no single shielding option exists at present to reduce crew exposure from GCRs below existing limits during the transit periods in space. It is possible that a combination of 2m+ regolith shielding for the surface stay portion of a mission in addition to the use of composites on transit vehicles and habitats may help to improve this outlook—but it is hard to quantify these numbers especially when the very first missions to Mars will likely involve either humans in orbit or a very short surface stay which negates the value of regolith shielding entirely while still incurring at least 500 days or more in transit in deep space.

These conclusions indicate two high-priority paths for further research that should be conducted on shields. First, detailed studies about the combination of composite vehicle and regolith shielding should be conducted to determine whether it is possible to reduce potential exposure levels below the limits for all gender and age groups on Long-stay mission models. Second, field based shields should be shifted to higher priority for funding and implementation within the next 20 years.

Another area that likely merits further research is the question of whether crew dosage with any medical countermeasure (for example, Amifostine) could serve to safely mitigate a large portion of the risk of GCR exposure, provided the dosing is given at a regular interval during the deep space transit periods of the mission. This is another question that may be hard to analyze given the ethical limitations of studying the effectiveness of these medicines with humans on Earth.

Finally, in terms of the existing crew exposure limits one must also ask the most challenging question of all—given NASA’s Space Worker Regulations include a section on the concept of autonomy, is it worth it to relax exposure limits for the earliest Mars missions provided the astronauts involved are willing to accept this risk for the potential of being the first explorers on another planet? Much like the “leap” that human kind made on the first Lunar missions, these increased risks may be far outweighed by the potential returns.

THIS PAGE INTENTIONALLY LEFT BLANK

## LIST OF REFERENCES

- Adams, J. H., D. H. Hathaway, R. N. Grugel, J. W. Watts, T. A. Parnell, J. C. Gregory, and R. M. Winglee. 2005. *Revolutionary Concepts of Radiation Shielding for Human Exploration of Space*. NASA/TM 2005–213688. Huntsville, AL: Marshall Space Flight Center. <http://hdl.handle.net/2060/20050180620>.
- Anzai, Kazunori, Nobuhiko Ban, Toshihiko Ozawa, and Shinji Tokonami. 2012. “Fukushima Daiichi Nuclear Power Plant Accident: Facts, Environmental Contamination, Possible Biological Effects, and Countermeasures.” *Journal of Clinical Biochemistry and Nutrition* 50(1): 2–8. doi:10.3164/jcbn.D-11-00021.
- Barcellos-Hoff, Mary Helen, Eleanor A. Blakely, Sandeep Burma, Albert J. Fornace, Stanton Gerson, Lynn Hlatky, David G. Kirsch et al. 2015. “Concepts and Challenges in Cancer Risk Prediction for the Space Radiation Environment.” *Life Sciences in Space Research* 6: 92–103. doi:10.1016/j.lssr.2015.07.006.
- Boston, P.J., S.M. Welch, and S.L. Thompson. 2003. “Extraterrestrial Caves: Science, Habitat, & Resources (A NIAC Phase I Study).” 07600-045. [http://www.niac.usra.edu/files/studies/final\\_report/428Boston.pdf](http://www.niac.usra.edu/files/studies/final_report/428Boston.pdf).
- Cellerant Therapeutics. 2016. “CLT-008 Myeloid Progenitor Cells.” <http://www.cellerant.com/pipeline/clt-008-myeloid-progenitor-cells.html>.
- Cucinotta, Francis A. 2015. “A New Approach to Reduce Uncertainties in Space Radiation Cancer Risk Predictions.” *PLoS ONE* 10(3): 1–15. doi:10.1371/journal.pone.0120717.
- Cucinotta, Francis A., and Marco Durant. 2010 “Risk of Radiation Carcinogenesis.” In *Human Health and Performance Risks of Space Exploration Missions*, edited by Jancy C. McPhee and John B. Charles, 119–169. Washington, DC: NASA.
- Cucinotta, Francis A., Myung Hee Y. Kim, and Lori J. Chappell. 2011. *Space Radiation Cancer Risk Projections and Uncertainties-2010*. NASA/TP-2011-216155. Hanover, MD: NASA Center for AeroSpace Information.
- Cucinotta, Francis A., Myung Hee Y Kim, Lori J. Chappell, and Janice L. Huff. 2013. “How Safe Is Safe Enough? Radiation Risk for a Human Mission to Mars.” *PLoS ONE* 8(10): 1–9. doi:10.1371/journal.pone.0074988.
- Dezfuli, Homayoon, Michael Stamatelatos, Gaspare Maggio, Christopher Everett, and Robert Youngblood. 2010. *NASA Risk-Informed Decision Making Handbook*. NASA/SP-2010-576-Version1.0. Washington, DC: NASA Office of Safety and Mission Assurance.

- Drake, Bret G, Stephen J Hoffman, and Kevin D Watts. 2009. *Human Exploration of Mars Design Reference Architecture 5.0 Addendum*. NASA/SP-2009-566-ADD. Hanover, MD: NASA Center for AeroSpace Information.
- Drake, Bret G and Kevin D Watts. 2014. *Human Exploration of Mars Design Reference Architecture 5.0 Addendum #2*. NASA/SP-2009-566-ADD2. Hanover, MD: NASA Center for AeroSpace Information.
- Drugs.com. 2016a. “Amifostine - FDA Prescribing Information, Side Effects and Uses.” Accessed November 25. <https://www.drugs.com/pro/amifostine.html>.
- Drugs.com. “Neupogen.” 2016b. *Drugs.com*. Accessed November 25. <https://www.drugs.com/neupogen.html>.
- Epelman, S., and D.R. Hamilton. 2006. “Medical Mitigation Strategies for Acute Radiation Exposure during Spaceflight.” *Aviation, Space, and Environmental Medicine* 77(2):130-139. <http://www.ingentaconnect.com/content/asma/ asem/2006/00000077/00000002/art00007>.
- Garner, Rob. 2015. “Real Martians: How to Protect Astronauts from Space Radiation on Mars.” NASA Journey to Mars. <https://www.nasa.gov/feature/goddard/real-Martians-how-to-protect-astronauts-from-space-radiation-on-Mars>.
- Harmon, Katherine, and Francie Diep. 2011. “Radioactive Omission: Where Are the Anti-Radiation Drugs?” *Scientific American*. <https://www.scientificamerican.com/article/radioactive-omission-where/>
- Hassler, Donald. 2013. “Measuring the Radiation Environment on Mars.” *Technology Today* Winter: 6–9. <http://www.swri.org/3pubs/ttoday/Winter13/pdfs/MarsRadiation.pdf>.
- Hassler, Donald, Cary Zeitlin, Robert Wimmer-Schweingruber, Bent Ehresmann, Scott Rafkin, Jennifer Eigenbrode, David Brinza, and Gerald Weigle. 2013. “Mars’ Surface Radiation Environment Measured with the Mars Science Laboratory’s Curiosity Rover.” *Science Express*, no. 9 December. doi:10.1126/science.1244797.
- Köhler, J., B. Ehresmann, C. Zeitlin, R. F. Wimmer-Schweingruber, D. M. Hassler, G. Reitz, D. E. Brinza, et al. 2013. “Measurements of the Neutron Spectrum in Transit to Mars on the Mars Science Laboratory.” *Life Sciences in Space Research* 5 (May 2013): 6–12. doi:10.1016/j.lssr.2015.03.001.
- Levine, Rachel. 2015. “Cleveland BioLabs Releases Entolimod Phase 1 Study Findings at ASCO.” *Marketwired*. <http://irdirect.net/pr/release/id/1326333>.



- Lindsey, Nancy J. 2003. "Lunar Station Protection: Lunar Regolith Shielding." In *International Lunar Conference 2003 Session 5: Science of, from and on the Moon: Life Sciences and Habitation, Hawaii Island, Hawaii*. Greenbelt, MD: Lockheed Martin Technical Offices.
- Miller, J, L A Taylor, M Digiuseppe, L H Heilbronn, G Sanders, and C J Zeitlin. 2008. "Radiation Shielding Properties of Lunar Regolith and Regolith Simulant." In *NLSI Lunar Science Conference 2008, Moffett Field, California*. Moffett Field, CA: NASA Lunar Science Institute.
- NASA Human Research Roadmap. 2016. "Risks." Last modified December 21. <https://humanresearchroadmap.nasa.gov/risks/>.
- NASA Journey to Mars. 2017. "Journey to Mars Overview." Last modified March 27. <https://www.nasa.gov/content/journey-to-Mars-overview>
- NASA Office of the Chief Technologist. 2016. "2015 NASA Technology Roadmaps." Last modified July 8. <https://www.nasa.gov/offices/oct/home/roadmaps/index.html>.
- NASA Science Beta. "Digging in and Taking Cover." 1998. *NASA Science Beta*. [https://science.nasa.gov/science-news/science-at-nasa/1998/msad20jul98\\_1](https://science.nasa.gov/science-news/science-at-nasa/1998/msad20jul98_1).
- NASA Space Radiation Analysis Group. 2016. "Spaceflight Radiation Health Program at JSC." Accessed August 4. <http://srag.jsc.nasa.gov/Publications/TM104782/techmemo.htm>.
- National Council on Radiation Protection and Measurements (NCRP). 2014. *RADIATION PROTECTION FOR SPACE ACTIVITIES : SUPPLEMENT TO PREVIOUS RECOMMENDATIONS*. NCRP Commentary No. 23. Bethesda, MD: NCRP.
- Onconova Therapeutics. 2016. "Recilisib (Ex-Rad)." <http://www.onconova.com/pipeline/#tab-id-4>.
- Phys.org. 2010. "Early Warning System Would Predict Space Storms on Mars." March 29. <http://phys.org/news/2010-03-early-space-storms-Mars.html>.
- Rojdev, Kristina, and William Atwell. 2015. "Hydrogen and Methane Loaded Shielding Materials for Mitigation of Galactic Cosmic Rays and Solar Particle Events." *Gravitational and Space Research* 3(1): 59-81. doi: 676-2472-1-PB.
- Sieffert, Alyssa Megan. 2014. "Astronaut Health & Safety Regulations Ionizing Radiation." *The SciTech Lawyer* 10(4): 20-22.

- Slaba, Tony C, Christopher J Mertens, and Steve R Blattnig. 2013. *Radiation Shielding Optimization on Mars*. NASA/TP-2013-217983. Hanover, MD: NASA Center for AeroSpace Information.
- Space Daily. 2016. "Active Tracking of Astronaut Rad-Exposures Targeted." July 22. [http://www.spacedaily.com/reports/Active\\_tracking\\_of\\_astronaut\\_rad\\_exposures\\_targeted\\_999.html](http://www.spacedaily.com/reports/Active_tracking_of_astronaut_rad_exposures_targeted_999.html).
- Spudis, Paul D. 2011. "Regolith, The 'Other' Lunar Resource." AIRSPACEMAG.COM. <http://www.airspacemag.com/daily-planet/regolith-the-other-Lunar-resource-156943194/>.
- Thibeault, Shiela, Catherine Fay, Sharon Lowther, Kevin Earle, Godfrey Sauti, Jin Ho Kang, and Cheol Park. 2012. *Radiation Shielding Materials Containing Hydrogen, Boron, and Nitrogen: Systematic Computational and Experimental Study - Phase I*. HQ-E-DAA-TN33851. Hampton, VA: NASA Innovative Advanced Concepts (NIAC).
- United States Nuclear Regulatory Commission. 2016. "§ 20.1004 Units of Radiation Dose." Accessed July 6. <http://www.nrc.gov/reading-rm/doc-collections/cfr/part020/part020-1004.html>.
- U.S. Food & Drug Administration. 2016. "FDA Approves Radiation Medical Countermeasure." Accessed November 25. <http://www.fda.gov/emergencypreparedness/counterterrorism/medicalcountermeasures/aboutmcmi/ucm443245.htm>
- Wetegrove, Megan. 2014. "Space Radiation - Interplanetary Radiation Belts." American Nuclear Society Aerospace Nuclear Science & Technology Division. <http://anstd.ans.org/2014/05/21/space-radiation-interplanetary-radiation-belts/>.
- Williams, Richard. 2015. *NASA Space Flight Human-System Standard Volume 1 , Revision A: Crew Health*. NASA-STD-3001, Volume 1, Revision A with Change 1. Washington, DC: NASA.

## INITIAL DISTRIBUTION LIST

1. Defense Technical Information Center  
Ft. Belvoir, Virginia
2. Dudley Knox Library  
Naval Postgraduate School  
Monterey, California